CMAC

# Poster Collection

2025

Engineering and
Physical Sciences
Research Council

# Contents

# Contents continued

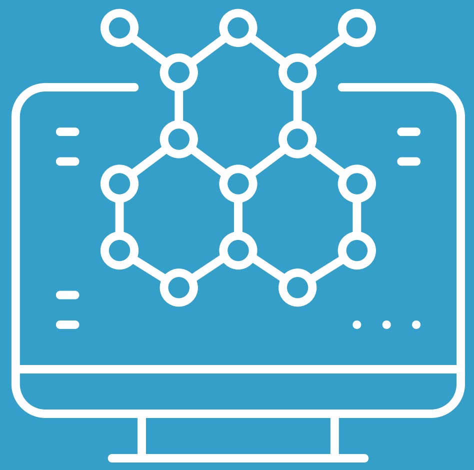

# Data & Digital Twins

POSTER 2

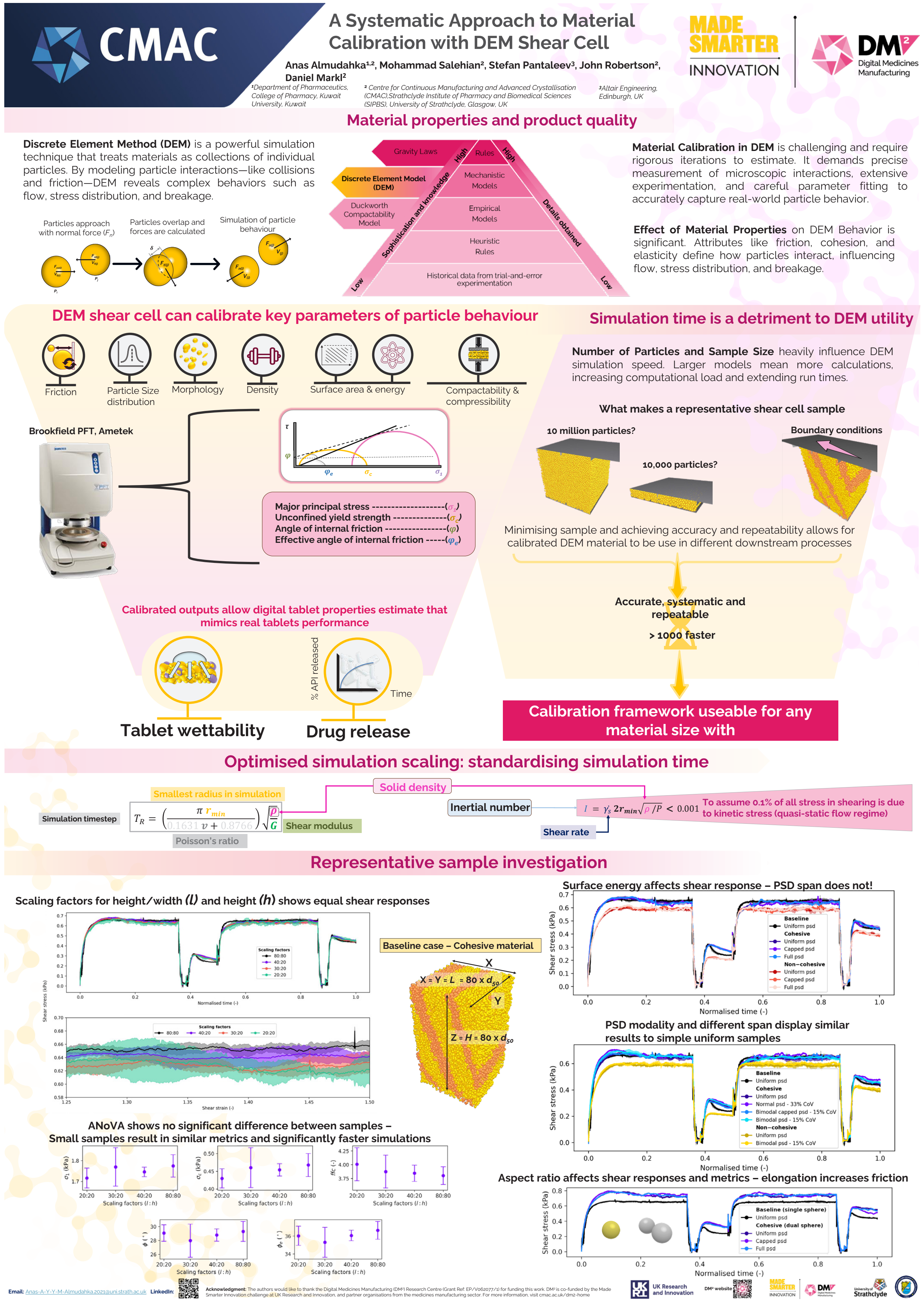

POSTER 3

# Balancing Performance and Manufacturability in Pharmaceutical Tablets

Faisal Alsharif [1,2], Natalie Maclean [1,2], Ibrahim Khadra [1], Daniel Markl [1,2]
[1]Strathclyde Institute of Pharmacy & Biomedical Sciences (SIPBS), University of Strathclyde, Glasgow
[2] Centre for Continuous Manufacturing and Advanced Crystallisation (CMAC), University of Strathclyde, Glasgow

## Introduction

Balancing tablet performance and manufacturability is essential in pharmaceutical formulation. Compression pressure and porosity influence tablet strength, disintegration, and dissolution, impacting drug release and production efficiency. This study evaluates these effects in Microcrystalline Cellulose (MCC)/Mannitol and Dicalcium Phosphate Anhydrous (DCPA) formulations to optimise tablet design.

## Aim & Objectives

- Investigate how compression pressure and porosity affect tablet performance & manufacturability.
- Examine their impact on disintegration, tensile strength, and liquid absorption using sessile drop analysis.
- Analyse drug release through dissolution testing.
- Optimise formulation parameters to improve tablet quality.

## Materials and Methods

| Formulation | Filler (1) 32% | Filler(2) 32% | API 30% | Disintegrant 5% | Lubricant 1% |
|---|---|---|---|---|---|
| 1 | MCC | Mannitol | Griseofulvin | Croscarmellose Sodium (CCS) | Magnesium Stearate (Mgst) |
| 2 | MCC | DCPA | | | |

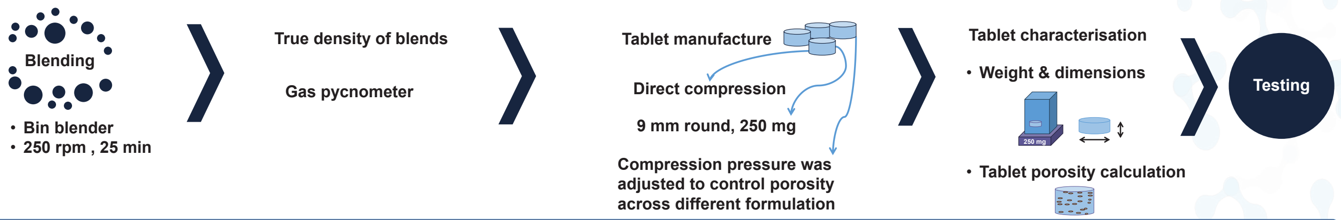


Tablet Characterisation

| Tensile strength | Sessile drop | | Disintegration | Dissolution |
|---|---|---|---|---|
| | Water | 0.4% Sodium Dodecyl Sulfate (SDS) In water | Water | 0.4% SDS in water |

## Result & Discussion

Manufacturability

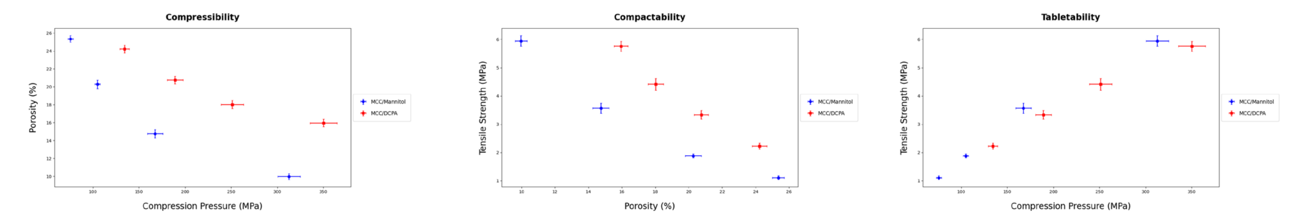


- Higher compression pressure resulted in lower porosity, leading to denser tablets.
- MCC/DCPA exhibited better compactability, achieving higher tensile strength at lower porosity compared to MCC/Mannitol.
- Compression pressure increased tablet strength in both formulations; however, MCC/Mannitol needed higher pressure to match MCC/DCPA

Performance

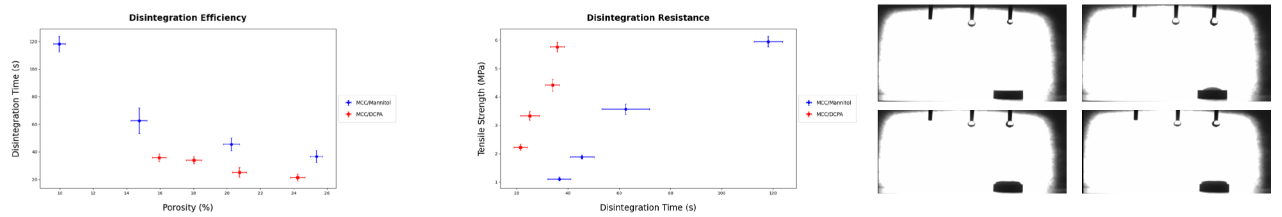


- Higher porosity led to faster disintegration and quicker drug release.
- MCC/DCPA disintegrated faster than MCC/Mannitol, indicating better wettability.
- Stronger tablets resisted disintegration longer, balancing strength and dissolution.

## Conclusion

- Balancing tablet strength, porosity, and disintegration time is crucial for optimising both performance and manufacturability.
- MCC/DCPA exhibited better compactability and faster disintegration, while MCC/Mannitol required higher compression pressure to achieve similar tensile strength.
- Higher porosity led to faster disintegration, while stronger tablets showed greater resistance to breakdown.
- Ongoing sessile drop and dissolution studies will provide further insights into liquid absorption and drug release.

POSTER 4

# PharmaCrystNet: Improving the predictive capabilities of Crystallisation Models in the Pharmaceutical Industry

*D. Alvarado, F. Paterson, C. J. Brown**
CMAC, Technology and Innovation Centre, University of Strathclyde, Glasgow, UK
*cameron.brown.100@strath.ac.uk

## Introduction

- Crystallisation is a crucial operation as it affects physical properties, stability, and final product performance.
- Modelling of crystallisation through population balance models (PBMs) helps understand process dynamics and the evolution of critical attributes throughout a process, such as crystal size distribution (CSD). This in turn provides guidance about process conditions necessary to ensure product meets quality standards and process has an acceptable efficiency.
- However, PBMs are not widely adopted due to limitations in terms of development time, large uncertainty, and required data quality. Thus, to bring about greater adoption, the following challenges must be address
  1. Improve transferability between chemical systems
  2. Reduce experimental burden needed to collect data and parameterise models
  3. Obtain models that fit better complex mechanisms.

## Aims

Thus, this project will develop a physics informed neural network (PINN) that addresses the mentioned challenges by achieving the following aims:

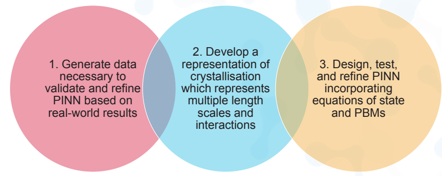


## Methods and Results

### 1. Selection of APIs

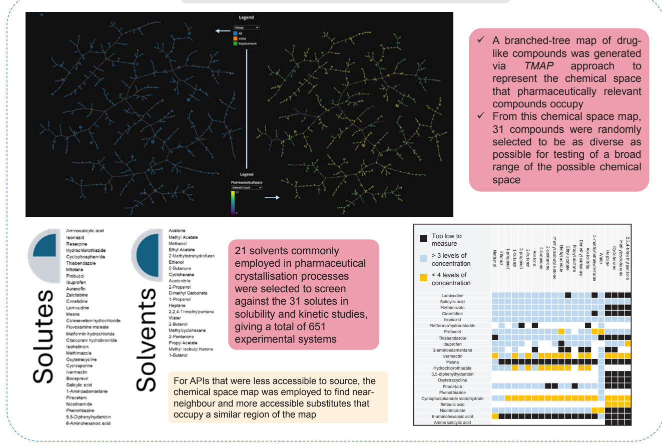


### 3. Dataset Construction

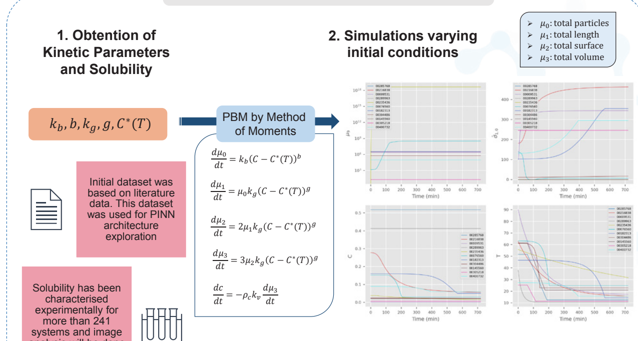


- >200K simulations for 20 systems corresponding to 9 solvents and 14 solutes varying process conditions such as initial and final temperature, cooling profile, seed mass and size.
- Within the systems characterised experimentally, ~30% of solute did not dissolve in the tested solvent, and ~25.5% systems did not nucleate.
- Solubility curve could be fitted with $R^2 \geq 0.95$ for 41 systems

### 2. Experimental Data Collection

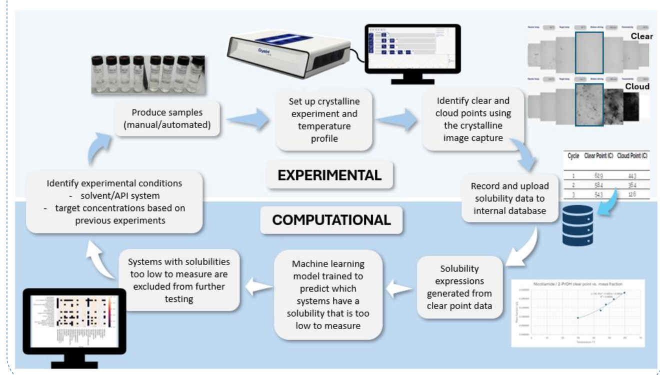


### 4. PINN Modelling

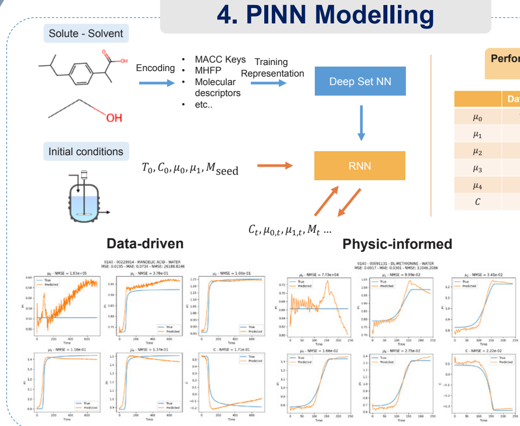


| | Data-driven | PI ($\beta$ = 0.01) |
|---|---|---|
| $\mu_0$ | 1.59e4 | 4.27e3 |
| $\mu_1$ | 0.325 | 0.097 |
| $\mu_2$ | 0.089 | 0.158 |
| $\mu_3$ | 0.025 | 0.165 |
| $\mu_4$ | 0.062 | 0.215 |
| $C$ | 0.042 | 0.824 |

- The inclusion of solute-solvent representation allows model to be more transferable to different systems
- RNN (LSTM) showed their capacity to learn general patterns for different systems, however more work is necessary to improve their accuracy

## Summary and future work

- Initial results showed that the proposed architecture (LSTM: long short-term memory RNN) can learn to predict crystallisation outcomes across time mostly for parameters related to length, surface, and volume.
- However, the performance of the model for systems where nucleation is negligible was poor to predict the number of particles ($\mu_0$), by which variations in architecture and physics incorporation will be carried out to improve this aspect as well as the overall accuracy
- Additionally, more specific analysis will be done to establish generalisation towards other systems not included in the training set.
- The results obtained are limited to 20 systems. Thus, future work will specially focus on obtention of solubility data for new combinations solute-solvent and the estimation of kinetic parameters for the characterised systems for their inclusion in the training and validation of the PINN

## References

- Wu, G., et al., Physics-informed machine learning for MPC: Application to a batch crystallization process. Chemical Engineering Research and Design, 2023. 192: p. 556-569.
- Raissi, M., P. Perdikaris, and G.E. Karniadakis, Physics-informed neural networks: A deep learning framework for solving forward and inverse problems involving nonlinear partial differential equations. Journal of Computational Physics, 2019. 378: p. 686-707
- Kumar Akkisetty, P., et al., Population Balance Model-Based Hybrid Neural Network for a Pharmaceutical Milling Process. Journal of Pharmaceutical Innovation, 2010. 5(4): p. 161-168.
- Boobier, S., et al., Machine learning with physicochemical relationships: solubility prediction in organic solvents and water. Nature Communications, 2020. 11(1): p. 5753.

Engineering and Physical Sciences Research Council
University of Strathclyde Glasgow

POSTER 5

# dm2dbpy: Putting the A in FAIR Data

John A. Armstrong, Christopher Boyle, Tabbasum Naz, Antony D. Vassileiou, Blair F. Johnston
j.armstrong@strath.ac.uk
*Continuous Manufacturing and Advanced Crystallisation (CMAC), Strathclyde Institute of Pharmacy & Biomedical Sciences, University of Strathclyde, Technology and Innovation Centre, 99 George Street, Glasgow G1 1RD, UK.*

## 1. Introduction & Motivations

- One of the key outcomes from DM² Platform 1 is to establish data schema and standards for medicines manufacturing datasets following FAIR (findable, accessible, interoperable, reusable) standards which was achieved through storage of data in a relational SQL database
- This data storage achieves the findability, interoperability and reusability of the data but not so much the accessibility since SQL itself is quite dense, and queries can be difficult to decipher
- Having a user-friendly application programming interface (API) built in Python allows researchers to **access and use data** without breaking the flow of research and in a programming language they are more familiar with

## 2. Database Schema

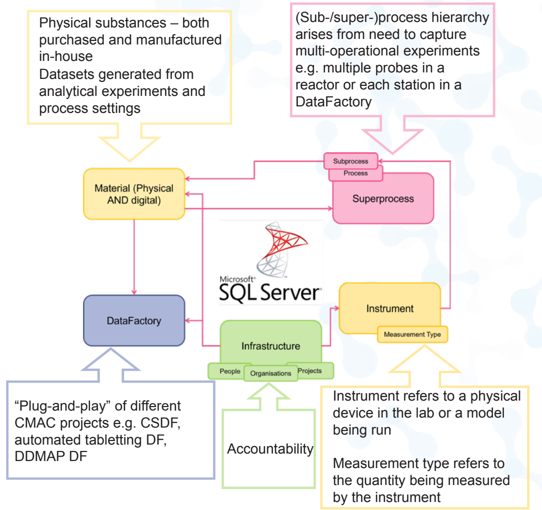


## 3. Interacting with the Database

SQLAlchemy

- Python API built on top of SQLAlchemy's Object Relational Mapper (ORM)
- Object-oriented approach:
  - Each table is a Python class which are linked via helper functions defining primary/foreign keys
- Inheritance mapping: instantiating table objects will load all dependent tables
- Built-in query caching and optimisation

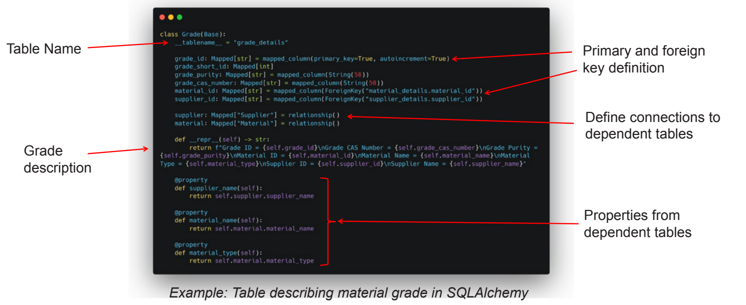


*Example: Table describing material grade in SQLAlchemy*

## 4. CRUD Operations

- Package provides easier accessibility of data to users, with defined functions for CRUD (create, read, update, delete) operations
- Abstraction of SQL queries:
  - Interact with DB using Python objects instead of raw SQL queries
  - Simplification of complex queries and DB operations
  - Function-based query construction
- Code readability: much nicer to read than raw SQL

**C: Create**

Query: "Create a tablet set with 10 tablets consisting of 10% cmac-1 API, 1% cmac-2 lubricant, 5% cmac-4 disintegrant and the rest cmac-3 filler."

Python:

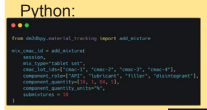

SQL:

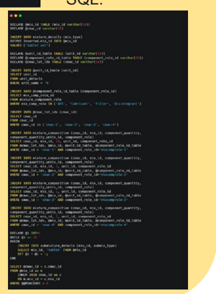

QOL: don't need to know arbitrary IDs e.g. for units or people, the CRUD functions will find the IDs for you based on distinguishing information e.g. mL or person's name

**R: Read/select**

Query: "Return all blends with 30% drug loading of griseofulvin containing 5% disintegrant."

Python:

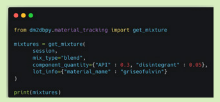

SQL:

"mixtures" is then a Python list of Mixture objects which are defined similar to the grade example above

**U: Update**

Python:

SQL:

**D: Delete**

Python:

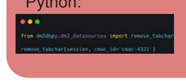

SQL:

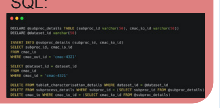

## 5. Use Case: DM² Tabletting DataFactory

- DataFactories generate a **lot** of data *very* quickly from a variety of instruments
- One such example is the DM² platform 2 tabletting DataFactory which generates pre-compaction, compaction and post-compaction data within a matter of minutes
- Following the schema above, each instrument in the DataFactory would be a subprocess with each run being a process and the overall manufacturing target being the superprocess
- Tracking the data between these interconnected tables can result in SQL queries 1000s of lines long but is simplified into a short Python script called at the end of each iteration to store data in appropriate and linked tables.

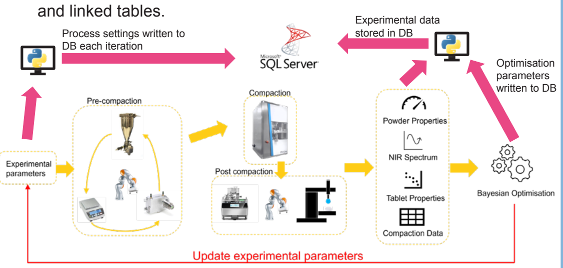


## 6. Installation & Contribution

- Python package is available upon request via the CMAC GitHub
- Public release on PyPI with full documentation to follow

SCAN ME

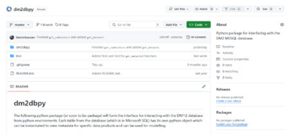

Collaborators welcome!

Get in touch to become a contributor to the project.

## 7. Conclusions & Future Work

- dm2dbpy **simplifies SQL queries** with a Pythonic approach, reducing burden for researchers
- Stepping stone on the way to plain English querying: Python is much more language-like than SQL
- **Faster database querying**: researcher spends less time getting data into Python
- Future work includes **developing web-based GUIs** for non-programmers to interact with the database easily and **integration with semantic technologies** for smart querying.

UK Research and Innovation | MADE SMARTER INNOVATION | DM² Digital Medicines Manufacturing

**Acknowledgment:** The authors would like to thank the Digital Medicines Manufacturing (DM²) Research Centre (Grant Ref: EP/V062077/1) for funding this work. DM² is co-funded by the Made Smarter Innovation challenge at UK Research and Innovation, and partner organisations from the medicines manufacturing sector. For more information, visit cmac.ac.uk/dm2-home

DM² website



POSTER 6

# SHARing data to accelerate Pharmaceutical manufacturing Efficiency across trusted Networks

CMAC: Blair Johnston, Subhaa Arumugam
CPI: Pamela Little, Martin Keane, Kamal Abu Hassan, Rab Leckie, Marvellous Mark, Mohamed Elpkash
CCDC: Andy Maloney, Matthew Lightfoot, Suzanna Ward
GDP: Rob Innes

## Research Goal

***Develop a Framework for Risk Assessing the Value of Federated Learning to Improve the Fidelity of Models in Pharmaceutical Manufacturing and to de-risk transformative (FASS) technologies in medicines manufacturing data sharing, to drive predictive science and to improve manufacturing efficiency.***

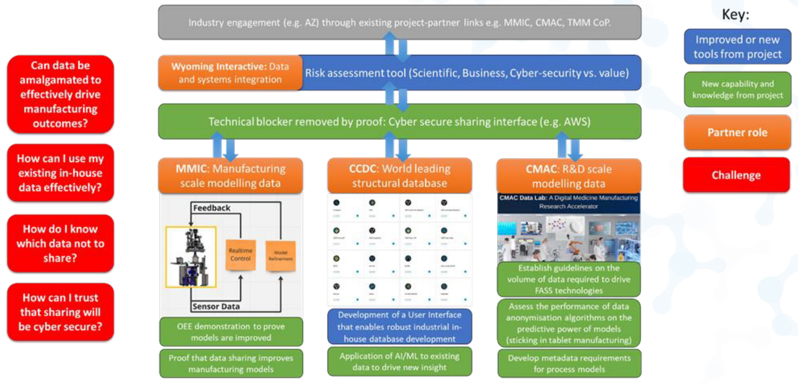


## Key Benefits

- Improved collaboration between organizations
- Faster model development and deployment
- Enhanced Data Privacy and Security
- Real-Time Research Data Utilization
- Better Predictive Modelling

## Federated Learning Architecture

- **Decentralized Data Training**
  - **Enables collaborative ML model training while preserving privacy and ensuring regulatory compliance by not sharing raw data.**
- **Federated Client-Server Architecture**
  - **Each client, hosted by different organizations, trains the model locally using private data and shares only model updates with the central server.**
- **Secure Model Updates & Aggregation**
  - **The central server aggregates these updates and sends back the improved global model to all the clients.**
- **Differential Privacy & Secure Computation**
  - **Sensitive data is protected from being reconstructed or inferred from model updates.**
- **Heterogeneous Data Handling**
  - **Model training can occur on diverse data sources across different organizations.**

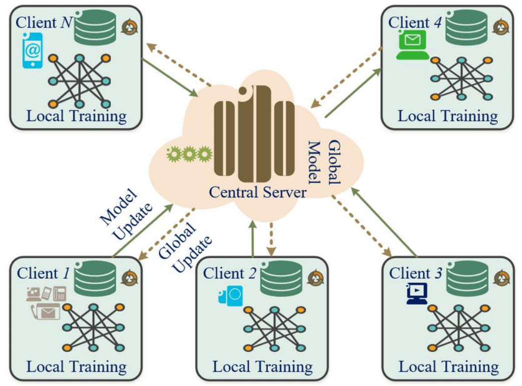


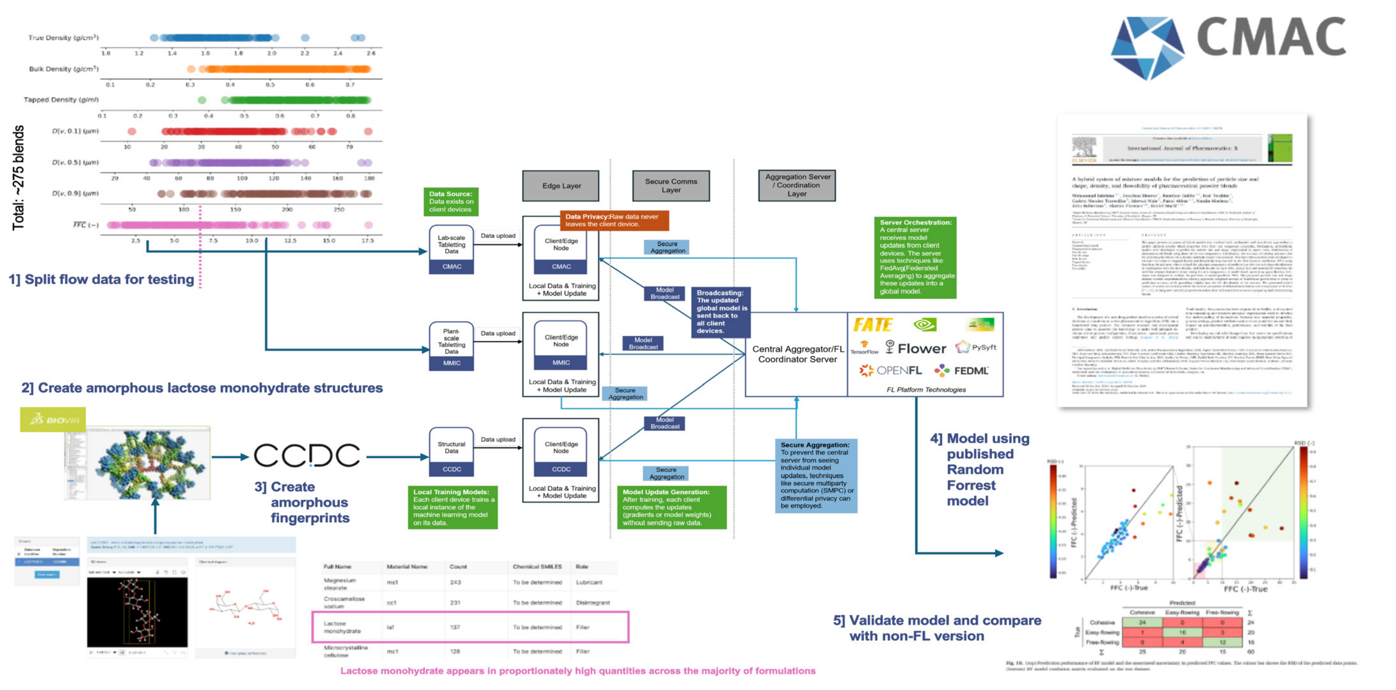

POSTER 7

# Physical & Chemical Analysis of Pharmaceutical Materials

Dr. Christoph Busche, Dr. María José Heras Ojea, MChem. Rachel Feeney, MChem. Mark McGowan
CMAC National Facility, University of Strathclyde, 99 George St, Glasgow, G1 1RD

## Introduction

Analytical characterisation plays an important role throughout the pharmaceutical manufacturing pipeline, specifically for testing the active pharmaceutical ingredients, excipients, blends and final solid dosage forms. Analytical techniques available at the CMAC National Facility include; particle sizing and morphology imaging, density measurements (bulk, tapped & particle), thermal stability measurements, surface area & energy, impurity detection & quantification, powder flow properties, tablet hardness and dissolution testing. Our techniques have also been used in a number of non-pharmaceutical related applications.

## Infrared microscope

IR-Microscopy can be used for chemical analysis of specific areas of interest. The example below shows it being used in forensic trace analysis, specifically gunshot residues and for the analysis of micro-bond resin droplets on glass fibres.

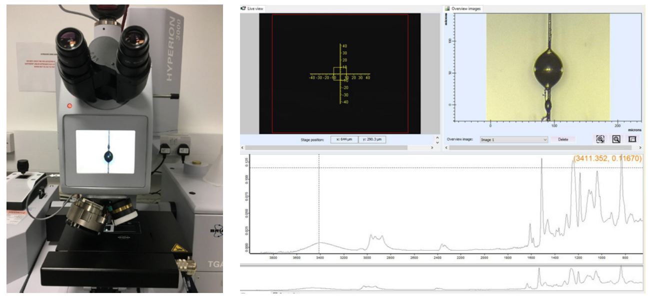

Microscope image and live IR spectra of a resin droplet.

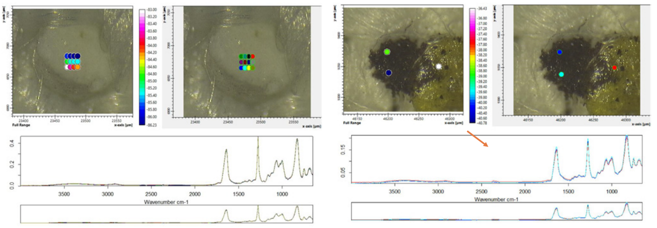

Original Cotton fabric.

Two different forms of gunpowder residue on cotton fabric.

## Optical coherence tomography (OCT)

OCT is a high-resolution imaging technique using coherent light to measure depth resolved images (up to 2mm) of scattering material.

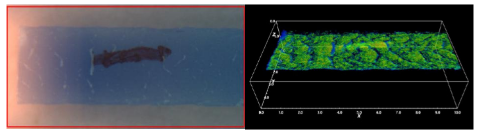

Surface profile of an extrudate.

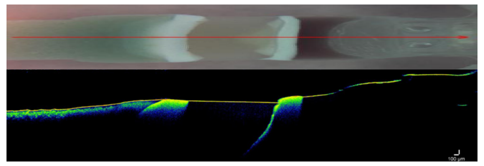

Depth profile of a multicomponent extrudate

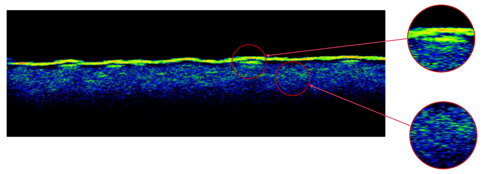

Cracks and “grains” below the surface of an extrudate

OCT can be used for the destruction free determination 3D imaging of structures in extrudates, tablets and other scattering material. Structures including coating thickness, cracks, domain/grain sizes

## Raman coupled Morphology

This is the combination of two analytical methods: morphological analysis (shape and size distribution) and chemical identification via Raman spectroscopy.

Raman spectroscopy can be used to identify polymorphism in a given sample.

The combination of morphological and chemical analysis can be used to “deformulate” a given blend. (here cold medicine is used as an example)

Reference spectra of three APIs: Paracetamol, Guaifenesin, Phenylephrine

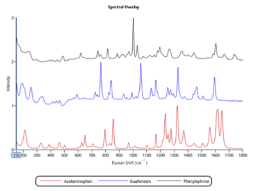

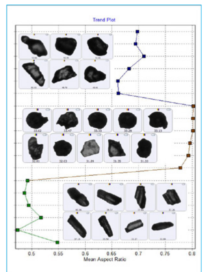

The components were identified by Raman spectroscopy and a trend of the aspect ratio could be seen
Starch
v
Paracetamol
v
Guaifenesin

Comparison between different brands of cold medicine. 8 components could be identified using an internal reference library.
Once identified the respective particle size distribution for a chosen component can be extracted.

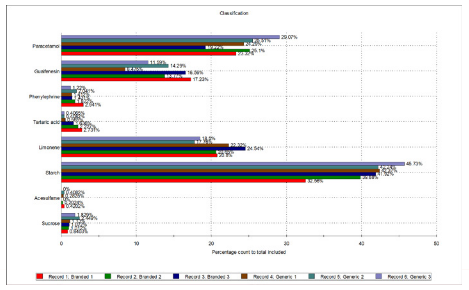

## Time of Flight Secondary Ion Mass Spectroscopy (ToF-SIMS)

ToF-SIMS is a surface analysis method which uses a $Bi_3^+$ primary ion beam map a surface via mass spectra. Other ions (Ar or $O_2$) can be used to remove surface layers to expose deeper parts of the sample. In this example, the effect of blending on the distribution of excipients and Mg stearate in the final tablet has been investigated (left = less blended) (right = more blended). The ion distributions of Magnesium Stearate (green), Lactose (blue) and Avicel (red) have been overlaid to compare distribution patterns.

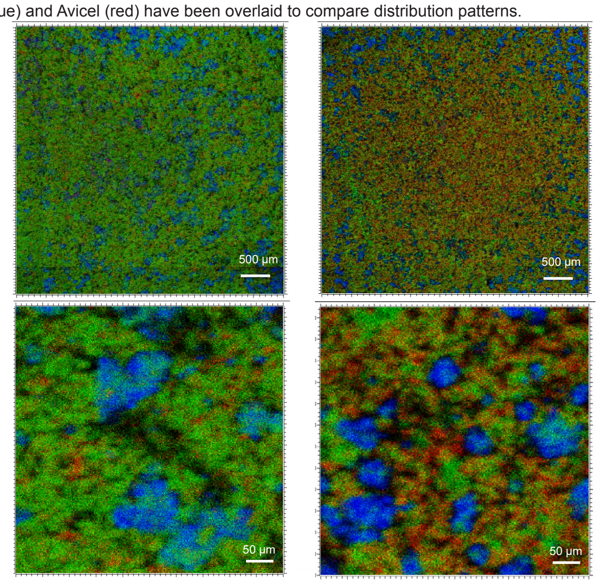


Acknowledgements: Examples of Raman coupled Morphology were provided by Dr. Jo Lothian, Malvern Panalytical Ltd. Micro-bond resin droplets were provided by David Bryce, Mechanical and Aerospace Engineering, University of Strathclyde. Gunpowder residue samples were provided by Hamad S. Rashed, Pure and Applied Chemistry, University of Strathclyde



POSTER 8

# Effect of simulation box size and shear on the structure of amorphous hydrochlorothiazide

Michael Devlin[a]*, Inês Martins[b], Andy Maloney[c], Thomas Rades[b], Blair Johnston[a], Alastair Florence[a]

[a] CMAC, Strathclyde Institute of Pharmacy and Biomedical Sciences (SIPBS), University of Strathclyde, UK
[b] Department of Pharmacy, University of Copenhagen, Copenhagen, Denmark
[c] The Cambridge Crystallographic Data Centre, United Kingdom
*Michael.s.Devlin@strath.ac.uk

## Overview

- **Molecular dynamics (MS) simulations used increasingly to understand structure and dynamics in amorphous pharmaceutical systems**
- **No general guidelines around simulation box seize for small molecule systems, despite numerous such reports for biomaterials**
- **Effect of box size systematically studied to determine limits for consistent simulations/ properties for amorphous hydrochlorothiazide (HCTZ)**
- **Learnings from box size investigation used to investigate impact of shear on the structure of amorphous HCTZ to replicate ball milling**

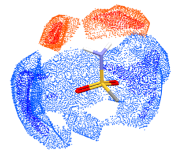

## Effect of box size on structural properties

### Implications for structural fingerprinting using pair distribution function

- PDFs calculated from structural models by

$$G_{calc}(r) = \frac{1}{r}\sum_i\sum_j\left[\left(\frac{f(Q)_i f(Q)_j}{\langle f(Q)\rangle^2}\right)\delta(r - r_{ij})\right] - 4\pi r\rho_0$$

- Poor consistency of PDF < 100 molecules
- Good agreement with experimental ≥ 250 molecules

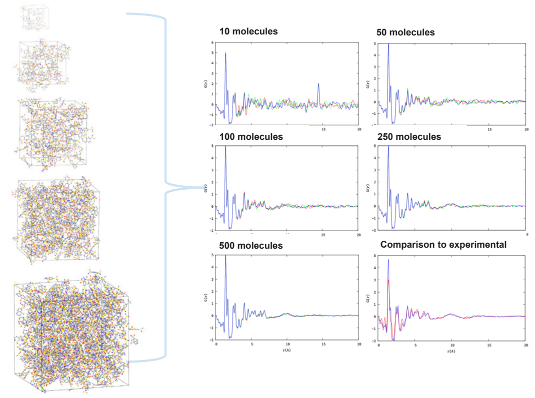


### Impact on intra- and inter- molecular structure

- Inconsistent structural properties < 100 molecules
- 250 molecules needed as minimum to replicate long-range intermolecular interactions consistently

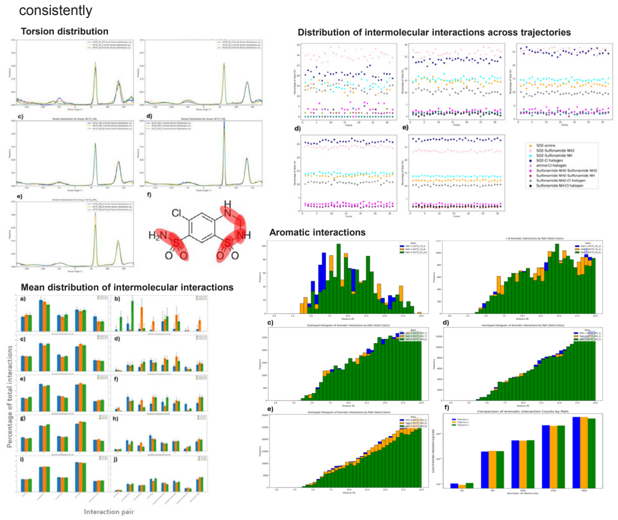


## Effect of shear on structure

### Shear simulations: Background and previous work

- Previous work from collaborators investigated polyamorphism in HCTZ with MD/ PDF
- Identified torsion distribution change depending on preparation route (melt-quench vs spray drying)
- Unable to replicate ball milling with simulation

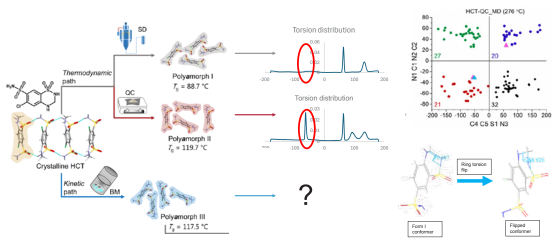


- Materials Studio used to simulate effect of pressure and shear on structure of amorphous HCTZ

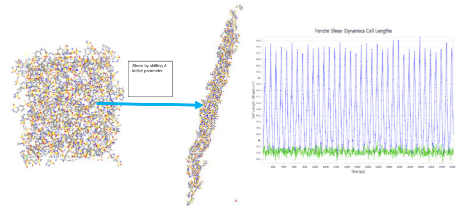

### Impact of shear on structural properties

- Shear/ pressure induces similar structural changes as melt quenching
- Increase in flipped conformer relative to ambient simulations
- Energy barrier between ring puckering states may explain process dependence of transition

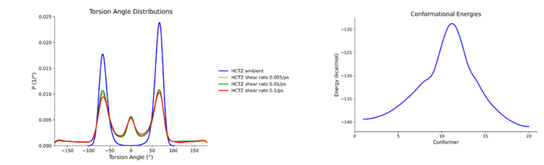


- Change in distribution of intermolecular interactions, often involving groups involved in conformational change

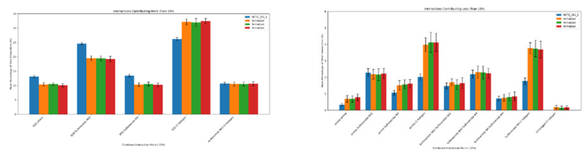

## Conclusions

Box size

- Local structure in MD simulations of amorphous HCTZ dependent on box size
- Inconsistent box packing when less than 100 molecules are used
- Long-range interactions not accounted for fully until ~250 molecules in the box

Effect of shear

- Shearing results in same intramolecular structural change as melt-quenching, possibly explaining preparation method-dependent properties of the amorphous form
- Intermolecular contacts also significantly affected by shear/ pressure

## References

(1) Anderson, B. D. and Xiang, T.-X. (2016) ‘Molecular Dynamics Simulations of Amorphous Systems’, in *Computational Pharmaceutical Solid State Chemistry*. Hoboken, NJ: John Wiley & Sons, Inc, pp. 331–373. doi: 10.1002/9781118700686.ch13.

(2) Martins, I. C. B. *et al.* (2023) ‘Unveiling polyamorphism and polyamorphic interconversions in pharmaceuticals: the peculiar case of hydrochlorothiazide’, *Chemical Science*. Royal Society of Chemistry, 14(41), pp. 11447–11455. doi: 10.1039/d3sc02802j.

(3) Zografi, G. and Newman, A. (2017) ‘Interrelationships Between Structure and the Properties of Amorphous Solids of Pharmaceutical Interest’, *Journal of Pharmaceutical Sciences*, 106(1), pp. 5–27. doi: 10.1016/j.xphs.2016.05.001.

POSTER 9

# Deep Learning Enhanced Correlation of Particle Descriptors to Sustainable Pharmaceutical Manufacturing Processes

Omar El-Habbak[1], Cameron Brown[1], Alexandru Moldovan[2], Helen Blade[3], Rachael Shinebaum[4], Alastair Florence[1]

[1] CMAC Future Manufacturing Hub, Strathclyde Institute of Pharmacy and Biomedical Science, University of Strathclyde, Glasgow, UK
[2] Cambridge Crystallographic Data Centre, 12 Union Road, Cambridge, UK
[3] Oral Product Development, Pharmaceutical Technology & Development, Operations, AstraZeneca, Macclesfield, UK
[4] Technical Operations & Scientific Innovation, Pharmaceutical Technology & Development, Operations, AstraZeneca, Macclesfield, UK

## 1. The Missing Piece?

- Currently, determining the suitability of powders for product development requires detailed, time-consuming experimental characterization of the bulk properties.
- Machine learning prediction of powder flowability based on crystal properties could positively influence critical decision-making during medicine manufacturing.

| Crystal Property | Modeling Parameter | Device Used |
|---|---|---|
| Flowability (bulk property) | Flow function coefficient | FT4 Powder Rheometer |
| Particle Size Distribution | D10, D50, D90, D[3,2] | QicPic Sympatec |
| Morphology and Energy Calculations | Total lattice energy, electrostatic energy, H-bond energy, VdW energy | Computationally acquired through CSD Python API |
| Surface Chemistry | H-bond donor density, aromatic bond density, H-bond acceptor density | Computationally acquired through CSD Python API |
| Surface Roughness | Rugosity, RMSD, skewness, Pearson kurtosis | Computationally acquired through CSD Python API |

## 2. Data Pipeline

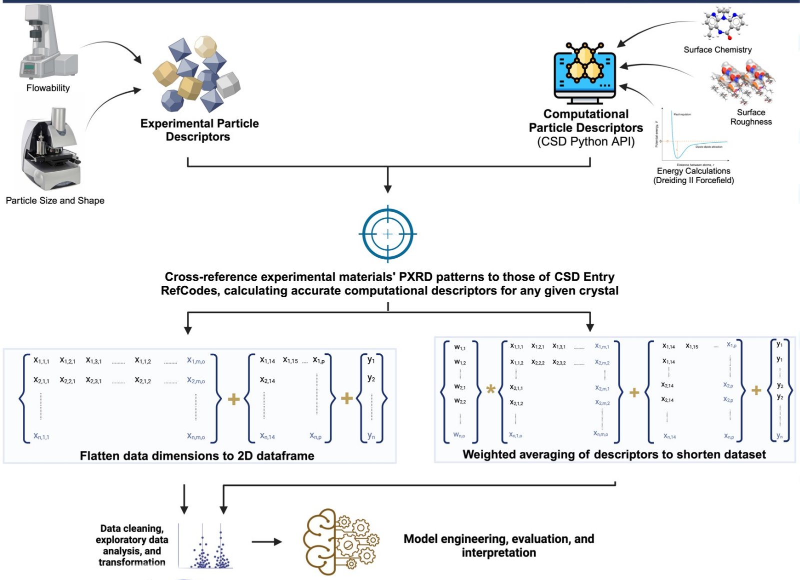


## 3. What the Models Tell Us

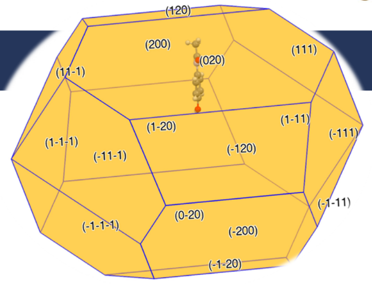

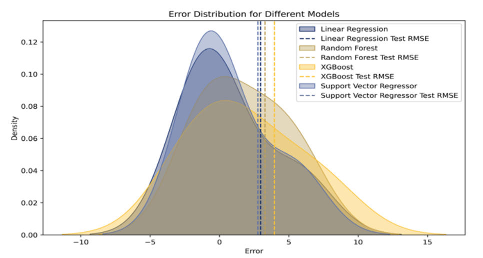


KDE Plot of Regression Error Residuals – All Faces (dotted lines are test RMSEs)

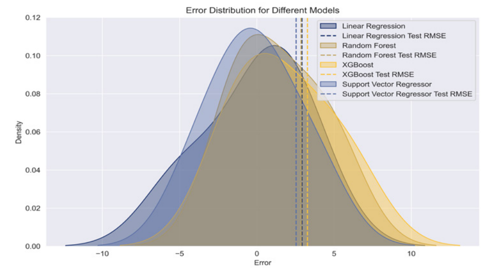


KDE Plot of Regression Error Residuals – 4 Faces with Highest Surface Energies (dotted lines are test RMSEs)

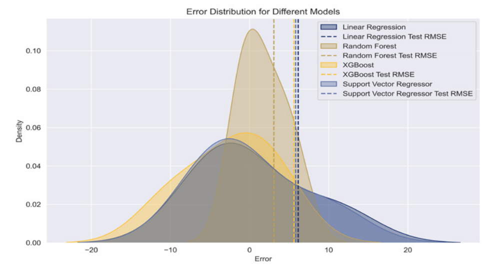


KDE Plot of Regression Error Residuals – 4 Most Morphologically Dominant Faces (dotted lines are test RMSEs)

**Key Findings:**

- Models run on the dataset of experimental + computational particle descriptors performed better than those run on experimental descriptors alone.
- Pearson and Spearman correlations showed high correlation between flowability and certain descriptors (total lattice energy, electrostatic energy, VdW attraction) highlighting the need of further exploration of descriptors to pinpoint their relevance to flowability.
- Models that were run on data representing particle descriptors of a crystal's four faces with the highest surface energies outperformed those run on data representing particle descriptors of all faces or the four most morphologically dominant faces, suggesting a face's surface energy has high impact on flowability.

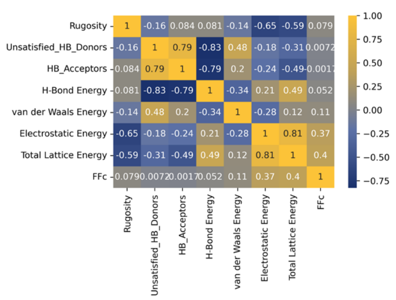


Pearson Correlation

## 4. What's Next?

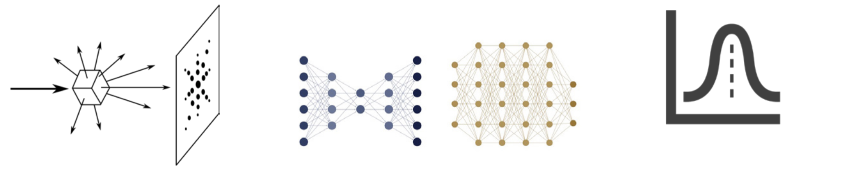

1. PXRD pattern analysis and mapping to CSD RefCode structures
2. Mitigate data scarcity by using active learning and synthetic data generation
3. Model particle size distributions instead of individual particle characteristics

POSTER 10

# Medicines Manufacturing Innovation Centre: research highlights from an industry-academia-government collaboration

Hikaru G. Jolliffe[1], Martin Prostredny[1], Carlota Mendez Torrecillas[1], Ecaterina Bordos[1], Bilal Ahmed[1], Maria A. Velazco-Roa, Collette Tierney[1], Michael Devlin[1], Nicolas Cabezudo Garcia, Ebenezer Ojo, Daniel Markl[1], and John Robertson[1]

hikaru.jolliffe@strath.ac.uk

1 CMAC, University of Strathclyde, Glasgow.

## 1. Medicines Manufacturing Innovation Centre

- Part of the Advanced Manufacturing Innovation District Scotland (AMIDS)
- MMIC project led by Centre for Process Industry (CPI), University of Strathclyde, AstraZeneca, GSK, UKRI, Scottish Enterprise, and the Scottish Government; other partners also (Pfizer, Gericke, DFE Pharma).
- *"…an international beacon for innovation in small molecule medicines manufacturing"*


## 2. Example CDC flowsheet

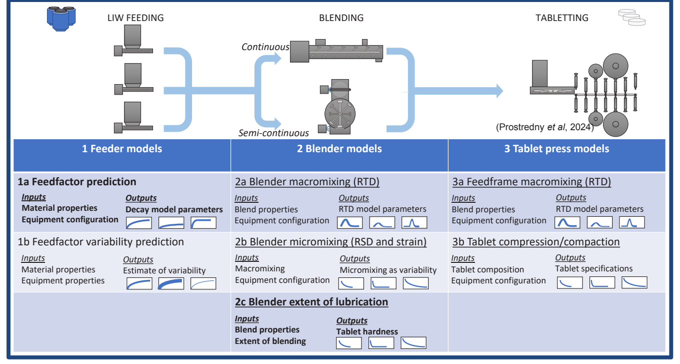


## 3a. Loss-in-Weight (LIW) feeder modelling

- LIW screw feeders: hopper above screws. As screws turn, material is dispensed.
- Can be measured in mass per revolution, the *feed factor* (g/rev).
- Feed factor can decay as hopper empties. Exact performance depends on material and equipment choice.
- Later, sharper decay (high $\beta$) or sooner, gradual decay (low $\beta$).
- Feed factor can also be lower or higher overall ($ff_{max}$).

$$ff = ff_{max} - ff_{max}e^{-\beta v}$$

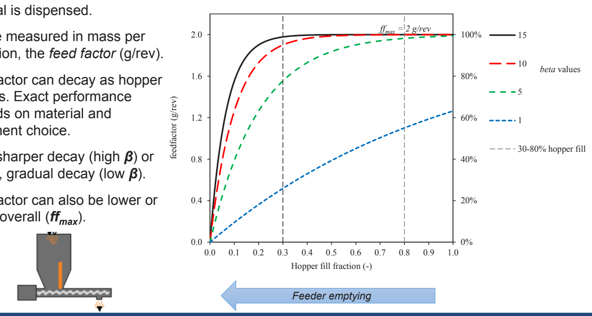


## 3b. Machine Learning for parameter prediction

- Use Machine Learning to predict LIW feeder process performance (model equation parameters) using material properties and equipment choice as inputs.

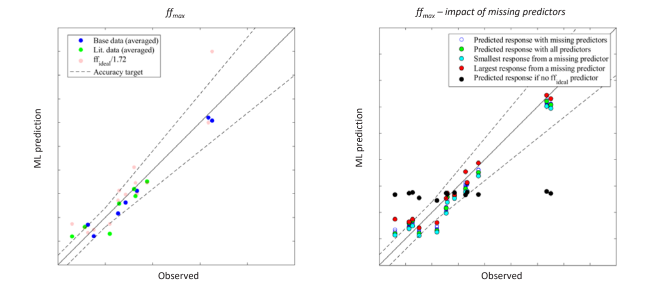


## 4a. Impact of batch blending on powders

- Low-shear Low-RPM $0 < Fr < 0.4$
- High-shear High-RPM $0 < Fr < ?$

$$Fr = \frac{\omega^2 r}{g}$$

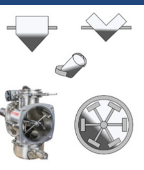

- Rate constant $\gamma$ should be formulation-dependent, and the same for all conditions (one curve)

$$\sigma_{SF=0.85} = \sigma_{SF=0.85,min} + (\sigma_{SF=0.85,max} - \sigma_{SF=0.85,min})e^{-\gamma V^{1/3}HR}$$

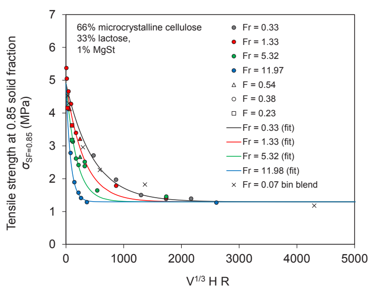


(Gericke AG, n.d.; Kushner & Moore, 2010; Kushner, 2012; Kushner & Schlack, 2014)

## 4b. Transferable equation: include a $Fr^{1/2}$ term

$$\sigma_{SF=0.85} = \sigma_{SF=0.85,min} + (\sigma_{SF=0.85,max} - \sigma_{SF=0.85,min})e^{-\gamma K} \quad K = V^{1/3}HRFr^n, \begin{cases} n = 0 & Fr < 1 \\ n = 2 & Fr > 1 \end{cases}$$

- Approach also works for CQA of tensile strength, content uniformity (API RSD), and other formulations.

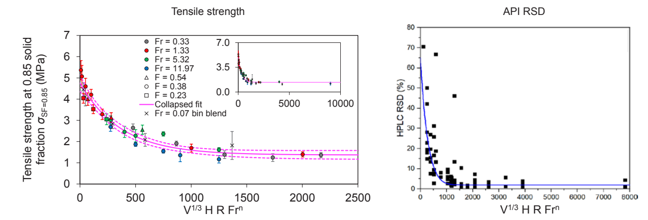


(Jolliffe et al., 2024a; Prostredny et al., 2024)

## 5. Continuous blender mass holdup

- Unexpected mass-holdup behaviour depending on equipment configuration.
- Hypothesis – some material forms inclined powder surface; when surface matches outlet angle, mass holdup is increased.

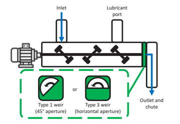


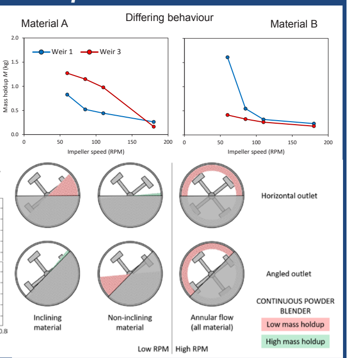


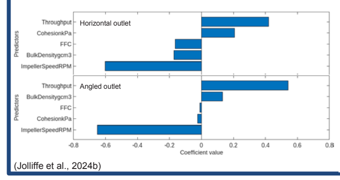


(Jolliffe et al., 2024b)

## 6. Summary & key publications

*Int. J. Pharm.*

*Pow. Tech.*

- **The Medicines Manufacturing Innovation Centre:** cutting-edge R&D centre for pharmaceutical manufacturing.
- **University of Strathclyde:** strategic partner, providing experimental expertise and leading research in experimental model development for secondary processing unit operations.
- **Digital tools:** employed to increase efficiency and research productivity.

## 7. References & Acknowledgements

- **Jolliffe et al.**, 2024a. *Int. J. Pharm.*, 659, 124232
- **Jolliffe et al.**, 2024b. *Powder Technology*, 449, 120440
- Kushner and Moore, 2010. *Int J. Pharm.*, 399, 19–30.
- Kushner, 2012. *Int J. Pharm.*, 429, 1–11.
- Kushner and Schlack, 2014. *Int. J. Pharm*, 475, 147–155.
- **Prostredny et al.**, 2024. *Powder Technology*, 448, 120224
- Gericke AG.

Many thanks to:

**Richard Elkes** (GSK), **Gavin Reynolds** (AstraZeneca), **Hugh Verrier** (Pfizer), **Yunfei Li Song** (GSK), **Martin Luis de Juan** (AstraZeneca), **Bernhard Meir** (Gericke), **Sara Fathollahi** (DFE Pharma), **Anders Sparén** (AstraZeneca), **Leonard Schmidt** (AstraZeneca), **Bastiaan Dickhoff** (DFE Pharma), **John Mack** (Applied Materials), **Gurjit Bajwa** (GSK), **Deborah McElhone** (CPI).

POSTER 11

## TBC

Deepak Kakde - CMAC,
University of Strathclyde

This poster will be available at the conference

POSTER 12

## An Intelligent Decision System for the Efficient Prediction of Thermodynamic and Thermal properties with a Successive Improvement Framework

Murray Knight – CMAC,
University of Strathclyde

This poster will be available at the conference

POSTER 13

# Hydrodynamic Challenges in Crystallisation: Leveraging CFD for Precision Reactor Optimisation

*Mitchelle Mandaza*[1,2 *], *Cameron Brown*[1,2] *and Jan Sefcik*[3]
[1]Strathclyde Institute of Pharmacy & Biomedical Sciences, University of Strathclyde
[2] EPSRC Future Manufacturing Hub for Continuous Manufacturing and Advanced Crystallisation, Technology and Innovation Centre, University of Strathclyde, UK
[3] Department of Chemical and Process Engineering, University of Strathclyde
* mitchelle.mnemo@strath.ac.uk

Scan me!

## INTRODUCTION

- Hydrodynamic factors like turbulence, micro-mixing, and energy dissipation affect supersaturation control, crystal size distribution, and process efficiency in crystallization.
- Optimising these factors improves reactor selection, scalability, and overall crystallisation outcomes

## RESEARCH OBJECTIVES

- Compare hydrodynamic performance across three reactor systems: Crystalline, EasyMax, and OptiMax.
- Evaluate velocity distribution, turbulence and shear stress using CFD simulations.

## METHODS

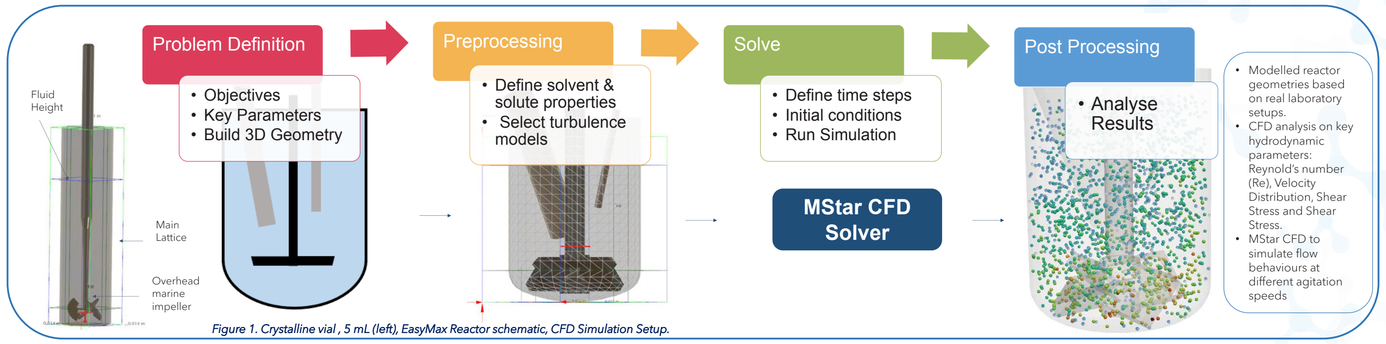


*Figure 1. Crystalline vial , 5 mL (left), EasyMax Reactor schematic, CFD Simulation Setup.*

## CFD RESULTS

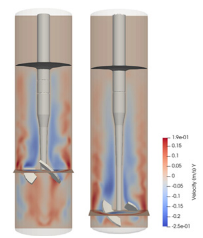

*Figure 2. Crystalline reactor vial with velocity contours at 400rpm. Operating at lower Re, resulting in weaker mixing and localized supersaturation gradients.*

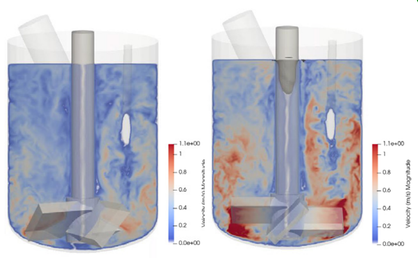

*Figure 3. 2D slices of EasyMax reactor with velocity magnitude profiles at 400 and 600rpm. More uniform velocity gradients with increase in agitation.*

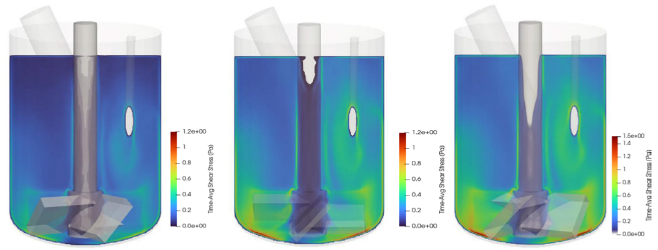


*Figure 4. 2D slices of EasyMax reactor with shear stress profiles at 400, 600 and 800 rpm.*

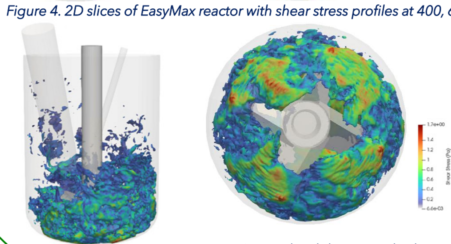


- Velocity fluctuations - highlight local
- turbulences and allow calculations for turbulent intensity.
- Turbulence intensity - observe if flow is turbulent or laminar and predict fluid flow properties
- EasyMax maintains higher levels of shear stress

*Figure 5. 3D CFD-predicted shear stress distribution in the EasyMax at 400rpm, highlighting uniform stress dispersion.*

## RESULTS

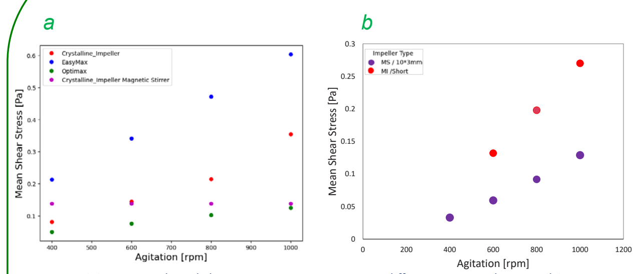


*Figure 6. (a) CFD-predicted shear stress variations across different reactor designs. (b) Experimentally estimated shear stress in the Crystalline reactor, providing comparison with simulation results.*

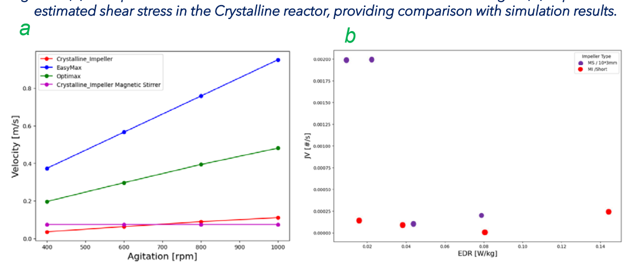


*Figure 7. (a) CFD-predicted velocity profiles. The average velocity changes with increasing agitation for each reactor. (b) Correlation between eddy dissipation rate (EDR) and nucleation rate (JV) highlights the impact of mixing intensity on crystallisation kinetics.*

- While shear rate is used for validation, energy dissipation rate (EDR) may provide deeper insight into nucleation kinetics and reactor performance. EDR directly represents turbulence intensity and micromixing, which are critical for supersaturation distribution and nucleation kinetics.

## Future work

- Validate CFD models with experimental data across diverse operating conditions.
- Develop industry-standard reactor design guidelines for better scalability and process control.

## Conclusions

- CFD analysis provides insight into how reactor design influences hydrodynamic performance.
- EasyMax exhibits the best uniformity, minimising turbulence-driven inconsistencies.

REFERENCES
1. Čelan, A., Ćosić, M., Penga, Ž., & Kuzmanić, N. (2024). Experimental and CFD Analysis of Hydrodynamics in Dual-Impeller Crystallizer at Different Off-Bottom Clearances. Processes, 12(10), 2183
2. Pohar, Andrej & Erklavec Zajec, Vivian. (2020). "A Review of Computational Fluid Dynamics (CFD) Simulations of Mixing in the Pharmaceutical Industry". Biomedical Journal of Scientific & Technical Research. 27. 10

ACKNOWLEDGEMENTS
EPSRC Future Manufacturing Hub for Continuous Manufacturing and Advanced Crystallisation, Technology and Innovation Centre, Neda Nazemifard (Takeda), National Manufacturing Institute Scotland (NMIS) and Scottish Research Partnership in Engineering (SRPe) and the University of Strathclyde.

NMIS National Manufacturing Institute Scotland | SRPe | Takeda | University of Strathclyde Glasgow

POSTER 15

# Discovery of a new high-pressure phase of Posaconazole

Banaz Fetah,[1] Daniel Markl,[1,2] Cheryl Doherty,[3] Iain D. H. Oswald,[1]
1. Strathclyde Institute of Pharmacy & Biomedical Sciences, University of Strathclyde, Glasgow, UK
2. EPSRC Future Manufacturing Research Hub for Continuous Manufacturing and Advanced Crystallisation (CMAC), University of Strathclyde, Technology and Innovation Centre, UK
3. GlaxoSmithKline, Stevenage, UK

## Aim of the project

To investigate the effect of pressure on Posaconazole through the use of X-ray diffraction to enable us to elucidate the changes to the structure as a function of applied pressure.

## INTRODUCTION

During the tablet manufacturing process in the pharmaceutical industry, crystalline materials are subjected to various external forces, most notably pressure during the compression stage.[1] Hence, it is important to investigate the effects of pressure on pharmaceutical materials to identify any phase transitions that may occur or understand how elastic or plastic the materials can be.[2] By investigation of materials under high pressure, it allows us to gain valuable insights for pharmaceutical researchers to develop more effective and stable drug formulations.

Posaconazole (POSA) is an antifungal compound used to treat infections in immunocompromised individuals. There are fourteen different polymorphs found, of which only 2 have their crystal structures reported but much less is understood about their properties.[3] Of the two structurally characterised forms, the thermodynamically stable form of POSA (Form I) crystallises in the monoclinic space group $P2_1$ with Z = 2 whilst Form II crystallises from the melt in the same space group $P2_1$ with Z =6. Form I is primarily used to produce oral suspensions.[4]

## METHODS

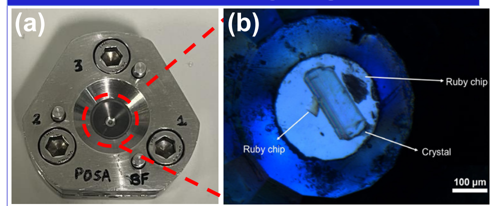


**Figure 1. (a) Conventional diamond anvil cell (DAC). (b) Single crystal of POSA with ruby chips loaded in DAC.**

The diamond anvil cell (DAC) is a method not widely employed across the board in studies. However, the DAC offers significant advantages such as its ability to reach pressures of up to 10 Gigapascal (10000 Megapascal) to identify new high-pressure phases.

The DAC is essentially composed of 2 opposing diamonds, a tungsten gasket and a sample chamber. Since diamonds are electromagnetically transparent, various spectroscopic and diffraction techniques (e.g., single-crystal X-ray diffraction) can be used.

Within the sample chamber ruby is added to measure the pressure inside the cell. Pressure transmitting medium (PTM), such as petroleum ether or silicone oil is added to create a hydrostatic environment which enables single crystal data to be collected.

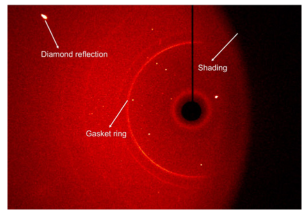


**Figure 2. Single crystal X-ray diffraction image.**

What are some of the limitations we face?
- Shading from the steel body limit the amount of data that we can access.
- Diamond reflections and gasket rings can increase background noise.

## RESULTS

On compression, we observed that Form I undergoes a phase transition between 0.17-0.25 GPa due to a sudden change in the unit cell parameters (Table 1). Our results show that POSA transforms to a new high-pressure polymorph where there is a tripling of one of the axes and a reduction in symmetry to P1. The number of formula units changes from Z=2 to Z=6 induced by a change in the conformation of the molecule; this form is different to Form II.

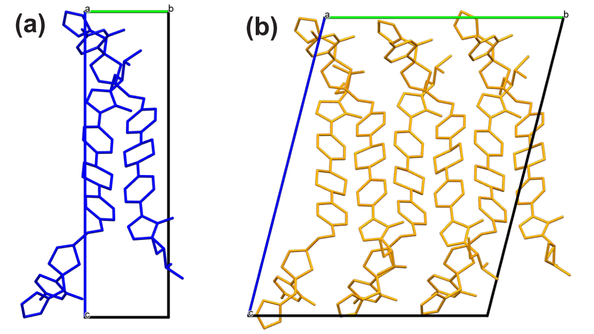


**Figure 3. (a) Ambient form ($P2_1$) with Z=2 in blue. (b) New high-pressure form (P1) with Z=6 in orange.**

**Table 1. Unit cell parameters of Form I and new high-pressure form.**

| Pressure (GPa) | *a* -axis | *b* -axis | *c* -axis | al(°) | be(°) | ga(°) | Volume |
|---|---|---|---|---|---|---|---|
| 0 | 12.5262 | 6.3499 | 22.7875 | 90 | 96.348 | 90 | 1801.41 |
| 0.25 | 11.9304 | 18.5528 | 23.9016 | 104.486 | 93.797 | 91.092 | 5107.5 |

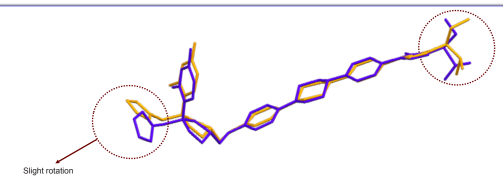


**Figure 4. Structural overlay of Form I (blue) and high-pressure form (orange).**

The overall structures are largely similar but a rotation in the end groups of the molecule can be observed, particularly the triazole ring (Figure 4). This change is significant enough to cause a change in symmetry and move to a more complex description of the structure bringing the amorphous form one step closer.

Previous investigation of POSA tablets by Huang *et al.* observed that Form I amorphized under compaction conditions at 0.4 GPa indicating a compression-induced phase transition.[5]

In this study, the crystal started deteriorating at 0.33 GPa, as shown by the striations (Figure 5) which made it difficult to collect good diffraction data beyond this point. Strain within the large crystal can result in a more disordered state and the overall structure can move closer to the characteristics of an amorphous state.

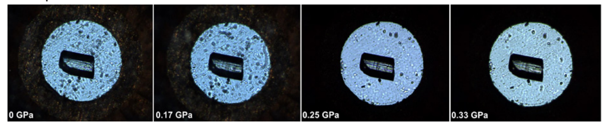


**Figure 5. Microscopic images showing incremental increases in pressure applied to single crystals of POSA in DAC.**

## CONCLUSION

This study demonstrates a pressure-induced phase transition of POSA at 0.25 GPa .There is a tripling of the *b*-axis and a reduction in symmetry in P1.
Structural overlay of the ambient form (Form I) and high-pressure form show that the structures are mostly similar with rotations in the end groups.

## FUTURE WORK

Explore the use of powder instead of a single crystal in the diamond anvil cell (DAC) to determine if comparable changes are observed.

## ACKNOWLEDGEMENT

This work is funded by through the Engineering and Physical Sciences Research Council (EPSRC) and GlaxoSmithKline.

## REFERENCES

1. Rogers, A., Hashemi, A. & Ierapetritou, M. Modeling of Particulate Processes for the Continuous Manufacture of Solid-Based Pharmaceutical Dosage Forms. *Processes* **1**, 67–127 (2013).
2. Park, H., Nie, H., Dhiman, A., Tomar, V. & Zhou, Q. T. Understanding Dynamics of Polymorphic Conversion during the Tableting Process Using *In Situ* Mechanical Raman Spectroscopy. *Mol. Pharmaceutics* **17**, 3043–3052 (2020).
3. Guidetti, M., Hilfiker, R., Kuentz, M., Bauer-Brandl, A. & Blatter, F. Water-mediated phase transformations of posaconazole: An intricate jungle of crystal forms. *European Journal of Pharmaceutical Sciences* **195**, 106722 (2024).
4. Lykouras, M., Orkoula, M. & Kontoyannis, C. Formation and Characterisation of Posaconazole Hydrate Form. *Pharmaceuticals* **16**, 65 (2022).
5. Huang, C. *et al.* Understanding Compression-Induced Amorphization of Crystalline Posaconazole. *Mol. Pharmaceutics* **16**, 825–833 (2019).

GSK GlaxoSmithKline | University of Strathclyde Glasgow | EPSRC Engineering and Physical Sciences Research Council | UKRI Engineering and Physical Sciences Research Council

POSTER 16

# Advanced mass transfer models to predict liquid-liquid phase separation

Irene Moreno[1, 2*], David McKechnie[1], Leo Lue[1] and Javier Cardona[1, 2, 3]

[1] Department of Chemical and Process Engineering, University of Strathclyde, Glasgow, UK.
[2] EPSRC Future Manufacturing Research Hub for Continuous Manufacturing and Advanced Crystallization (CMAC), Glasgow, UK.
[3] Department of Electronic and Electrical Engineering, University of Strathclyde, Glasgow, UK.

irene.moreno@strath.ac.uk

## The models, *chico*, they never lie

*...or do they?*

## 1. Background and motivation

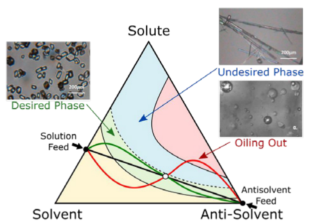


**Figure 1.** Ternary phase diagram illustrating that the mixing path dictates the outputs.

Poor understanding of **mixing** in antisolvent crystallization

LEADS TO... Oiling out, unexpected polymorphs, uncontrolled nucleation and growth

SOLUTION: Development of better-suited **mass transfer models**

Lack of adequate **experimental data** to inform them

## 2. CHAC-KKS phase-field model

$$\partial c/\partial t = \nabla(M/f_{,cc}\cdot\nabla\mu_c);\ \mu_c = f_{\alpha,c}(1-H) + f_{\beta,c}H$$

$$\partial\eta/\partial t = -L\mu_\eta;\ \mu_\eta = \left[f_\beta - f_\alpha - (c_\beta - c_\alpha)f_{\beta,c_\beta}\right]H + Wf_{Land} - \kappa\eta$$

- Penalty coefficient for the α-β interface
- Barrier height for η double well

- c is composition, η is the phase variable
- **Double-well** potential for **η**
- Probability of **nucleation** depends on **local supersaturation** (S) [1, 2]

$$\sigma = \frac{1}{3}\sqrt{\frac{\kappa W}{2}}$$ Interfacial free energy

$$2\lambda = \sqrt{2\kappa/W}$$ Interfacial thickness

### Model results: phase fields and DF comparison

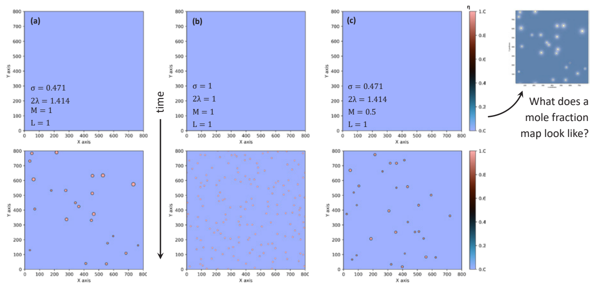


**Figure 2.** Effect of the interfacial free energy and thickness, and CH mobility. **(a, b)** A lower interfacial thickness leads to a thinner transition zone, and higher interfacial free energy leads to slower growth, and more nucleation. The latter is governed by the KKS model, in which the probability of nucleation depends only on S. Less growth means higher S at a given time, and thus more nuclei. **(c)** CH mobility is related to the diffusion coefficient, with a lower value resulting in slower mass transfer and thus slower particle growth.

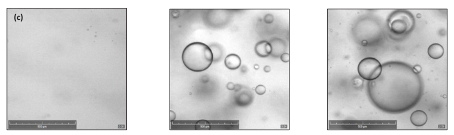

**Figure 3:** DataFactory images of liquid-liquid phase separation in a salicylic acid – heptane system. Qualitatively, it is easy to see how the CHAC-KKS model would be able to reproduce these results – with the added benefit of being able to map the composition inside the new liquid phase.

**Acknowledgements:** CMAC (https://cmac.ac.uk/), the University of Strathclyde, and Thomas Pickles for gathering the Datafactory images of Figure 3. **References:** QR on top.

## 3. CaHiMaS combined diffusion model

### Equation and model behaviour

$$\frac{\partial x_A}{\partial t} + \nabla(\mathbf{v}x_A) = \nabla[D_{AB}\cdot\nabla x_A] + \nabla[D_{AB}x_A\cdot\nabla[A(1-x_A)^2 - \varepsilon^2\nabla^2 x_A]]$$

- **Chemical potential gradient** + Maxwell-Stefan
- **Margules activity model**
- Interface free energy ($\varepsilon^2\nabla^2 x_A$)

Margules parameter · Interface free E coef.

Incorporating an activity model allows to make phase separation theoretically possible; by adding the interfacial free energy term, it is possible to model this behaviour accurately, as shown below.

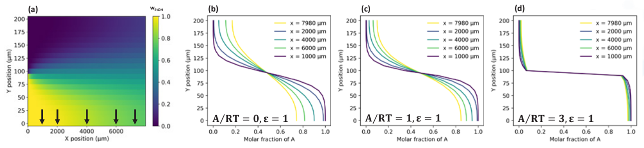


**Figure 4(a):** example of steady state mixing map gathered with Fick's law; **(b-d):** composition profiles at the marked mixing map points for Fick (b) and CaHiMaS (c, d). All of them gathered with $D = 1600\ \mu m^2/s$.

### How has this model been validated?

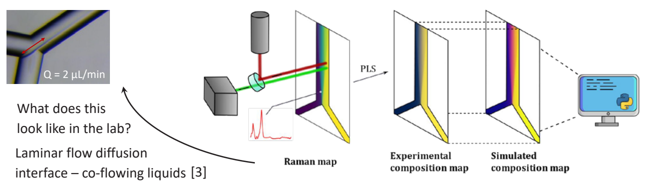


### Experimental and optimization results

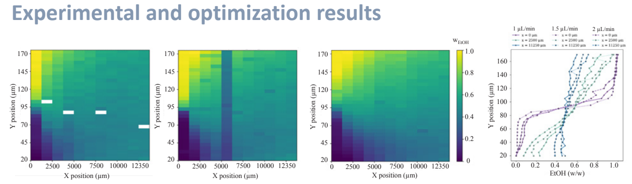

**Figure 5.** Flowrate effect on map collection: EtOH-$H_2O$ composition (w/w) maps obtained at 2, 3 and 4 µL/min (left to right, respectively), and their composition profiles at x = 0, 2500 and 11250 µm.

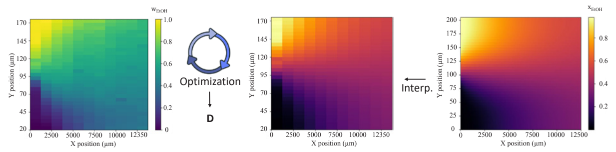


**Figure 6.** Example of the maps generated during the optimization, for the case of 100-000 at 4 µL/min. **Left:** experimental map. **Right:** simulated map obtained with the final D guess. **Middle:** interpolated simulated map.

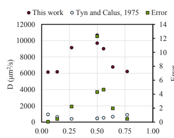

So... where is this error coming from?

Misalignment between optical and Raman + the channel shape led to **inaccuracy in the Y positions**

Air entering at the connections can lead to **flow inaccuracies**

AstraZeneca · Chiesi · Lilly · Pfizer · Roche · sanofi · Takeda · ucb

POSTER 17

# Benchmarking the Predictive Capabilities of the SAFT-γ Mie EoS for Properties of Interest in Pharmaceutical Systems

Saman Naseri Boroujeni, Gaurav Seth, George Jackson, Amparo Galindo, Claire Adjiman

Department of Chemical Engineering, Sargent Centre for Process Systems Engineering, Institute for Molecular Science and Engineering, Imperial College London, South Kensington Campus, London SW7 2AZ, United Kingdom

## I. Introduction

**Why?** The significance of thermodynamic modelling in computer-aided molecular and process design within pharmaceutical process engineering.

Active pharmaceutical ingredients (APIs), featuring multiple functional groups, serve as an ideal benchmark for evaluating the accuracy and reliability of the SAFT-γ Mie equation of state.

**What?**

- **8** Active Pharmaceutical Ingredients
- **7** Amino Acids
- **24** Organic Solvents

**How?**

- Solubility of APIs in Pure Organic Solvents
- Solubility of APIs in Mixed Solvents
- Solubility of AAs in Pure Organic Solvents
- Solid-Liquid-Liquid Equilibrium of API + Pure Solvents
- Solid-Liquid-Liquid Equilibrium of API + Mixed Solvents
- Eutectic Mixtures
- Octanol-Water Partition Coefficients

## II. Methods

$$\frac{A}{Nk_BT} = \frac{A^{ideal}}{Nk_BT} + \frac{A^{mono.}}{Nk_BT} + \frac{A^{chain}}{Nk_BT} + \frac{A^{assoc.}}{Nk_BT}$$

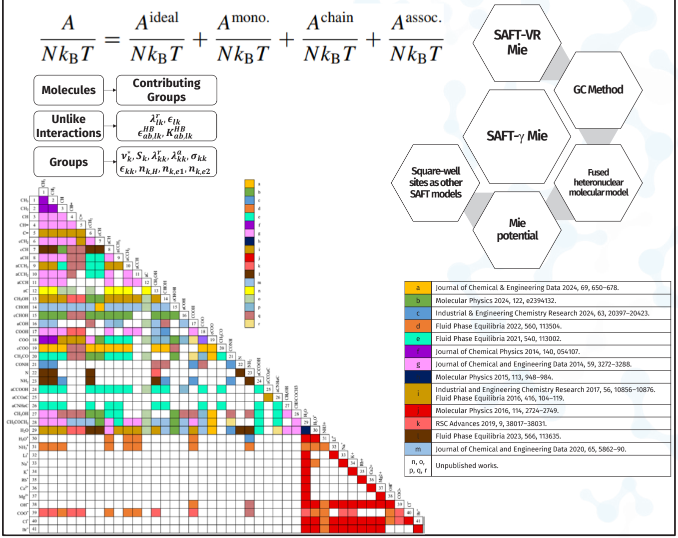


## III. Results & Discussion

### IIIa. Active Pharmaceutical Ingredients

Aspirin · Benzoic Acid · Paracetamol · Lidocaine · Ketoprofen · Mefenamic Acid · Ibuprofen · Lovastatin

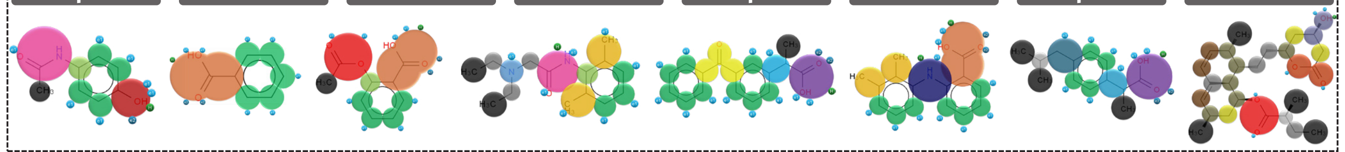

### IIIb. Solubility in Pure Solvents

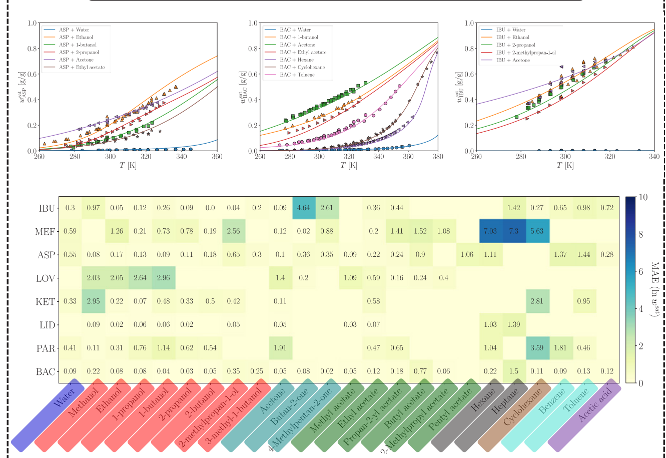

### IIIc. SLE & SLLE Phase Diagrams

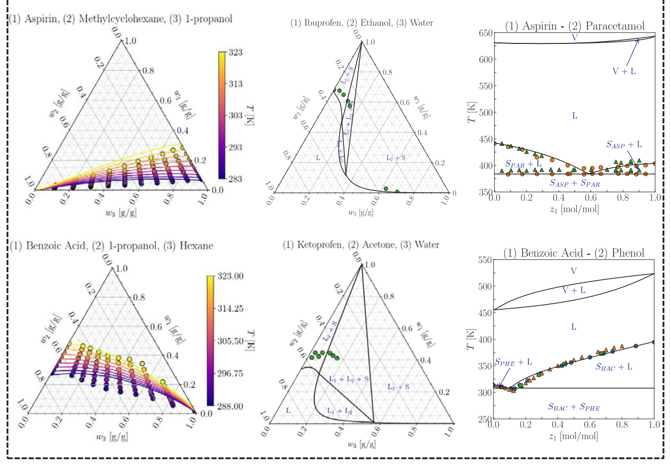


## IV. Conclusions

MAE of the $w_{API}^{sat}$ for all APIs: 0.052 [g/g], MAE of the $\log_{10} w_{API}^{sat}$ for all APIs: 0.094 [-]

| | Aspirin | Benzoic Acid | Paracetamol | Lidocaine | Ketoprofen | Mefenamic Acid | Ibuprofen | Lovastatin |
|---|---|---|---|---|---|---|---|---|
| MAE of the $w_{API}^{sat}$ | 0.023 | 0.019 | 0.067 | 0.083 | 0.121 | 0.024 | 0.082 | 0.071 |
| MAE of the $\log_{10} w_{API}^{sat}$ | 0.284 | 0.132 | 0.652 | 0.162 | 0.890 | 1.531 | 0.457 | 0.284 |

**Take Home Message:**

SAFT-γ Mie EoS can be employed confidently regarding its accuracy and reliability in predicting thermodynamic properties of APIs.

LinkedIn · Molecular Systems Engineering · Sargent Centre for Process Systems Engineering · UKRI Engineering and Physical Sciences Research Council · IMPERIAL · University of Strathclyde Glasgow

POSTER 18

# Data-Driven Virtual Knowledge Graph for Pharma

**Tabbasum Naz**, Blair Johnston

tabbasum.naz@strath.ac.uk, blair.johnston@strath.ac.uk

Continuous Manufacturing and Advanced Crystallisation (CMAC), Strathclyde Institute of Pharmacy & Biomedical Sciences, University of Strathclyde, Technology and Innovation Centre, 99 George Street, Glasgow G1 1RD, UK.

## 1- Abstract

Currently, medicine manufacturing data is difficult to access and query as it is in a) unstructured format, ii) scattered at multiple locations in variety of formats iii) without meta-data and stored in files. To solve these problems, we have proposed a Digital Medicine Manufacturing - Extract-Transform-Load (DM² ETL) tool to derive maximum value from the data acquisition effort to date and to allow future data to be integrated easily. DM² ETL, with multiple components, is responsible for extraction, transformation and loading of heterogeneous medicine manufacturing data related to multiple instruments. Schema for experimental data in the medicine manufacturing domain has been designed that provides a structure for data and establishes linkage to meta-data. For central repository in structured format, we have used MS-SQL server.

Once data is structured in MS-SQL, server, we have performed semantic integration of medicine manufacturing data using virtual knowledge graph. Medicine manufacturing data virtualisation is performed through integration of ontotext ontop platform. To achieve this task, we have developed Ontology Based Data Access (OBDA) mappings defined from DM² database. OBDA file descriptors are developed to map relational schema to graphs. This helps us to access the medicine manufacturing data via SPARQL endpoint. This allows medicine manufacturing experts to access and query the overall data assets in an integrated way, by exploiting the semantics of the extracted information. As data is in interoperable format so its easy to connect it to other existing ontologies in the domain.

## 2- MS-SQL Database Overview

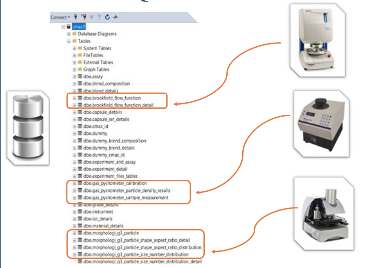

## 3- Virtual Knowledge Graph Approach for Medicine Manufacturing Data

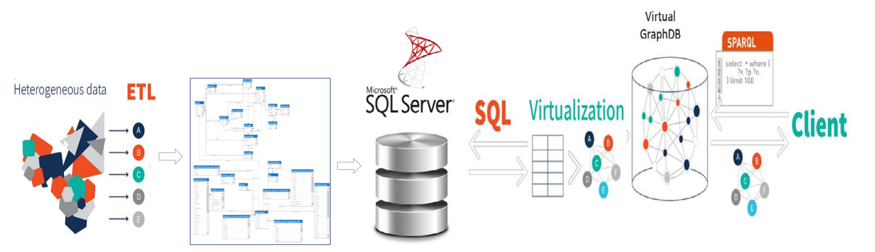


## 4- Methodology

- ✓ Database schema for multiple instruments has been designed including
  - ✓ Morphologi G3
  - ✓ Gas pycnometer
  - ✓ Autotap
- ✓ Meta-data schema has also been designed
- ✓ Linkage of instrument's data with meta-data
- ✓ DM² ETL has been designed fto load instrument's data
- ✓ Data Virtualisation with GraphDB via ontotext ontop open-source platform

## 5- Search Data Using SPARQL

- ✓ Medicine manufacturing data can be searched via SPARQL
- ✓ SPARQL query to search "experiment details"

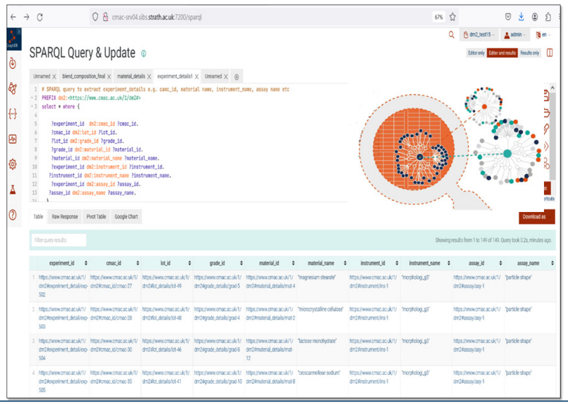

## 6- Navigation of Virtual Knowledge Graph

Navigation of "blend/mixture composition" using SPARQL query

- ✓ blend_1 and blend_10

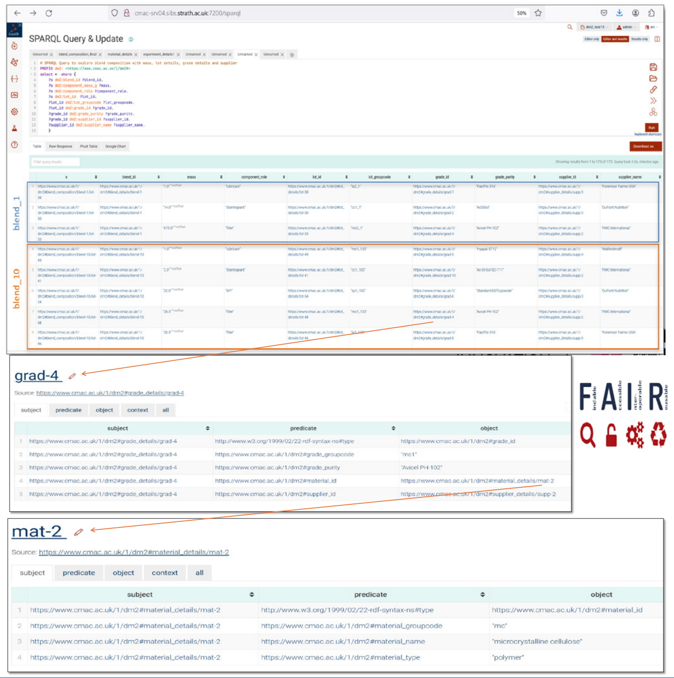


## 7- DM² - Data Visualisation from Knowledge Graph

- ➢ Data visualisation of "particle shape - aspect ratio" of different materials from Morphologi-G3 via knowledge graph.

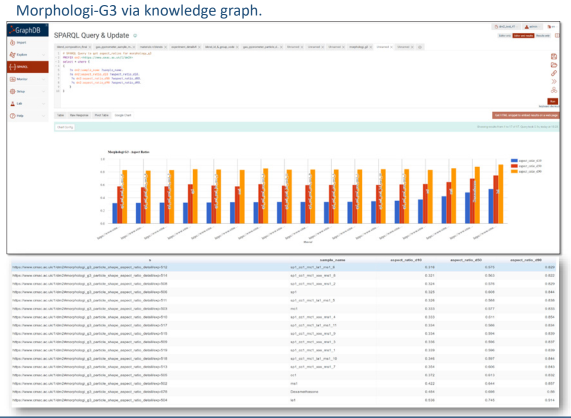

## 8- Conclusion

- ✓ Medicine manufacturing data integration and access based on virtual knowledge graphs (VKG)
- ✓ Towards FAIR data
- ✓ Medicine manufacturing data available in relational database and virtual knowledge graph
- ✓ Fully structured data that can be linked with other resources
- ✓ Data is also available in MS-SQL server that can easily be linked with Tableau visualisation software and provides interactive data visualization

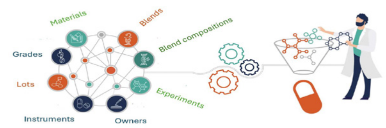


UK Research and Innovation

MADE SMARTER INNOVATION

DM² Digital Medicines Manufacturing

**Acknowledgment:** The authors would like to thank the Digital Medicines Manufacturing (DM²) Research Centre (Grant Ref: EP/V062077/1) for funding this work. DM² is co-funded by the Made Smarter Innovation challenge at UK Research and Innovation, and partner organisations from the medicines manufacturing sector. For more information, visit cmac.ac.uk/dm2-home

POSTER 19

# Improved Extraction of Biomedical Relations from Text

Abiola Obamuyide and Blair Johnston

CMAC, University of Strathclyde, Glasgow

{first}.{last}@strath.ac.uk

## Background

- The task is that of identifying entities (e.g. drugs, proteins, genes, diseases) and identifying relationships between them from e.g. scientific literature, clinical trial reports, etc.
- Useful for constructing pharmaceutical knowledge graphs, medicine repurposing/re-use, adverse medicine reaction detection, discovery of new medicines etc.

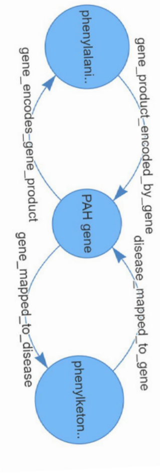


**Figure 1: Knowledge Graph extracted from the following text:** "Aberrant splicing of phenylalanine hydroxylase mRNA: the major cause for phenylketonuria in parts of southern Europe. We report a mutation within the phenylalanine hydroxylase (PAH) gene that causes aberrant splicing of the mRNA and that is in tight association with chromosomal haplotypes 6, 10, and 36. Because of the high frequency of these particular haplotypes in Bulgaria, Italy, and Turkey, it appears to be one of the more frequent defects in the PAH gene causing classical phenylketonuria in this part of Europe. The mutation is a G to A transition at position 546 in intron 10 of the PAH gene, 11 bp upstream from the intron 10/exon 11 boundary. It activates a cryptic splice site and results in an in-frame insertion of 9 nucleotides between exon 10 and exon 11 of the processed mRNA. Normal amounts of liver PAH protein are present in homozygous patients, but no catalytic activity can be detected. This loss of enzyme activity is probably caused by conformational changes resulting from the insertion of three additional amino acids (Gly-Leu-Gln) between the normal sequences encoded by exon 10 and exon 11"

## Data

- Existing datasets have limitations, e.g. assume a classification setting, are noisy, do not have annotations for end-to-end RE, etc.
- We introduce a new dataset suitable for end-to-end generative biomedical RE obtained from UMLS and Wikipedia.

UK Research and Innovation

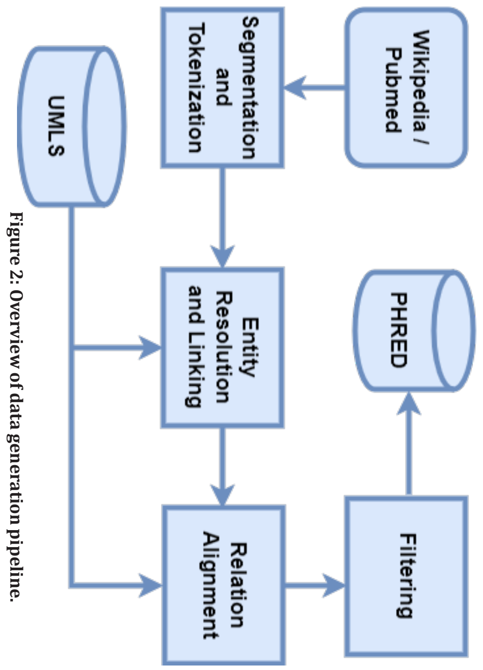


**Figure 2: Overview of data generation pipeline.**

## Experimental Details

- Each instance in dataset consists of text (e.g. a sentence) together with all relation triples expressed in the text.
- Dataset has a total of about 107k instances which we split into 106k/500/500 train/val/test split. Baseline models include *BART*, *GENIE*², and *BIOGPT*³.
- Our proposed approach combines elements from previous methods for true end-to-end generative pharmaceutical relation extraction.

MADE SMARTER INNOVATION

DM² Digital Medicines Manufacturing

## Results

| MODEL | Precision | Recall | F1 |
|---|---|---|---|
| BART | 23.16 | 14.95 | 18.17 |
| GENIE | 34.10 | 42.57 | 37.86 |
| BIOGPT | 39.02 | 41.10 | 40.04 |
| OURS | **45.42** | **46.18** | **45.79** |

**Table 1: Results showing performance of our approach compared to other methods from the literature.**

## References

1. Lewis, M., Liu, Y., Goyal, N., Ghazvininejad, M., Mohamed, A., Levy, O., Stoyanov, V., & Zettlemoyer, L. (2020). *BART: Denoising Sequence-to-Sequence Pre-training for Natural Language Generation, Translation, and Comprehension.*
2. Josifoski, M., De Cao, N., Peyrard, M., Petroni, F., & West, R. (2022). GenIE: Generative Information Extraction. *NAACL 2022 - 2022 Conference of the North American Chapter of the Association for Computational Linguistics: Human Language Technologies, Proceedings of the Conference.*
3. Luo, R., Sun, L., Xia, Y., Qin, T., Zhang, S., Poon, H., & Liu, T.-Y. (2022). BioGPT: generative pre-trained transformer for biomedical text generation and mining. *Briefings in Bioinformatics.*
4. Cabot, P. L. H., & Navigli, R. (2021). REBEL: Relation Extraction by End-to-end Language generation. *Findings of the Association for Computational Linguistics, Findings of ACL: EMNLP 2021.*
5. Elsahar, H., Vougiouklis, P., Remaci, A., Gravier, C., Hare, J., Simperl, E., & Laforest, F. (2019). T-Rex: A large scale alignment of natural language with knowledge base triples. *LREC 2018 - 11th International Conference on Language Resources and Evaluation*, 3448–3452.

**Acknowledgment:** The authors would like to thank the Digital Medicines Manufacturing (DM²) Research Centre (Grant Ref: EP/V062077/1) for funding this work. DM² is co-funded by the Made Smarter Innovation challenge at UK Research and Innovation, and partner organisations from the medicines manufacturing sector. For more information, visit cmac.ac.uk/dm2-home

**DM² website**

POSTER 20

# Physics Informed Neural Networks For Fluid Dynamics In Channels

Thomas Ralph, Cameron Brown, Alastair Florence.
University of Strathclyde, Glasgow.
thomas.ralph@strath.ac.uk

## 1. Background

Computational fluid dynamics (CFD) is the current best approach to simulating virus deactivation, however these simulations are often very computationally expensive, and can also take months to finish execution. This creates a computational bottleneck within the equipment design phase for the discovery of new medicines.

The aim of this project is to adequately predict the outputs of virus inactivation simulations using artificial intelligence (AI), machine learning, neural networks, and so on. These predictions need to be faster than CFD and still reliably accurate.

Neural networks are capable of predicting fluid velocity within desired geometries and may possess the ability in the future to bypass the need to rely on CFD for, not just fluid, but for all kinds of Multiphysics simulations.

## 2. Aims

- Aim 1: Create a physics informed neural network (PINN) with square-shaped obstacles using NVIDIA Modulus to use as a base model for transfer learning.
- Aim 2: Create multiple channels with varying parameter set ups / obstacle shapes and train new PINNs using transfer learning with the base model.
- Aim 3: Create fluid validation data for each of the models using COMSOL to compare with the PINN results.
- Aim 4: Analyze the error between the validation and prediction data of each of the variables of interest (x-velocity, y-velocity, and pressure), to gauge accuracy of each model.

## 3. Target Application

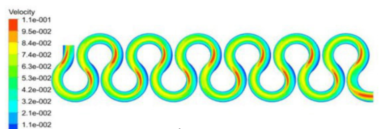


Figure 1

Figure 1 shows the axial velocity of fluid flow as it moves through a 2D serpentine channel from [1]. The change in velocity is in response to centrifugal forces. This simulation was produced using Fluent Ansys.

The velocity of the fluid can be used to generate a virus deactivation diagram. The PINNs in this poster is aimed at generating flow predictions similar to the CFD results shown in Figure 1.

## 4. Base Model Specifications

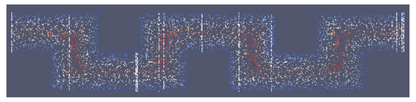

Figure 2

The base model in Figure 2 was trained using 5,000 interior points, 64 inlet and outlet points, 2,000 boundary points, 10 integral continuity lines, and 500,000 training steps.

The integral continuity lines are randomly placed throughout the chan nel to specify the average velocity at each vertical line.

The standard distance function is colored blue to red, indicating interior points closest and furthest from the channel boundaries.

## 5. Base Model For Transfer Learning

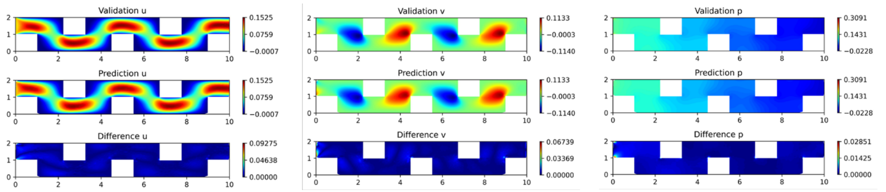


Figure 3

Figure 3 shows the validation, prediction, and difference data for u, v, and p. The difference/error for each variable is very close to zero. This model has been used as a base model to use for transfer learning of other PINNs with varying geometries. MAE for u, v, and p is 0.0028, 0.0016, and 0.0012 respectively.

## 6. Transfer Learning Fluid Flow PINN For Square Channel

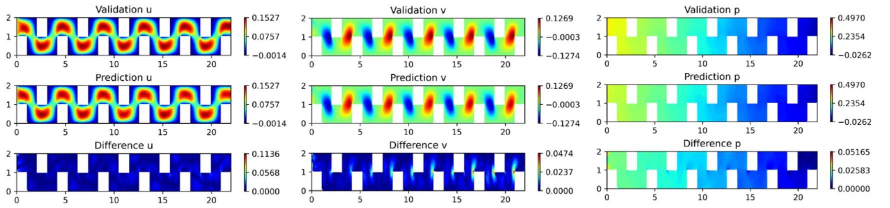


Figure 4

Figure 4 shows the validation, prediction, and difference data for u, v, and p. This model was trained using only 100,000 training steps and used the transfer learning model in Figure 2 to aid in its predictions. This model is a length and obstacle number expansion of the model in Figure 2. We can notice v error getting higher towards the outlet of the channel. The p difference is relatively close to zero but not as accurate as the p difference seen in Figure 2. MAE for u, v, and p is 0.0056, 0.0041, and 0.013 respectively.

## 7. Transfer Learning Fluid Flow PINN For Door-Knob Channel

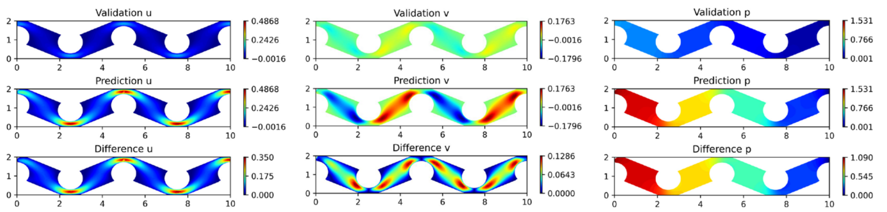


Figure 5

Figure 5 shows the validation, prediction, and difference data for u, v, and p. This model was trained using only 100,000 training steps and used the transfer learning model in Figure 2 to aid in its predictions. We can see high error magnitude in this model for u, v, and p. Particularly at the narrow passages within the channel. This was a common trend seen in other channels with narrow passages. MAE for u, v, and p is 0.041, 0.026, and 0.59 respectively.

## 8. Transfer Learning Fluid Flow PINN For Serpentine Channel

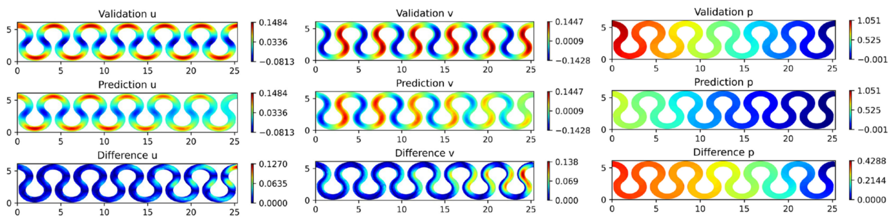


Figure 6

Figure 6 shows the validation, prediction, and difference data for u, v, and p. This model was trained using only 100,000 training steps and used the transfer learning model in Figure 2 to aid in its predictions. We can see higher error in u and v towards the channel outlet. For p, we see the opposite. This channel closely resembles the channel seen in Figure 1 except the inlet and outlet locations differ. MAE for u, v, and p is 0.012, 0.019, and 0.25 respectively.

## 9. Future Work (3D Coil Simulation)

Figure 7

Figure 7 shows a 3D CFI generated using COMSOL (CFD software). Exploring the possibilities of generating 3D fluid simulations using NVIDIA Modulus would be suitable for future work. The geometry would appear like the CFI in Figure 7.

Once such fluid predictions have been simulated in a 3D CFI, exploring the possibilities of applying virus inactivation kinetics to the velocity particles to generate a graph of virus inactivation in 3D would be an appropriate future step.

## 10. References

1) Design, Construction, and Optimization of a Novel, Modular, and Scalable Incubation Chamber for Continuous Viral Inactivation, October 2016

2) Modular Coiled Flow Inverter with Narrow Residence Time Distribution for Process Development and Production, February 15 2019

3 Design of a novel continuous flow reactor for low pH viral inactivation, 13 November 2017

4 Continuous Cooling Crystallization in a Coiled Flow Inverter Crystallizer Technology—Design, Characterization, and Hurdles, 29 August 2021

5 MINIATURIZED TUBULAR COOLING CRYSTALLIZER WITH SOLID-LIQUID FLOW FOR PROCESS DEVELOPMENT, June 10-13, 2018

POSTER 21

# A Prototype Crystallisation Knowledge Graph

Jason K. Robertson [1,2], Michael Chrubasik [3], Blair F. Johnston [1,2]

[1] Strathclyde Institute of Pharmacy and Biomedical Sciences, University of Strathclyde, Glasgow, UK
[2] Continuous Manufacturing and Advanced Crystallisation (CMAC) Future Manufacturing Hub, University of Strathclyde, Glasgow, UK
[3] National Physical Laboratory, Glasgow, UK

## Introduction

Although the literature has many examples of crystallisation processes and outcomes, these are difficult to search and analyse because there are not many papers containing detailed experimental methods with data in a structured, machine-readable format. The aim of this project is to create a crystallisation knowledge graph to describe crystallisation experiment process elements along with experimental methods and data.

**What will this give us?**

- Refined or even new approaches to crystallisation experiments, through knowledge graph-enabled machine learning analyses
- A structured dataset for training AI models to predict crystallisation outcomes.
- Enables generative AI models to assist in data interpretation and hypothesis generation.
- Allows researchers to easily query and retrieve crystallisation conditions, results, and trends
- Researchers can ask complex scientific questions in natural language
- Pharmaceutical and materials science industries can use the graph for process optimisation
- Helps in screening and designing crystallisation processes for better drug formulation and material synthesis.

## What are Ontologies and Knowledge Graphs?

An ontology describes how concepts within a domain are related to each other in a way which is computationally useful. For example, a crystallisation experiment could be described as (this is a fragment for brevity):

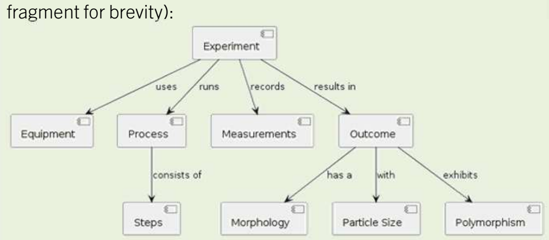


When data are added to the concepts, the ontology becomes a knowledge graph. A search might ask "Which EXPERIMENTS including a seeding STEP at a temperature MEASUREMENT over 60 deg. C resulting in a particular MORPHOLOGY?" The knowledge graph would answer this easily; the same query on flat data tables would be more difficult.

Since the knowledge graph contains data, and the relationships between those data, it is more computationally useful than data on its own. Knowledge graphs are therefore well-suited to storing data for machine learning applications.

## Populating the Knowledge Graph

Although there is a web-based user interface for inputting experimental data, it is anticipated that most data will be ingested via the Application Programmers' Interface (API).

The API will accept exported data by lab equipment, automatically entering it into the knowledge graph without the researcher's intervention.

Using this automated approach, the aim is to import data from existing sources (such as CMAC's Data Factory, which collects and Integrates large volumes of managed data from sources including laboratory experiments, production lines, and simulation models) to rapidly grow the available dataset.

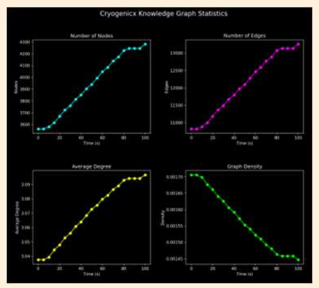


## Acknowledgements and Contact

We would like to acknowledge NPL (EPSRC ICASE), and University of Strathclyde (EPSRC DTP REA) for funding, and would like to thank Amal Osman for sample solubility data.

jason.robertson@strath.ac.uk, BlueSky: @cryogenicx.bsky.social

## Early Testing using Generative AI

Although knowledge graphs are powerful tools for representing related data, information is traditionally retrieved from them using the SPARQL query language. This has to be learned and is more difficult to work with than the database query language SQL.

Large Language Models, however, can write SPARQL based on plain English prompts and return analyses on the data within graph.

A Large Language Model (LLM) was provided with the graph file and prompted with some basic information about its structure:

"Here's a knowledge graph in RDF/XML format. The experiment data are held as data property assertions, and each experiment is made up of steps which share a common experiment UUID, which is also a data property assertion. Analyse the graph so that you can locate all the data."

Following this initial prompt the LLM was asked:

"List the solutes, solvents and concentrations from each experiment. Don't show the full experiment IRI, only show data after the # in the IRI."

It went on to examine the file, and after an initial mis-step which it dealt with itself, provided the required list (right, table trimmed for space reasons).

Extracted Experiment Data

| | Experiment UUID | Solutes | Solvents | Concentrations |
|---|---|---|---|---|
| 16 | ae859e70-b57f-49f7-9380-31e0fcc75ec3 | Salicylic_Acid | 2-propanol | 0.3902654516640253 |
| 17 | b386f173-6995-4fb6-a766-7ca35eafcb7a | Salicylic_Acid | Cyclohexane | http://www.w3.org/1999/02/22-rdf-syntax-ns#nil |
| 18 | 796622e1-8f64-455b-86ff-9c2a0ca50afa | Salicylic_Acid | Water | 0.0045000000000000005 |
| 19 | b8828634-b369-421e-8c81-3b708b54d9ef | Salicylic_Acid | Water | 0.0045000000000000005 |
| 20 | 6ea7b028-19c5-4fab-83e1-3aa7e18d4856 | Salicylic_Acid | Water | 0.017214228617106316 |

Clear Point Temperature Data

| | Experiment UUID | Clear Point Temperatu | Standard Deviation |
|---|---|---|---|
| 1 | ef34b53a-4985-4fd0-bab8-c0b09d79a6d0 | 58.2, 55.8, 54.7 | 1.7898 |
| 2 | 7a940d00-d842-48b1-9e8d-c4bcadc67e5b | 50.3, 51.6, 54.9 | 2.3714 |
| 3 | d07f95e8-b22a-44e0-95b0-676634481ed2 | 51.5, 50.3, 52.7 | 1.2 |

The next prompt was: "Each experiment has cloud and clear points. For each experiment, show me the clear point temperatures and the standard deviation of the clear point temperatures."

It returned this information (left). The standard deviations were checked by another method and were correct.

The LLM was asked to provide this list again with solvents and concentrations, and to order the table by solvent, which it was able to do (below).

| Experiment UUID | Clear Point Temperatu | Standard Deviation | Solutes | Solvents | Concentrations |
|---|---|---|---|---|---|
| ef34b53a-4985-4fd0-bab8-c0b09d79a6d0 | 58.2, 55.8, 54.7 | 1.7898 | Salicylic_Acid | 2-propanol | ('0.3902400054151355') |
| 02effa73-92e2-4f91-a2f2-ea0fbda7b427 | 72.0, 67.9, 71.4 | 2.2143 | Salicylic_Acid | 2-propanol | ('0.4947999807089309') |
| c8735f71-c34b-407c-aa7e-1384d32be72b | 45.3, 47.0, 45.2 | 1.0116 | Salicylic_Acid | 2-propanol | ('0.299399968581436') |
| 781dbff8-ac64-4929-b598-33ce5fe7c3bc | 56.8, 58.4, 60.0 | 1.6 | Salicylic_Acid | 2-propanol | ('0.4040400026702355') |

### Conclusion

Although this session was promising, due to the probabilistic nature of LLM responses, on some other tests it was not always able to interpret the knowledge graph correctly. Further work will be to use better initial prompts to steer the LLM down the correct interpretation pathway. Graph plotting is also possible within the LLM and will be tested.

## Architecture

The knowledge graph is the cornerstone of the project; the entire application is built around it.

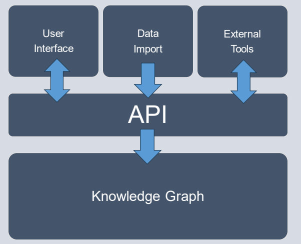


- The knowledge graph is at the core;
- The knowledge graph completely controls the user interface – to change the UI we simply change the knowledge graph;
- An industry-standard REST API abstracts users from the knowledge graph file;
- The user interface communicates with the knowledge graph via the API to fetch the crystallisation experiment framework and to send back researcher contributions;
- The API allows automated contributions, enabling any future front ends or tools.

## Next Steps

- Further work with the LLM on natural language analyses
- Data from more sources, both real-time and whole experiment
- Continue engagement with industry and academics
- Incorporate other pre-existing ontologies e.g. for unit conversion

POSTER 22

# Computer-aided Design of Optimal Solvent Blends for Crystallisation of Mefenamic Acid (MA)

Gaurav Seth, Saman Naseri Boroujeni, Amparo Galindo, George Jackson, Claire S. Adjiman*

Department of Chemical Engineering, The Sargent Centre for Process Systems Engineering, Imperial College London, South Kensington Campus, London SW7 2AZ, United Kingdom

## Introduction

80% of small molecule pharmaceuticals – solid crystals

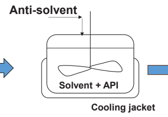


Crystallisation - Widely used in pharma manufacturing


Solvent(s) choice, process conditions

- Solubility
- API yield
- Solvent consumption

## Aim

- ❑ Formulate computer-aided mixture/blend design (CAM[b]D)
- Identify optimal solvent mixtures, process temperatures and mixture composition
- Minimize the Process E-factor or PEF (g waste/g crystals)
- ❑ Use SAFT $\gamma$ - Mie group contribution method – predicting thermodynamic properties within optimisation framework.

## System and key performance indicators (KPIs)

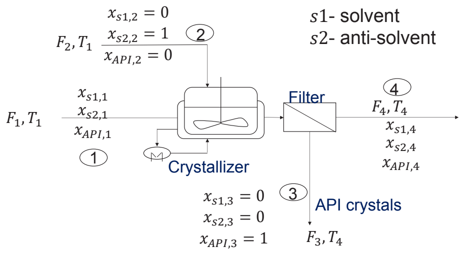


$s1$- solvent
$s2$- anti-solvent

Fig: Process diagram

**For $i^{th}$ component, $i \in \{s1, s2, API\}$, and $j^{th}$ stream, $j \in \{1,2,3,4\}$ :**

- Molar mass of components – $MW_i$
- Mass of $i^{th}$ component in $j^{th}$ stream - $w_{i,j} = MW_i F_j x_{i,j}$
- Mass of API crystallized - $w_{API}^c = MW_{API} F_3$

**KPIs:**

- SEF (g solvents waste/g crystals produced) - $\mathrm{SEF} = (w_{s1,4}+w_{s2,4})/w_{API}^c$
- PEF (g material waste/g crystals produced) - $(w_{s1,4}+w_{s2,4}+w_{API,4})/w_{API}^c$
- Crystallisation yield, $Y_c = (w_{API}^c/w_{API,1}) * 100$

## Process model and design constraints

**Mass balance:**

$$F_1 x_{s1,1} = F_4 x_{s1,4}$$
$$F_1 x_{s2,1} + F_2 = F_4 x_{s2,4}$$
$$F_4 x_{API,1} = F_4 x_{API,4} + F_3$$
$$x_{s1,1} + x_{s2,1} + x_{API,1} = 1$$
$$x_{s1,4} + x_{s2,4} + x_{API,4} = 1$$

**Propylbenzene**

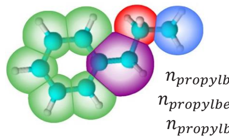

$$n_{propylbenzene,aCH} = 4$$
$$n_{propylbenzene,aCCH_2} = 1$$
$$n_{propylbenzene,CH_2} = 1$$
$$n_{propylbenzene,CH_3} = 1$$

**Solvent assignment constraints:**

$$y_{ii,k} = \begin{cases} 1, \text{ if the solvent is assigned to } s1 \text{ or } s2 \\ 0, \quad \text{otherwise} \end{cases}$$

$$\sum_{k \in N_s} y_{ii,k} = 1, ii = \{s1, s2\}$$

$$\sum_{ii \in \{s1,s2\}} y_{ii,k} \le 1, \qquad \forall k \in N_s$$

**Relating the solvents to functional groups**:

$$\tilde{n}_{ii,l} = \sum_{k \in N_s} y_{ii,k} n_{k,l}, \forall l \in N_g$$

$N_s$ – set of candidate solvents
$N_g$ – set of functional groups
$n_{k,l}$ – number of functional group $l$ in solvent $k$

**Process constraints:**
Solid liquid equilibrium for streams 1 & 4:

$$x_{API,j}\gamma_{API,j} = \exp\left[\frac{\Delta H_{API}^m}{R}\left(\frac{1}{T_{API}^m} - \frac{1}{T_j}\right)\right], j \in \{1,4\}$$

$\gamma_{API,j}$ – activity coefficient of API in $j^{th}$ stream

**Constraints on temperatures:**

$$T_1 \le \min(T_1^b - T_0, T_{s2}^b - T_0)$$
$$T_4 \le T_4^b - T_0$$
$$T_{b,s2} = M_T(1 - y_a) + y_a T_{s2}^{b*}$$
$$y_a = \begin{cases} 1, \text{ if antisolvent is used in stream 2} \\ 0, \quad \text{otherwise} \end{cases}$$

$T_1^b$ – bubble temperature of stream 1
$T_{s2}^{b\,*}$ – bubble temperature pure solvent $s2$
$M_T$ – a large value

Note :- Stability of ternary mixtures for stream 1 and stream 2 is confirmed using gSAFT within gPROMS

## Optimization problem

**Decision Variables**:
$\mathbf{X} = [y_{ii,k} \;\; y_a \;\; F_1 \;\; F_2 \;\; x_{s2,1} \;\; T_1 \;\; T_4]^T$
**Optimization problem (MINLP):**

$$\min_{\mathbf{X}} \quad PEF$$

*subject to* : Mass Balance
Design Constraints
$0 \le x_{s2,1} \le 1$
$SEF \ge 3.5$
$0 \le F_1 \le 50$ mol/sec
$0 \le F_2 \le 50 y_a$ mol/sec
$290.15 \le T_1 \le 400$ K
$290.15 \le T_2 \le 400$ K
$w_{API}^c = 100$ g/sec
$Y_c \ge 0.9$

Process constraints
Fixed API production
Minimum yield

## Results

**API** - Mefenamic Acid (MA)
**Set of candidate solvents ($N_s$)** - Water, 1-2-Propanediol, Acetic acid, Isobutyl acetate, Isopropyl acetate, 2-methyl-1-Propanol, Butyl acetate, ethanol, 1-butanol, 1-pentanol, Acetone, Ethyl acetate

Stream table

| S.No. | $s1, s2$ | s1 (g/sec) | s2 (g/sec) | PEF (g/g) | $Y_c$ (%) | $T_1$ (K) | $T_4$ (K) | $y_a$ |
|---|---|---|---|---|---|---|---|---|
| 1 | 1,2-Propanediol<br>water | 340.14 | 9.86 | 3.5 | 99.88 | 400 | 290.15 | 0 |
| 2 | 1-pentanol<br>- | 350 | - | 3.5 | 99.75 | 398.61 | 290.15 | 0 |
| 3 | Butanol<br>Isobutyl acetate | 349.18 | 0.82 | 3.51 | 99.48 | 383.92 | 290.15 | 0 |
| 4 | Isobutyl acetate<br>Ethyl acetate | 322.56 | 27.44 | 3.54 | 95.83 | 377.71 | 290.15 | 0 |

## Conclusions

- Results suggest the use of cooling crystallization to minimize the solvent consumption.
- Multiple high-performance solutions generated by including integer cuts in MINLP.
- Using high inlet temperature – high yield.

## Ongoing/Future work

- Solvent recycling
- Effect of adding impurities
- Additional design criteria – energy balance, crystal shape, particle size distribution

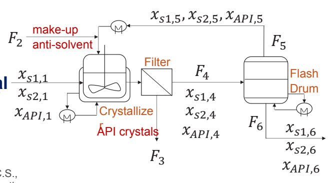


References:
1. Wang, J. and Lakerveld, R., 2018. Integrated solvent and process design for continuous crystallization and solvent recycling using PC-SAFT. *AIChE Journal*, *64*(4), pp.1205-1216.
2. Watson, O.L., Jonuzaj, S., McGinty, J., Sefcik, J., Galindo, A., Jackson, G. and Adjiman, C.S., 2021. Computer aided design of solvent blends for hybrid cooling and antisolvent crystallization of active pharmaceutical ingredients. *Organic Process Research & Development*, *25*(5), pp.1123-1142.

POSTER 23

# Pharmaceutical supply network design for advanced manufacturing technology interventions

Ettore Settanni – CMAC, University of Cambridge

This poster will be available at the conference

POSTER 24

# Discovery and Applications of a Novel Solid-state Arrangement: Water Bridge Salt Form

Saadia Tanveer,[1,2] David Remick,[3] Paul Meenan,[4] Marianne Langston,[5] Anton Peterson,[5] Martin R. Ward,[6] Chantal Mustoe,[6] Iain D.H. Oswald,[1] Alastair J. Florence,[1,2]

[1]Strathclyde Institute of Pharmacy and Biomedical Sciences, University of Strathclyde, Glasgow, UK. [2]EPSRC Future Hub for Manufacturing and Advanced Crystallisation, Technology and Innovation Centre, University of Strathclyde, Glasgow, UK. [3]Synthetic Molecule Design & Development (SMDD), Eli Lilly and Company, Indianapolis, IN 46285, USA. [4]Drug Product Design, Pfizer Inc. Groton CT 06340, USA. [5]Pharmaceutics Research – Analytical Development, Takeda Pharmaceuticals International Co., Cambridge, MA 02139, USA. [6]National Facility, CMAC, University of Strathclyde Glasgow, UK

## Introduction

**Salt formation** is a common technique to modify the properties and enhance the solubility and bioavailability of an Active Pharmaceutical Ingredient (API). However, salts tend to convert back to their free (unionised) form under certain conditions via a reaction known as **salt *disproportionation***.

**Industry Challenge:** Disproportionation poses significant challenges for the pharmaceutical industry by impacting **stability** and **solubility** of d***rug formulations***

## Disproportionation Reaction

**Salt *disproportionation*** *is an acid-base reaction involving a proton exchange process under certain conditions and changes* the chemical composition of API. Salt form stability is indicated by maximum solubility pH (pHmax)

$$pH_{max} = pK_a + \log \frac{S_0}{\sqrt{K_{SP}}}$$

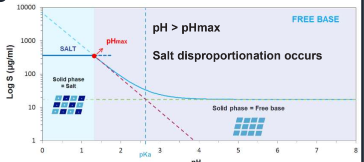


**Figure 1**: pH solubility profile of a weakly basic compound [2]

## Aim & Objectives

- This project aims to build a fundamental understanding of the salt "water bridge" structure, its propensity to form, stability, and structure-property relationships
- To design and apply a disproportionation monitoring workflow and test the stability behaviour of salt hydrates with and without bridging water motif between the API and counter ions

## Potential Benefits

- The study provides insights into the pH-dependent stability of miconazole salts, highlights the potential benefits of the water-bridging structure present in MM DH as a contributing factor to its sustained stability

## Case study: Miconazole Mesylate Dihydrate (MM DH)

It has been reported that the rate and extent of salt disproportionation for Miconazole Mesylate (MM) salt (amorphous AMO, anhydrous AH, dihydrate DH) in the presence of excipient is significantly different, and MM DH was resistant to disproportionation over the time studied [1]

### Water bridge salt hydrate

A "**water-bridge salt hydrate"** is a salt where counter ions (such as miconazole and mesylate) are linked indirectly via water molecules forming hydrogen bond bridges. This structural arrangement relies on water molecules to mediate the interactions between the cation and anion, stabilizing the salt hydrate.

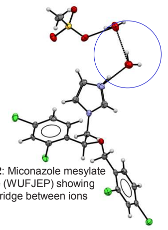

**Figure 2**: Miconazole mesylate dihydrate (WUFJEP) showing water-bridge between ions

## Disproportionation monitoring Workflow

A workflow has been developed to monitor the disproportionation process using alkalimetric titration of an aqueous salt solution by adding aliquots of NaOH. In-situ Raman spectroscopy and continuous pH monitoring are employed to detect the phase change, and the results are validated using PXRD and HPLC

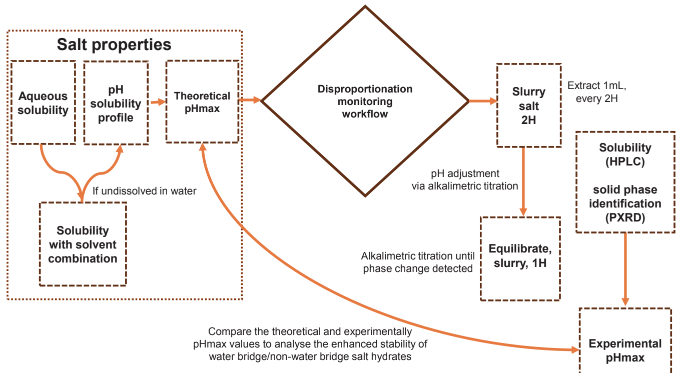


**Figure 3**: Schematic diagram of the disproportionation monitoring workflow

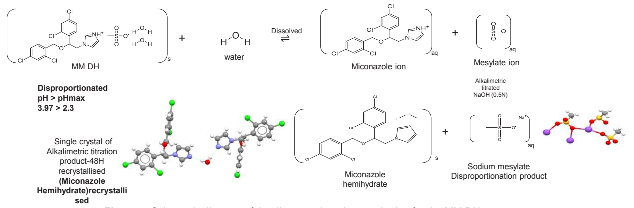


**Figure 4**: Schematic diagram of the disproportionation monitoring for the MM DH system

## Results and Discussion

**Disproportionation behaviour of miconazole mesylate dihydrate (water bridge salt) at varying pH conditions**

- Theoretical $pH_{max}$ of MM DH (SWB) is **2.3**
- The phase change was detected by a sudden decrease in the Raman peak area for the salt (@1268) and a sharp increase in the free base peak area (@1506) at a pH of **3.97**. Additionally, a sudden drop in pH was observed during the transition. The solid was assessed by PXRD and validated the change to the miconazole hemihydrate.
- MM DH disproportionation at **3.97** indicates an enhanced stability compared with normal salt behaviour

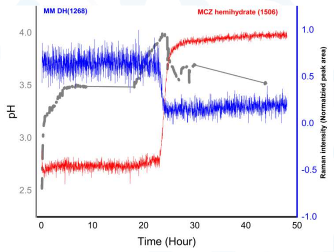


**Figure 5**: The peak area of Raman characteristic peak for miconazole (1506cm$^{-1}$) and MM DH (1268 cm$^{-1}$) and pH as a function of time. At pH 3.97 there is a sharp change in pH and the Raman bands of the two solids

**Disproportionation behaviour of miconazole chloride dihydrate salt MCZ Cl DH (non-water bridge)**

- The pHmax of MCZ Cl DH (non SWB) is calculated as **3.77**
- The onset of disproportionation is at ~pH 3.46, which corresponds well to the calculated pHmax.
- The solid form precipitated during this disproportionation reaction is also **miconazole hemihydrate**

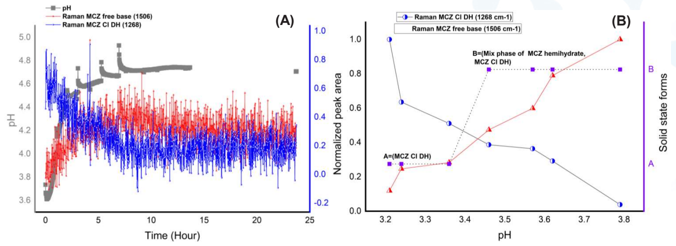


**Figure 6:** Peak area of Raman characteristic peaks for miconazole (1506 cm$^{-1}$) and MCZ Cl DH (1268 cm$^{-1}$) as a function of time and pH **(A)** and as a function of pH with PXRD results indicating phase composition **(B)**

**Nucleation behaviour of MCZ free base and influence of water bridging between counterions**

- The impact of seeding was tested via two experiments depicted in Figure 7
- Via either method there is no impact of seeding on nucleation of the MCZ free base the product remained as MM DH after 48 hours as revealed by Pawley refinement of XRD data

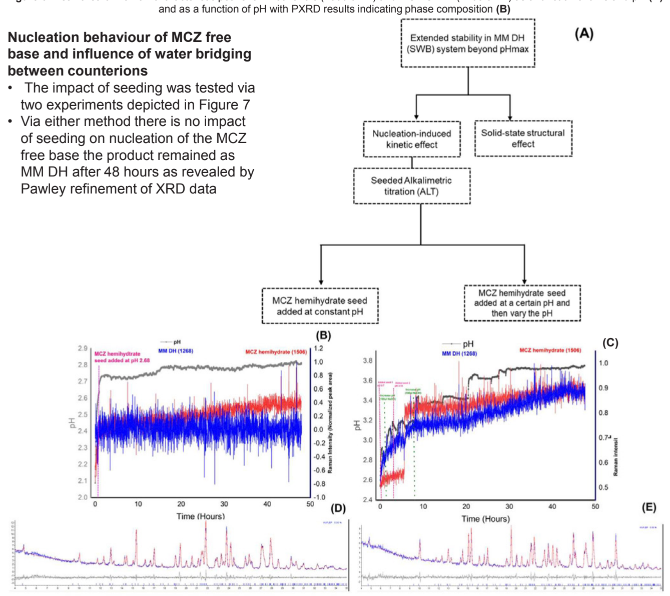


**Figure 7: (A)** Schematic diagram of the experimental workflow. In-situ monitoring of the characteristic peak for miconazole (1506 cm$^{-1}$) and MM DH DH (1268 cm$^{-1}$) and pH as a function of time for: **(B)**; Seeding at constant pH **(C)**; and seeding at variable pH **(D).** Pawley refinement of a product after 48H (seed addition at constant pH, **(E)** or (seed addition and varying pH, using the unit cell parameters from MM DH (WUFJEP).

## Conclusion & Future Work

- The developed workflow has been applied to miconazole salts and distinct changes in disproportionation behaviour are observed between MM DH and MCZ Cl DH despite having the same API molecule.
- The different counter ions have introduced a difference in the connectivity between the ions and the water molecules. We believe a water-bridging motif in MM DH salt contributes to enhanced stability. A larger pool of observations will enable a more robust set of guidelines to be developed so that salt "water bridge" forms can be a valid solid form for drug delivery.
- Charge distribution analysis will be performed to identify the impact of structural motifs in the known water bridge salt system with enhanced stability.
- Comparison will be made between the known water bridge system and traditional hydrates to develop a workflow for pharmaceutical compounds using crystallographic data and physicochemical properties.

## Acknowledgements:

This work is funded jointly by Lilly, Takeda and Pfizer and has been carried out within the CMAC Future Manufacturing Research Hub. Authors have no conflict of interest to declare.

## References:

[1] Patel, M.A., Luthra, S., Shamblin, S.L., Arora, K., Krzyzaniak, J.F. and Taylor, L.S., 2018, *Molecular Pharmaceutics*, *15*(1), pp.40-52.
[2] Abouselo, A., Rance, G.A., Tres, F., Taylor, L.S., Kwokal, A., Renou, L., Scurr, D.J., Burley, J.C. and Aylott, J.W., 2021, *Molecular Pharmaceutics*, *18*(9), pp.3247-3259.

Engineering and Physical Sciences Research Council

# DataFactories & Model-driven Experiments

POSTER 25

# Self-driving Tableting DataFactory to Accelerate Process Development

Faisal Abbas[1,2], Mohammad Salehian[1,2], Peter Hou[1,2], Jonathan Moores[1,2] , Jonathan Goldie[1,2] , Alexandros Tsioutsios[1,2], Victor Portela[3], Paul Chapman[3], Quentin Boulay[4], Roland Thiolliere[4], Jean-Jacques Schwartz[5], Jerome Guerin[5], Alastair Florence[1,2], Daniel Markl[1,2]
[1]Centre for Continuous Manufacturing and Advanced Crystallisation (CMAC), University of Strathclyde
[2]Strathclyde Institute of Pharmacy and Biomedical Sciences (SIPBS), University of Strathclyde
[3]School of Innovation and Technology, Glasgow School of Art
[4]Medelpharm
[5]DEC Group

## Introduction to DM2 Platform II

- Increasing complexity with more excipients, formulation and process parameters
- Process automation to support model-based experimentation
- Increased process efficiency and less waste of time material

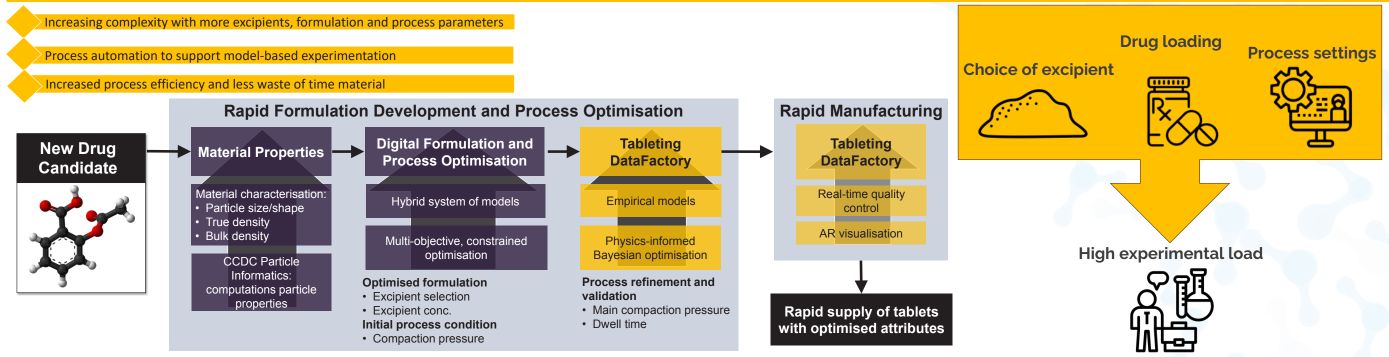


## The Microscale Tablet Manufacturing System

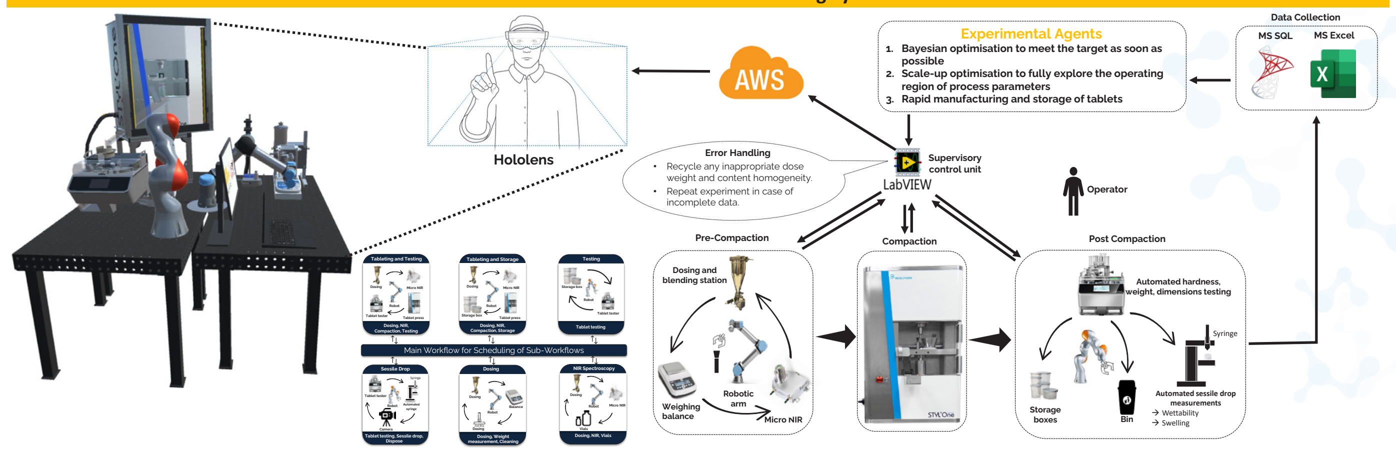


## Self-Driven Experiments

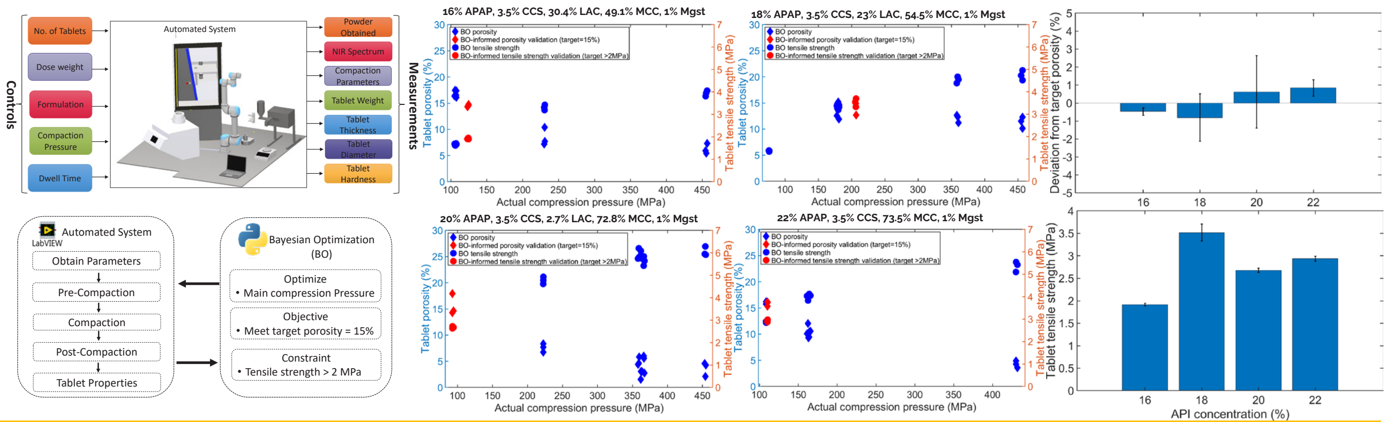


## Real-Time Data Quality Control

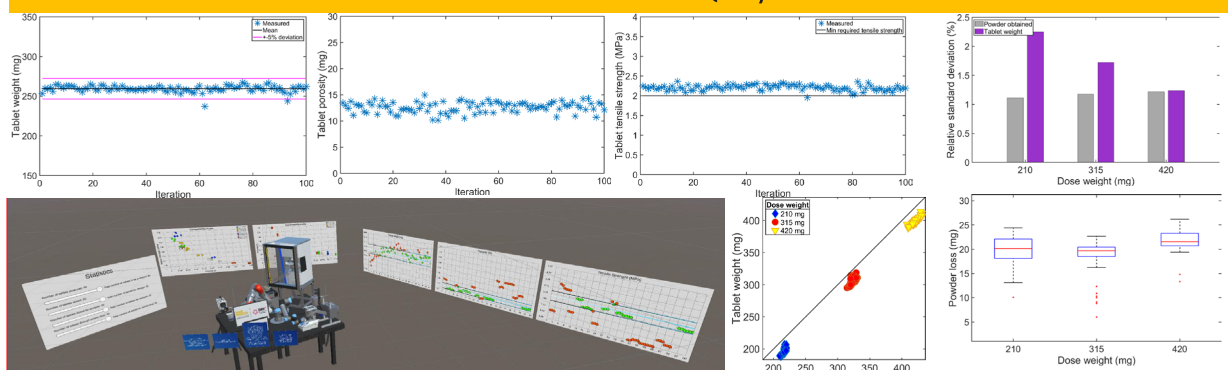


UK Research and Innovation

MADE SMARTER INNOVATION

DM² Digital Medicines Manufacturing

**Acknowledgment:** The authors would like to thank the Digital Medicines Manufacturing (DM²) Research Centre (Grant Ref: EP/V062077/1) for funding this work. DM² is co-funded by the Made Smarter Innovation challenge at UK Research and Innovation, and partner organisations from the medicines manufacturing sector. For more information, visit cmac.ac.uk/dm2-home

DM² website

DM² Video Demo



POSTER 26

# Machine-Learning for Mechanistic Model Identification

## Can Symbolic Regression Outperform Standard models?

[1]Aaron Bjarnason (presenting), [1]Thomas Pickles (contributor),
[1]Cameron Brown (academic supervisor), [1]Alastair Florence (academic supervisor)
[1]University of Strathclyde

## Symbolic Regression

Symbolic regression (SR) is a powerful machine learning technique with the ability to **autonomously discover** mathematical expressions describing complex systems. Unlike traditional regression, which fits data to predefined models, SR searches an expansive equation space to identify compact, **interpretable relationships**.


This makes it particularly valuable for scientific applications, where the precise underlying mathematics are unknown.

By leveraging PySR, a high-performance symbolic regression tool in Python, we uncover crystal growth expressions directly from experimental data. This data-driven approach enables predictive accuracy while maintaining physical interpretability, offering a novel alternative to conventional empirical and semi-empirical models in crystallisation process development.

## Experimental Setup

The crystallization experiments were conducted using an **automated platform** controlled remotely via LabOS, ensuring precise and reproducible process conditions. This system enabled automated control of temperature, stirring, and dosing, allowing for high-throughput experimentation with minimal manual intervention.

Solution concentration was measured using **High-Performance Liquid Chromatography (HPLC)**, providing accurate, time-resolved quantification of the solute during crystallization. This allowed for the monitoring of supersaturation levels, which are critical for understanding crystal growth kinetics.

To characterize particle size, a **BlazeMetrics probe** was employed to measure **chord length distributions (CLD)** in real time. The CLD data were later analyzed to determine the **volume mean diameter**, $\mu_{43}$ serving as a key parameter for modeling crystal growth.

This integrated setup provided high-quality kinetic data, essential for developing accurate crystallization models.

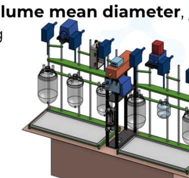

## Data-Driven Model Building

Accurate model form selection in mechanistic model building is essential for process optimization, yet traditional models can have ambiguous reliability, as they may not fully capture complex crystallisation behaviour

A lack of understanding about underlying mechanics and interactions further complicates model development

**Symbolic regression**, (SR) a data-driven approach, offers a potential solution. By discovering explicit mathematical expressions directly from experimental measurements, we may begin to build more accurate predictions of crystallisation behaviour. While expressions gleaned from SR may best serve in a system-specific manner, the directly derived mathematics may also help to glean some understanding of the physical behaviour underneath.

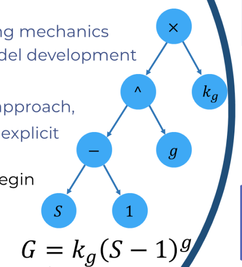


$$G = k_g(S-1)^g$$

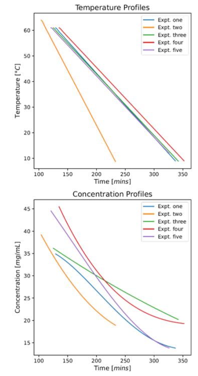


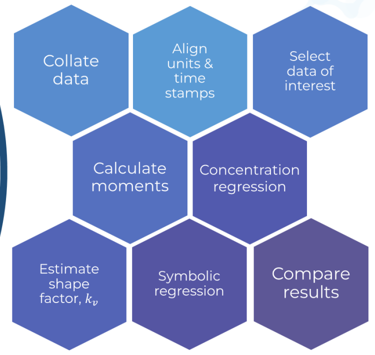


## Methodology & Preliminary Results

1. Clean/align data from various sources
2. Regression of time-sparse concentration data for comparison with time-dense measurements
3. Determine lamivudine (form II) shape factor, $k_v$, by optimization of Blaze data vs concentration data.
4. Perform Symbolic Regression to determine growth rate from concentration, solubility and size measurements
5. Selection of workable candidate expressions
6. Projection of particle size under discovered growth rate expression in comparison to:
   - experimental measurements
   - optimized standard growth expression predictions

| *Expression Origin* | *Mathematical Expression* | *SSE vs Measurement* |
|---|---|---|
| Standard Form | $G = k_{g1}(S-1)^{g1}$ | 21502 |
| Symbolic Regression | $G = \frac{k_{g2}C^*(T)}{C(t)}$ | 29472 |
| Comparative Error | N/A | +37.1% error |

Comparison of SR Expression to Optimised Standard Form

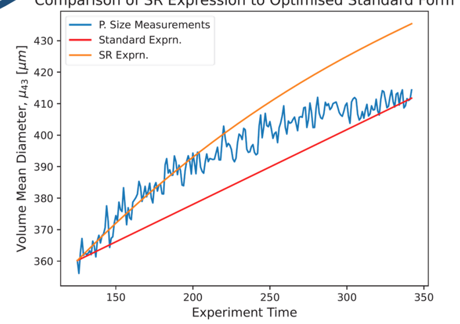


*Conclusion and Further Work:*

- Symbolic regression can develop an expression to model crystal growth with only a few experiments
- SR equation was outperformed by a standard growth expression with optimised parameters.
  - But more accurately captured the curvature of the modelled data
- Interim results could likely be improved by further exploration
- Gathering data using a more growth-dominated system may glean more accurate results
- The method can be deployed using the Snapdragon crystallisation platform and beyond.

AstraZeneca Chiesi Lilly Pfizer Roche sanofi Takeda ucb

POSTER 27

# Automated Cooling Crystallisation in the Crystallisation Screening DataFactory

Christopher Boyle*, Parandeep Sandhu, Sahil Salekar, Javier Cardona, Blair Johnston
CMAC, University of Strathclyde, Glasgow, UK. *christopher.boyle.101@strath.ac.uk

## Motivation

**Efficient high throughput solvent screening**
Leveraging robots and state of the art machine learning to explore solvent space for API.

**Crystallisation Classification System**
Model API-solvent interactions to predict key parameters like solubility, particle shape, oiling out, and agglomeration.

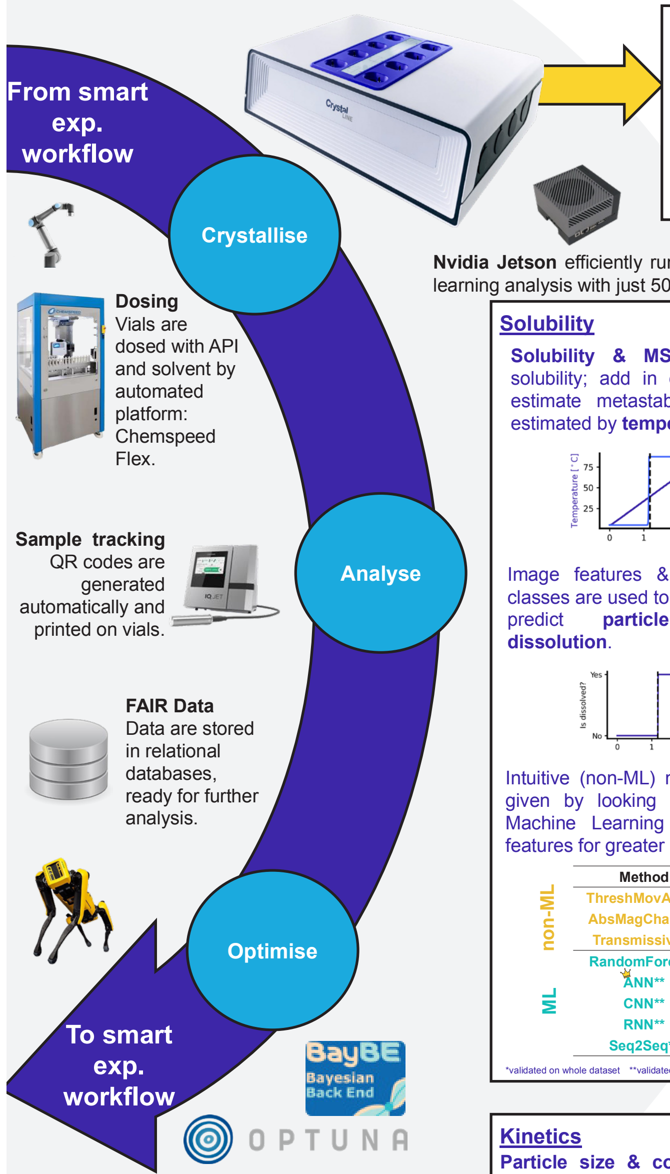


**Dosing**
Vials are dosed with API and solvent by automated platform: Chemspeed Flex.

**Sample tracking**
QR codes are generated automatically and printed on vials.

**FAIR Data**
Data are stored in relational databases, ready for further analysis.

**Nvidia Jetson** efficiently runs deep learning analysis with just 50W.

## Crystallise

**Small scale crystallisation**
The Technobis Crystalline is used to perform cooling crystallisation experiments.

**Data rich measurements**
Array of 6 crystalline platforms each with temperature control, transmissivity probes, and on-line imaging.

**Bespoke experiment control**
Our custom software interfaces with our data architecture while enabling flexible control based on state machines.

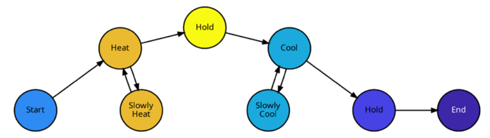


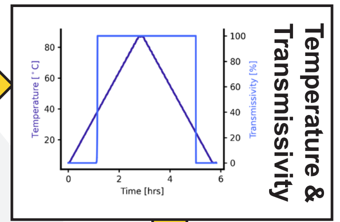


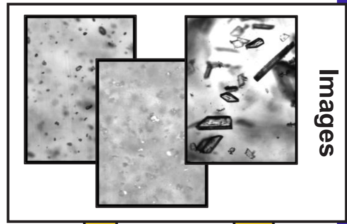


## Analyse

### Solubility

**Solubility & MSZW.** Clear point gives solubility; add in cloud point and we can estimate metastable zone width. This is estimated by **temperature cycling.**

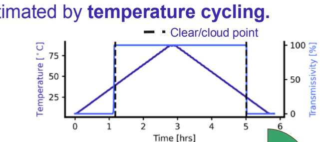


Image features & classes are used to predict **particle dissolution.**

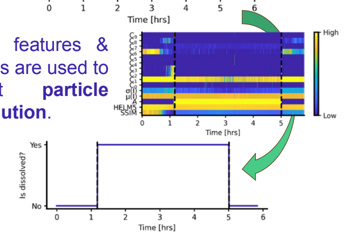


Intuitive (non-ML) models predict clear/cloud given by looking for changes in features. Machine Learning (ML) methods combine features for greater accuracy & generalisation.

| | Method | | RMSE (°C) |
|---|---|---|---|
| non-ML | ThreshMovAvFA* | | 9.9 |
| | AbsMagChange* | | 14.7 |
| | Transmissivity* | | 20.9 |
| ML | RandomForest** | [1] | 16.7 |
| | ANN** | | **4.8** |
| | CNN** | | 9.0 |
| | RNN** | | 6.8 |
| | Seq2Seq** | | 6.0 |

*validated on whole dataset **validated on representative subset

### Image Classification

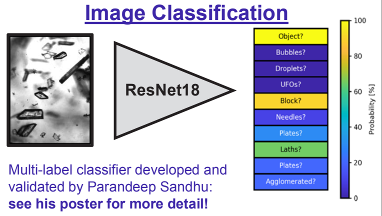


Multi-label classifier developed and validated by Parandeep Sandhu: **see his poster for more detail!**

### Image Segmentation

**Training data** composed of images annotated to identify particles using CVAT [1].

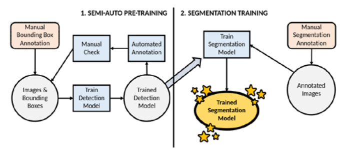


**Images segmented** by YOLOv8 [2]. Trained model attains mAP of 66.9%.

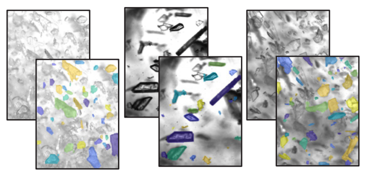

### Kinetics

**Particle size & count** are tracked over time to estimate growth rate and nucleation rate or can be passed on to population balance models.

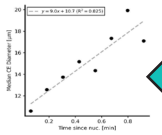


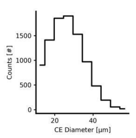


**Particle Size Distributions** Obtained from batches of images for a representative indication of particle size and shape.

## Optimise

**Smart experimentation**
Efficient design space exploration using Bayesian optimisation: quickly find optimal solvent and process parameters depending on the current target.

**Target** specific **growth rates**, particle shape or size, or emphasise solvent environmental impact while meeting industrial processability goals *e.g.*, Black's rules, meeting temperature requirements, and/or achieving **desired yield**.

### References & Acknowledgements

Thanks to DataFactory team (Amal Osman, Connor Clark, Fraser Paterson, Farha Kamal) for running experiments. Thanks to John Armstrong for getting our models to run on the Nvidia Jetsons efficiently and implementing the Seq2Seq model.

[1] Scikit-learn: Machine Learning in Python. doi:10.5555/1953048.2078195
[2] Computer Vision Annotation Tool. doi:10.5281/zenodo.3497105
[3] D. Reis et al. (2024) arxiv:2305.09972

MADE SMARTER INNOVATION
CMAC DATALAB
DM² Digital Medicines Manufacturing

POSTER 28

# A Workflow for the Automation of Pharmaceutical Salt Selection and Screening Process

Connor Clark[1,2], Martin Prostredny[1,2], Blair Johnston[1,2], Alastair Florence[1,2]
1 Strathclyde Institute of Pharmacy and Biomedical Sciences, University of Strathclyde, Glasgow, UK
2 Continuous Manufacturing and Advanced Crystallisation (CMAC) Future Manufacturing Research Hub, University of Strathclyde, Glasgow, UK

## Introduction

With over 60 % of novel active pharmaceutical ingredients (APIs) in recent years exhibiting low aqueous solubility and bioavailability, pharmaceutical salts have had an increased importance over time. However, salt screening, the process to find viable salt forms, can be a lengthy and complex process exploring different counterions and crystallisation conditions to find new crystalline forms. The use of tools to predict solubility or crystal packing coupled with artificial intelligence/machine learning for salt formation would be invaluable in reducing the experimental burden and uncertainty in salt selection, alongside improving sustainability through reduced material and energy usage and carbon footprint. Overall, this project aims to develop an automated workflow for model-driven salt selection and process development. This work introduces a workflow for the prediction and development of salt forms of APIs.

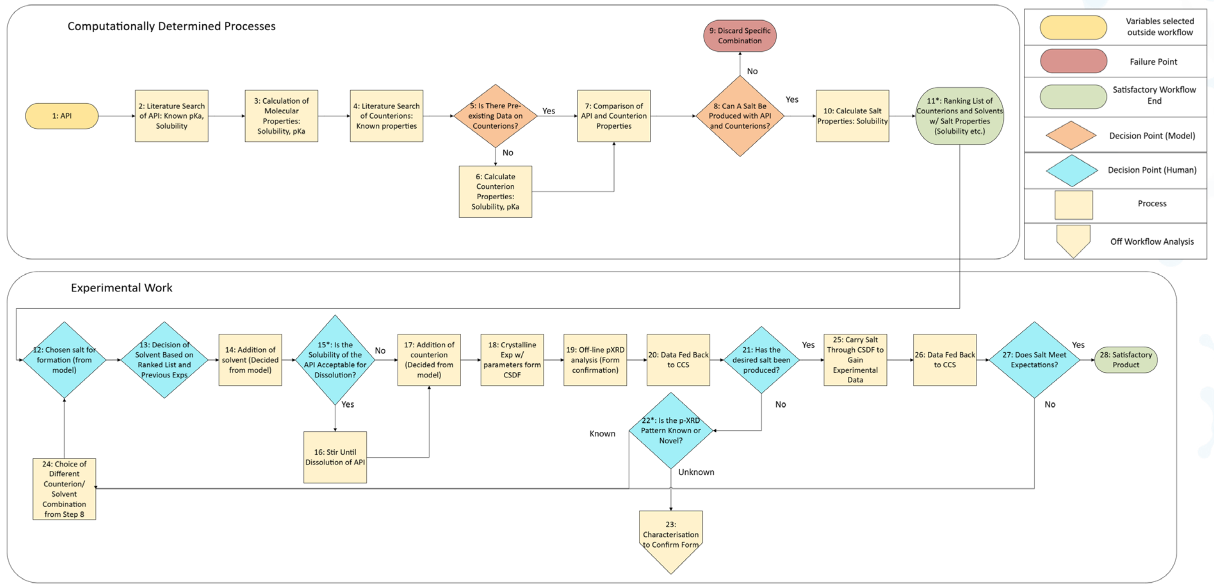


Figure 1: Initial Workflow for an Automated Salt Selection Process

## Generation of Training Data/Current Work

- Small-scale salt formation experiments are currently being carried out on APIs of interest in the Crystallisation Screening DataFactory (CSDF) in order to prepare appropriate data for training a model.
- Amantadine was selected as the first compound as it exhibits low aqueous solubility and is available commercially in form of a hydrochloride salt
- A Python script was used to compare pKa values and solubility data for the API and selected counterions generated from COSMO calculations.
- Suitable combinations of solvents and counterions for amantadine are presented in Table 1.

Table 1: Suitable Counterions and Compared Solubilities of Amantadine

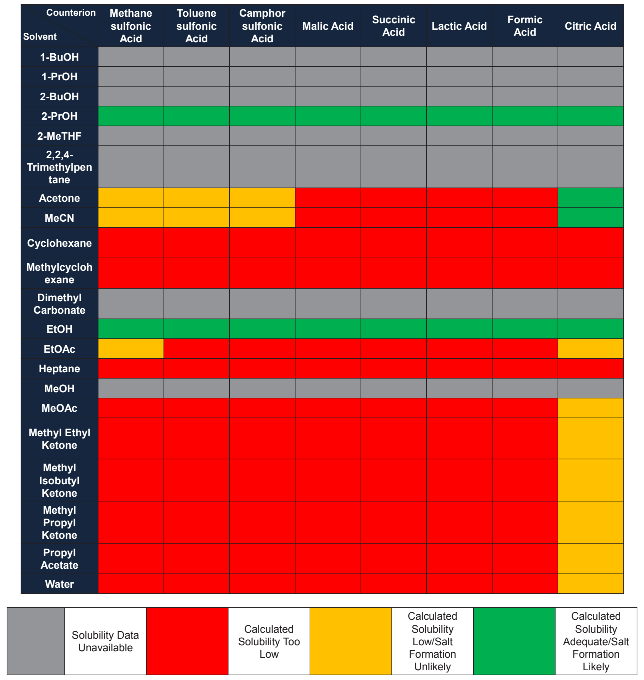


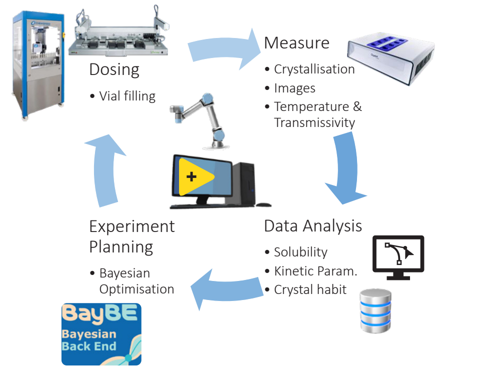


Figure 2: Crystallisation Screening DataFactory (CSDF) Workflow

## Next Steps/Future Work

Future work for this project will involve the development of the model, including generation of data through the CSDF, to fuel predictive tools. Alongside this, future translation of the workflow examined with amantadine to other compounds, which when aligned with the wider research in this space in CMAC, will lead to a toolbox available for efficient salt selection for increased solubility of future APIs.

POSTER 29

# Data Uncertainty within the Small-Scale Crystallisation Screening DataFactory (CSDF)

Amal Osman[1,2], Connor Clark[1,2], Christopher Boyle[1,2], Martin Prostredny[1,2], Chantal Mustoe[1,2], Murray Robertson[1,2], Michael Chrubasik[3], Paul Duncan[3], Blair Johnston[1,2], Alastair Florence[1,2]

1. Strathclyde Institute of Pharmacy and Biomedical Sciences, University of Strathclyde, Glasgow, UK
2. Centre for Continuous Manufacturing and Advanced Crystallisation, University of Strathclyde, Glasgow, UK
3. National Physical Laboratory, Glasgow, UK

## Introduction - DataFactory Goals and Objectives

Self-driving labs offer
- Increased efficiency
- Enhanced safety
- Improved accuracy
- Increased equipment utilisation

Resulting in
- Accelerated research & development
- Improved data collection
- Cost savings
- Improved environmental sustainability

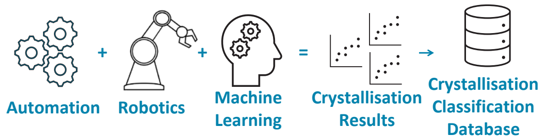


## Methods

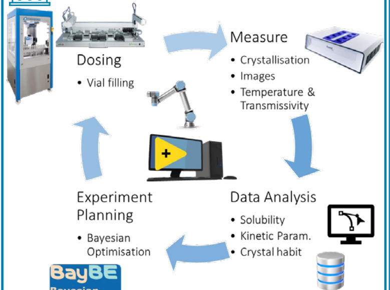


Figure 1: The crystallisation screening Datafactory (CSDF) automated workflow

## Current and future data capabilities

Generation of various crystallization parameter data including
- Solubility
- Kinetics
- Crystal morphology
- Crystal forms

An example of a dataset produced by the CSDF is shown in Figure 2

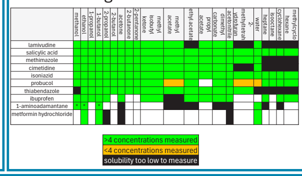

Figure 2: A solubility matrix of the top 10 investigated APIs investigated during a period of three months. Blank: experiments not started. * indicates that the compound did not nucleate therefore multiple experiments were required to generate triplicate data.

## Why focus on data uncertainty?

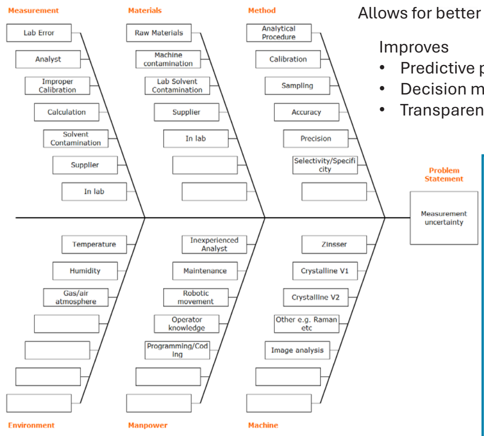

Figure 3: Known sources of measurement uncertainty seen within the CSDF

Allows for better understanding of accuracy and precision

Improves
- Predictive power and validity of models
- Decision making
- Transparency and trust in data

### Research Aims

- Understand **capabilities** & **limitations** of the CSDF in producing reliable and consistent crystallisation data
- Investigate **data uncertainty** produced within the CSDF & its **propagation**
- Quantify the possible overall **confidence level** of the data produced by the CSDF

## Results and Discussion

Three areas of uncertainties within the Crystalline were examined – heating rates, confidence in solubility data and temperature validation.

### Heating Rates

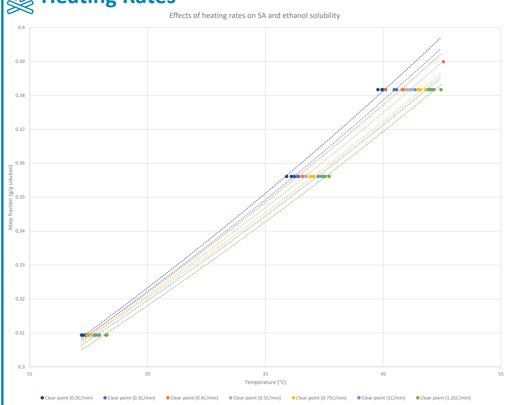

Figure 4: Solubility plots demonstrating the variability of clear points for three different concentrations of salicylic acid in ethanol at various heating rates (0.2°C, 0.3°C, 0.4°C, 0.5°C, 0.75°C, 1°C and 1.25 °C per min). * denotes the heating rate (0.5°C) used by previous DataFactory researchers[3]

Figure 4 shows how a range of heating rates between 0.2 – 1.25°C leads to a variation in results of up to +/- 5°C. This highlights how heating rates can influence accuracy of experimental measurements. This trend has been reported in Cashmore et al[4]. Further research is required to optimize the heating profile to get clear points as quickly but as accurately as possible by varying the rates within one experiment.

### Temperature Validation

External thermocouples were used to investigate the efficiency of the crystalline's temperature controls in various solvents and how solvent volume has an impact on results.

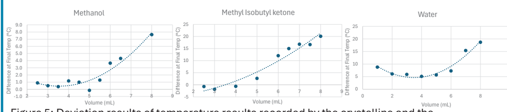

Figure 5: Deviation results of temperature results recorded by the crystalline and the thermocouple depending on solvent volume. Results were based on final temperature hold which was 10°C below the corresponding solvent boiling point

Figure 5 shows how volume of solvent can affect the efficiency of the crystalline's ability to heat solvents. In most cases, when working with 2-5mls of solvent, there is a temperature error margin of up to +/-2°C recorded by the crystalline. This reflects the working volumes highly recommended by Technobis. One exception was water where an error margin was seen to be up to +/-5°C. Further investigations will be carried out to understand the extent of the uncertainty when working with water as a solvent.

## Results and Discussion (continued)

### Confidence in Solubility Data

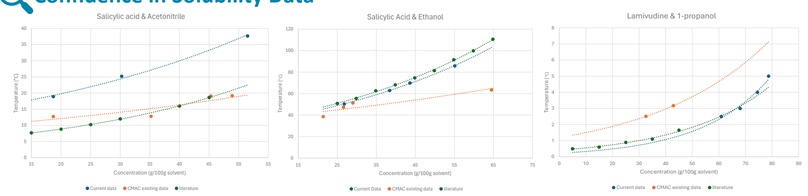

Figure 6: Solubility plots demonstrating the variability of clear points for three different API/Solvent combinations based on recent lab data, CMAC existing data and literature data [1,2]. Dotted lines represent exponential fits.

Figure 6 shows how various factors could affect the accuracy of solubility data such as type of Crystalline used, experiments carried out by different researchers and possible variation in data analysis.

A suggestion to improve the confidence in solubility data was to develop a crystalline troubleshooting workflow. This proposed preliminary workflow was designed to recommend best next experiments based on results during a solubility experiment as shown below in Figure 7.

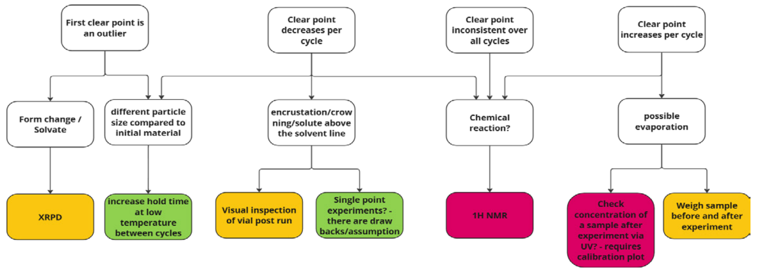


Figure 7: Proposed preliminary workflow on next best experiments based on solubility experiment outcomes. Colour codes refer to possible automation capabilities as follows: green = automatable now, amber = could be automatable, burgundy = manual intervention required

References:
1. Matsuda, H., Kaburagi, K., Matsumoto, S., Kurihara, K., Tochigi, K., Tomono, K., (2009) "Solubilities of Salicylic Acid in Pure Solvents and Binary Mixtures Containing Cosolvent", *Journal of Chemical & Engineering Data* 54 (2), doi: https://doi.org/10.1021/je800475d
2. Jozwiakowski, M., Nguyen, N., Sisco, J., Spancake, C., (1996), "Solubility Behaviour of Lamivudine Crystal Forms in Recrystallisation Solvents", *Journal of Pharmaceutical Sciences* 85(2). doi: https://doi.org/10,1021/js9501228.
3. Pickles, T., Mustoe, C., Brown, C. & Florence, A., (2022) "Autonomous DataFactory: High-throughput screening for large data collection to inform medicine manufacture", *British Journal of Pharmacy* 7(2). doi: https//doi.org/10.5920/bjpharm.1128
4. Cashmore, A., Miller, R., Jolliffe, H., Brown CJ., Lee, M., Haw, MD., Sefcik, J., (2023) "Rapid Assessment of Crystal Nucleation and Growth Kinetics: Comparison of Seeded and Unseeded Experiments", *Cryst Growth Des* (7):4779-4790. doi: 10.1021/acs.cgd.2c01406

Acknowledgments:
Many thanks to Thomas Pickles, Farha Kamaal, Javier Cardona, Jan Sefcik and Cameron Brown for their expertise and support with regards to the DataFactory

POSTER 30

# The Relationship Between Functional Group Orientation and Crystal Facet Behaviours

Dave Collins – CMAC, University of Leeds

This poster will be available at the conference

POSTER 31

# Development of Combination Amorphous Solid Dispersions utilizing Automated Excipient Screening Tools

## Jonathan Currie – University of Copenhagen

This poster will be available at the conference

POSTER 32

CMAC

# From Powder to Tablet: Predicting Moisture Sorption and Understanding Physical Stability Changes

Isra' Ibrahim[1,2], James Mann[3], Alexander Abbott[3], Fredrik Winge[4], Adrian Davis[5], Bart Hens[6], Ibrahim Khadra[1], Daniel Markl[1,2]

[1]Strathclyde Institute of Pharmacy & Biomedical Sciences, University of Strathclyde, Glasgow, UK.
[2]Centre for Continuous Manufacturing and Advanced Crystallisation, University of Strathclyde, Glasgow, UK.
[3]Global Product Development, Pharmaceutical Technology & Development, Operations, AstraZeneca, Macclesfield, UK.
[4]Global Product Development, Pharmaceutical Technology & Development, Operations, AstraZeneca, Gothenburg, Sweden.
[5]Analytical R&D, Pharmaceutical Sciences Small Molecules, Pfizer, Sandwich, UK.
[6]Drug Product Design, Pfizer, Zaventem, Belgium.

## Introduction

- Ensuring the physical stability of immediate-release tablets is crucial to maintain their quality and performance during storage, where the storage-induced changes can lead to altered tablet properties, potentially affecting drug release.
- How do the intrinsic properties of particles and their interactions in bulk powder and compacts influence the tablets physical stability under storage? and to what extent can these effects be predicted?

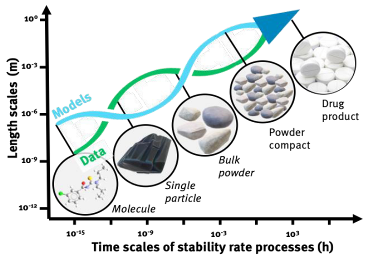


## Methods

**Raw Material Characterisation**
- Moisture sorption (DVS and modelling).
- Swelling (Morphologi 4).

**Tablets Manufacturing**
- Direct compression.
- 5 placebo Formulations.
- 4 porosities.

**Tablets Characterisation**
- Moisture Sorption.
- Weight and swelling)
- Porosity (modelling)
- Hardness

**Tablets Performance**
- Disintegration time
- Liquid absorption and swelling (sessile drop)

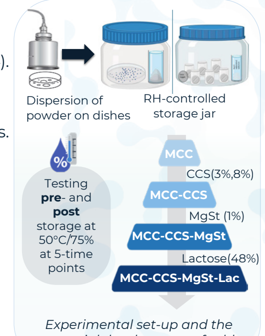


*Experimental set-up and the sequential development of tablet sets.*

## Results

Time-scale

DVS

Real storage

Length-scale

Tablet

Powder

### Using DVS to link powder and tablet moisture behaviour

- DVS powder data predicts tablet moisture content at a given RH, independent of porosity with possible overestimation at high RH. Sorption rate constant depends on porosity but not RH, enabling tablet sorption rate estimation from powder.

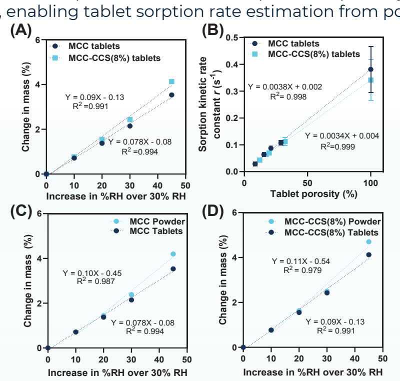


*Effect of (A) RH and (B) porosity on moisture content and sorption rate. (C) MCC and (D) MCC-CCS powder correlated with tablet moisture uptake.*

### Scaling DVS data to real storage tablet data

- A scaling factor from DVS and real storage data enables long-term storage predictions. Scaling was unaffected by porosity or formulation, though formulation impact remains uncertain.
- Variabilities in model prediction due to averaging multiple tablets at each time point and differences in initial weights.

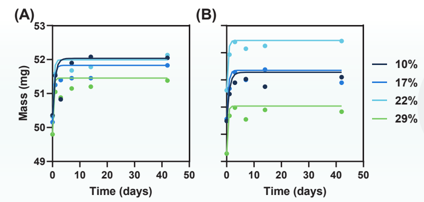


*Moisture-induced mass increase for MCC and MCC-CCS (8%) tablets at different porosities. Model predictions (lines) derived from one measurement of DVS powder data and experimental data (points).*

**Reasonable use of materials** (Hundreds of grams to few milligrams)

**Cost reduction**

**Time saving** (Several days or weeks to few hours)

### Effect of formulation on storage-induced physical instability

- Excipients and porosity both influenced changes in tablet mass and volume during storage.
- All tablets showed a significant reduction in tensile strength within the first day of storage.

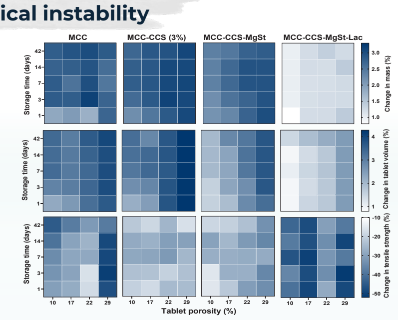


*The average relative change in tablets mass, volume and tensile strength after storage at 50°C/75% RH.*

- The addition of magnesium stearate and lactose slowed disintegration, with a more pronounced effect attributed to MgSt, rather than other excipients.
- Sessile drop measurements indicated reduced wettability after storage, leading to lower liquid uptake and a decreased swelling over time.

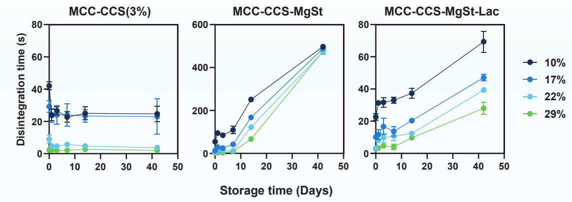


*Disintegration time of tablets before and after storage at 50°C/75% RH.*

## Future work

- Investigating the behaviour of magnesium stearate (MgSt) after storage by analysing potential surface redistribution using Raman spectroscopy.
- Extending DVS studies to improve the scaling factor model by identifying the parameters affecting it (Formulation and storage conditions variations).

AstraZeneca CAMS Pfizer

## POSTER 36

# Comparative Analysis of Antisolvent Crystallisation Screening: Determination of Solubility and Kinetic data through Small-scale Crystallisation Experiments

Farha Kamaal[1,2], Jan Sefcik[1,2], Javier Cardona[1,2,3]
1 Department of Chemical & Process Engineering, University of Strathclyde, United Kingdom
2 EPSRC Future Manufacturing Research Hub for Continuous Manufacturing and Advanced Crystallisation (CMAC), University of Strathclyde, United Kingdom
3 Department of Electronic and Electrical Engineering, University of Strathclyde, United Kingdom

### Introduction

- Antisolvent crystallisation is one of the approaches used in pharmaceutical manufacturing to enhance drug purity and yield. [1]
- Understanding solvent-API interactions during antisolvent crystallisation is key to optimising the process. By adjusting solvent composition and mixing rates, crystallisation outcomes and product properties can be controlled.
- The experiments will compare temperature cycling for pre-mixed samples with isothermal antisolvent addition, evaluating their effects on crystallisation behavior, including crystal size, morphology, and yield.
- This study provides key solubility and kinetic data for various API-solvent-antisolvent systems using the CMAC Crystallisation Screening DataFactory (CSDF).

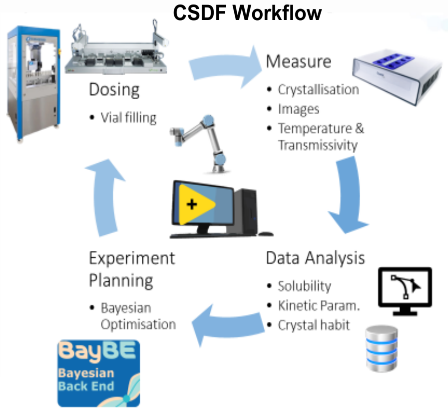


### Methodology

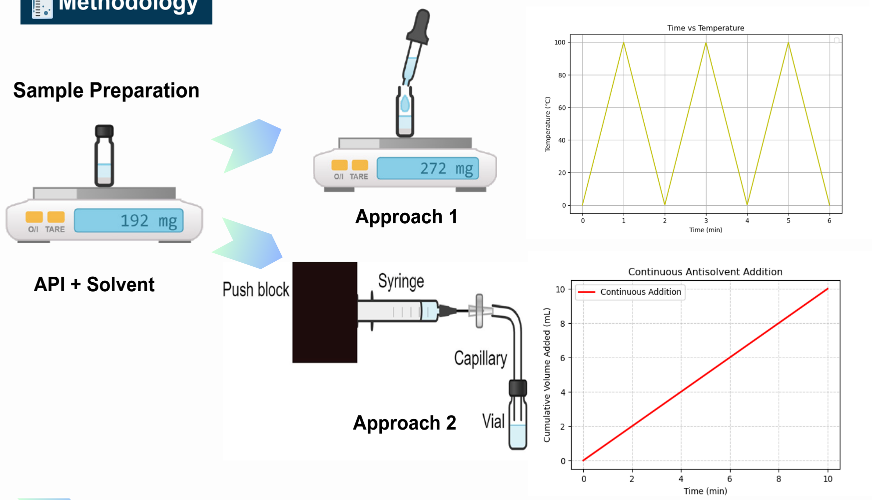


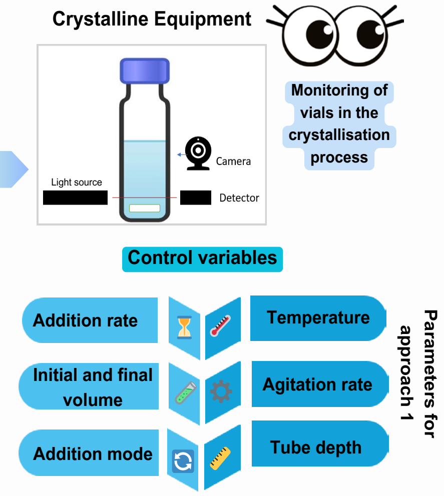


Crystalline showed nucleation trends, while XRPD confirmed phase and polymorphism.

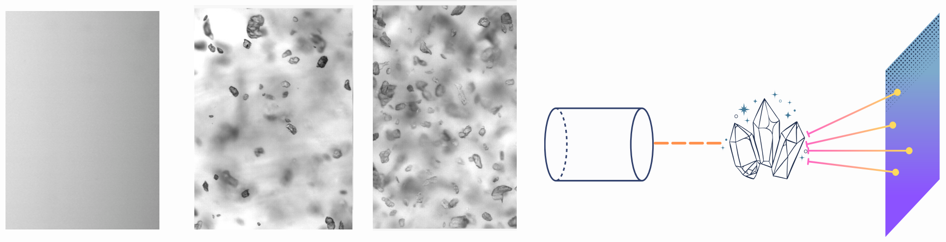

Nucleation & growth rate from Crystalline images

XRPD for crystal form

Parameters for approach 2

- Holding time
- Heating/cooling rate
- End Temperature
- Agitation rate
- Cap type
- Number of cycles

### Future Work

- Begin experimentation with the following API-solvent-antisolvent systems:
  - **Glycine-Water-Ethanol**
  - **Paracetamol-Ethanol-Water**
- Simultaneously study diffusive mixing in antisolvent crystallisation through microfluidic experiments.

**Targets**

- Size, Shape/habit
- Nucleation rate
- Growth rate
- Crystal form
- Detect unwanted outcomes

### References

QR on top

Acknowledgement: EPSRC Continuous Future Manufacturing and Advanced Crystallisation Research Hub (EP/P006965/1) and the University of Strathclyde

## POSTER 37

# A mother liquor recycling approach to recover API and solvent in cooling crystallisation

Yusuf Khan[1,2*], Scott Brown[1,2], Chris J. Price[1,2], Jan Sefcik[1,2], Anna Jawor-Baczynska[3] and Kirstie Milne[3]
1 Department of Chemical and Process Engineering, University of Strathclyde, Glasgow, UK.
2 Centre for Continuous Manufacturing and Advanced Crystallization (CMAC), Glasgow, UK.
3 Chemical Development, Pharmaceutical Technology & Development, Operations, AstraZeneca, Macclesfield, UK.
yusuf.khan@strath.ac.uk

### 1. Introduction

- Recycling the mother liquor in crystallisation operation increases the product yield but also leads to impurity buildup.
- This study investigates the effect of different process topologies on the yield and impurity profile in the mother liquor in crystallization of paracetamol in the presence of two impurities (acetanilide & metacetamol) and methanol as solvent.

### 2. Mother Liquor Recycling (Batch Experiment)

- A simple material balance model was prepared with to obtain the impurity profile and yield for various recycle fractions.

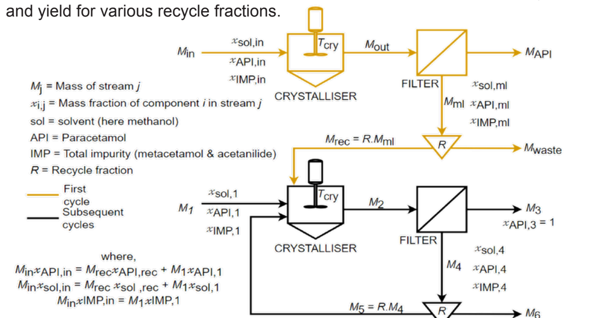


| Component | Mass (g) |
|---|---|
| $M_{in}\,x_{sol,in}$ | 60 |
| $M_{in}\,x_{API,in}$ | 30 |
| $M_{in}\,x_{IMP,in} = M_1\,x_{IMP,1}$ | 1.2 |
| $M_1\,x_{sol,1}$ | 24 |
| $M_1\,x_{API,1}$ | 18.05 |
| $T_{cry}$ | 25°C |

- Mother liquor recycling experiment was carried out at 0.6 recycle fraction of mother liquor for the verification of the model in EasyMax 100 reactor.

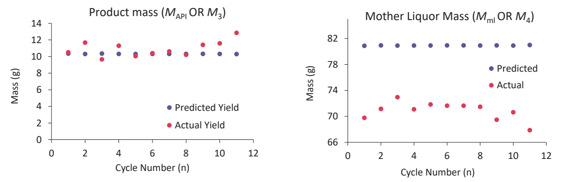


- Product yields were close to the predicted values. As no washing step was carried out, impurities found in the product were significant.

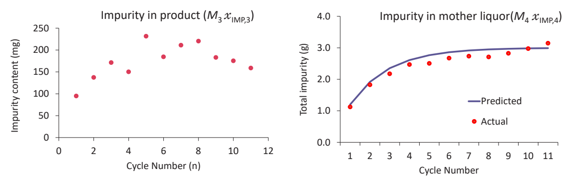


- The model predicted the total impurity content would level off after 10 cycles.
- The impurity in the mother liquor lost was calculated and added to get an the actual impurity content in the mother liquor.
- The difference between the actual and predicted values is due to the assumption in the model that all the impurities are present in the mother liquor and none in the product crystals themselves.

### 3. Mother Liquor Recycling (Rotavap Experiment)

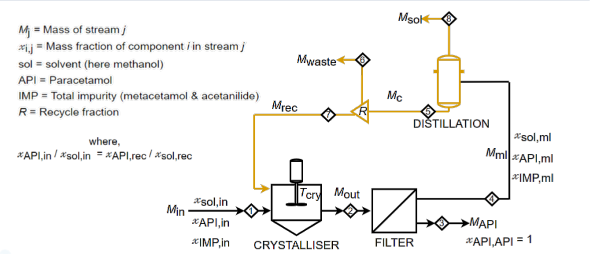


- A material balance model was prepared where the recycle stream was concentrated back up to the initial starting concentration and a fraction of it was recycled to the crystalliser.

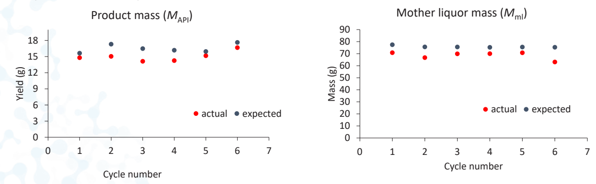


- Experiments were carried out starting from the steady state impurity concentration. A rotary evaporator was used to concentrate the mother liquor back up to the starting concentration and recycle a fraction of it back to the crystalliser.

| Component | Mass (g) |
|---|---|
| $M_{in}\,x_{sol,in}$ | 60 |
| $M_{in}\,x_{API,in}$ | 30 |
| $M_{in}\,x_{IMP,in}$ | 1.5 |
| $T_{cry}$ | 10°C |

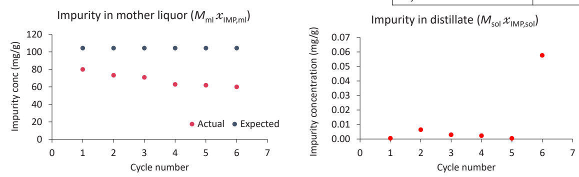


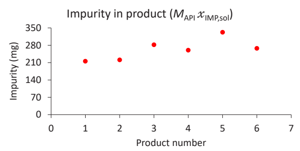


- The impurity profile does not build-up since we started from steady state impurity profile for 0.6 recycle fraction.
- The distillate collected is pure solvent and can be reused as a wash solvent.
- The impurity found in product is significant as we did not carry out a washing step.

### 4. Mother Liquor Recycling (Genevac Experiment)

- Experiments were carried out using a genevac evaporator. The recycle operation consists of 3 steps:-
  1. in which the mother liquor was concentrated further to crystallise API, stopping just before impurities crystallise,
  2. the mother liquor was decanted off as waste and the cake was washed,
  3. the recovered API was recycled back by dissolving it using the recovered solvent.
- The fresh feed from cycle 2 was added such that the input to the crystalliser matches the initial API and solvent amount.
- Impurity amount in fresh feed was kept the same for it to build-up.
- In this topology, API can be lost as waste through stream 7 & 11. Loss of API can be further reduced by using a cold wash and by decanting the liquid off at higher temperature.

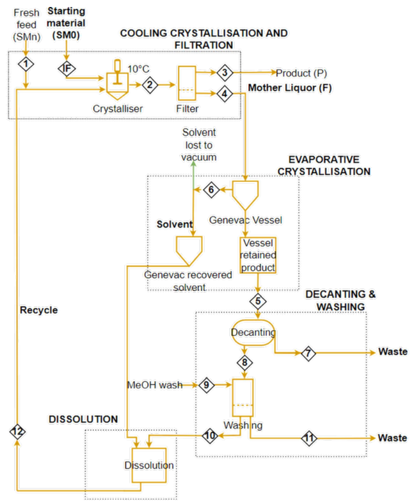


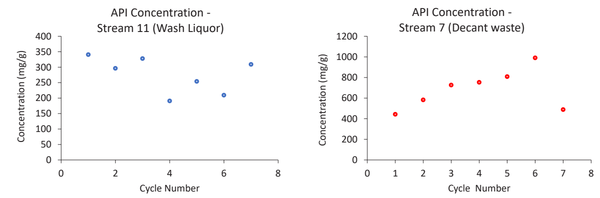


- Since the decanting was done manually and the time between evaporation and decanting operation was not always the same, the API concentration in decanted waste is not consistent.
- The impurity in the mother liquor does not build-up despite feeding the same amount in each cycle. The product obtained is more pure than the previous experiments.
- With further optimizations in the decanting and washing operations, higher yield and purity can be achieved in this topology.

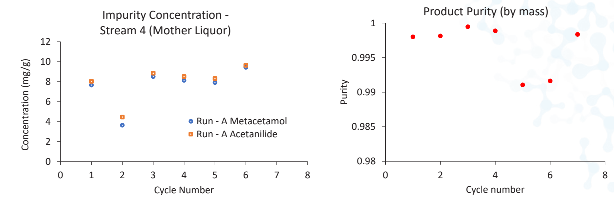


### 4. Conclusion & Future Work

- Mother liquor recycle reduces the solvent waste and increase the yield in API manufacturing.
- Future work will include extending the models to include impurity incorporation during crystal growth.
- The use of other equipment such as membranes for recycle stream concentration and solvent recovery will be investigated.

**Acknowledgement:** Centre for Continuous Manufacturing and Advanced Crystallization (CMAC) and the University of Strathclyde.

**References:** QR on top.

POSTER 38

# Exploring Interfacial Effects on Heterogeneous Crystal Nucleation Using Molecular Dynamics

Mae Macleod[1], Paul A. Mulheran[1], Jan Sefcik[1,2], Karen Johnston[1]

1 Department of Chemical and Process Engineering, University of Strathclyde
2 Future Continuous Manufacturing and Advanced Crystallisation Research Hub, University of Strathclyde

## Motivation

- Nucleation is vital for many industrial processes.
- The majority of crystallisation takes place via heterogenous nucleation, where the nucleus forms at an interface.
- This can be undesirable, causing fouling in vessels, or in other cases nucleants are added to induce nucleation or produce a desired polymorph.
- A greater understanding of heterogeneous nucleation will provide valuable insight into how to better enhance or inhibit nucleation.

## Simulating Nucleation

Nucleation is difficult to observe experimentally due to the time and physical scale of the process. Computational simulation, can provide insight into the initial formation and dynamics of the nuclei.

Nevertheless, due to the rare nature of nucleation, direct simulations of nucleation becomes unfeasible on account of long computation time.

Instead, enhanced sampling methods e.g. metadynamics[1] are used. Though rigorous, they are computationally expensive. A **seeding method** was developed as an alternative, less expensive, approximate method[2].

There are few examples of heterogeneous nucleation simulations, particularly from solution[3].

## Seeding Method

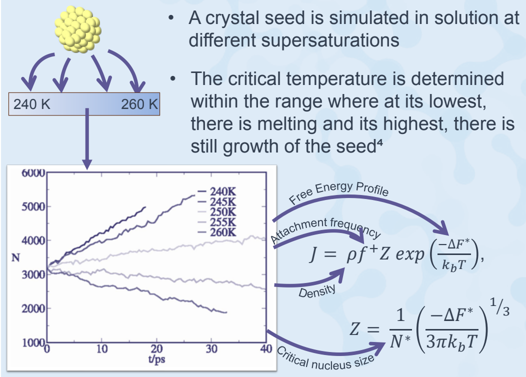


- A crystal seed is simulated in solution at different supersaturations
- The critical temperature is determined within the range where at its lowest, there is melting and its highest, there is still growth of the seed[4]
- The reliability of the seeding method is limited by how the phase of each particle is determined.

## Interfacial Concentration Enhancement Effect

An increased nucleation rate has been observed **experimentally** where a hydrophobic surface is present.

When a **PTFE**[5], or **tridecane**[6] surface was introduced, glycine nuclei were found to preferentially form at the interface rather than in the bulk solution.

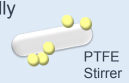


Experimental

This was unexpected, due to the hydrophobic nature of the material, as glycine is a polar, hydrophilic molecule. Similar effects have also been observed experimentally for urea.

To investigate the cause of this effect, the interaction between glycine solution with air, and an oil interface were simulated.

Simulation

The figures below show the density profiles from the **simulation** of glycine at a solution-air and solution-oil interface, carried out by McKechnie[6].

It was found that there was an **increased concentration** of glycine at the tridecane interface. This was thought to be due to dispersion interactions.

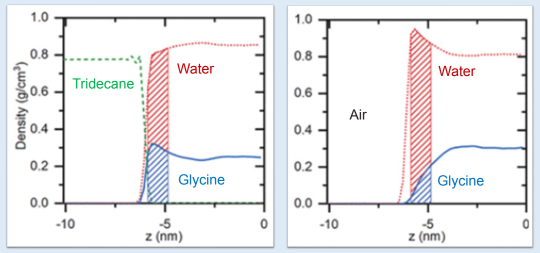


To further study the interface effects, the next stage is to investigate the crystal phase by:

- Planting a crystal seed in the bulk solution.
- Planting a seed on a surface.
- Comparing stability.

## Urea Model

Specialised modelling software is continuously improving, and migrating to new software can be challenging. Previous urea simulations[7] were carried out in LAMMPS, which although versatile, simulation time can be long, making it necessary to transfer to a more efficient software.

### One Urea Molecule

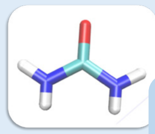

The initial energy values from the simulation of one urea molecule are in excellent agreement between software.

| Energy (kJ/mol) | LAMMPS | GROMACS |
|---|---|---|
| Bond | 302.99 | 302.99 |
| Angle | 0.10 | 0.10 |
| Dihedral | 33.48 | 33.48 |
| Improper | 0.03 | 0.03 |
| Lennard Jones | -0.60 | -0.60 |
| Coulomb | -759.51 | -759.51 |

### Solution Properties

Density

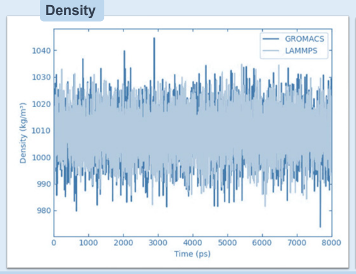


Radial Distribution Function

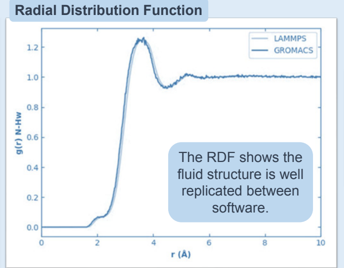


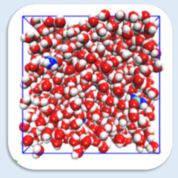

Simulation Snapshot

**Average** (kg/m³) L: 1008.95 ± 0.088, G: 1008.94 ± 0.162

## Future Work

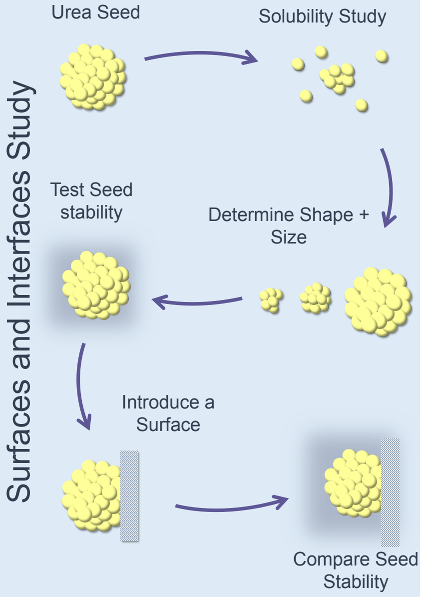


## References

1. M. Salvalaglio,C. Perego,F. Giberti,M. Mazzotti,& M. Parrinello, Molecular-dynamics simulations of urea nucleation from aqueous solution, Proc. Natl. Acad. Sci. U.S.A. 112 (1)
2. P. Lamas, C. and R. Espinosa, et al. Homogeneous nucleation of NaCl in supersaturated solutions. The Royal Society of Chemistry 2021; 23 (47)
3. Finney AR, Salvalaglio M. Molecular simulation approaches to study crystal nucleation from solutions: Theoretical considerations and computational challenges. WIREs Comput Mol Sci. 2024; 14(1)
4. Espinosa JR, Vega C, Valeriani C, Sanz E. Seeding approach to crystal nucleation. J Chem Phys. 2016;144(3):03450
5. Vesga, Maria J. and McKechnie, David et al. Conundrum of γ glycine nucleation revisited: to stir or not to stir? The Royal Society of Chemistry 2019; 21(14)
6. McKechnie D, Anker S, Zahid S, Mulheran PA, Sefcik J, Johnston K. Interfacial Concentration Effect Facilitates Heterogeneous Nucleation from Solution. J Phys Chem Lett. 2020 Mar 19;11(6)
7. Samira Anker, David McKechnie, Paul Mulheran, Jan Sefcik, and Karen Johnston. Assessment of GAFF and OPLS Force Fields for Urea: Crystal and Aqueous Solution Properties.Crystal Growth & Design 2024 24 (1)

University of Strathclyde Engineering

POSTER 39

# Multi-Route Data Factory for Amorphous Solid Dispersion: From Amorphous Solid Dispersions to Oral Solid Dosage Forms

Abdelazeez Mohamednour 1 ,Ecaterina Bordos1, Daniel Markl1, John Robertson1,

Future Manufacturing Hub for Continuous Manufacturing and Advance Crystallisation, Technology and Innovation Centre,
University of Strathclyde, 99 George Street, Glasgow, G1 1RD, UK

## 1- Aim and Context of Work

To transform Amorphous Solid Dispersions(ASDs) produced via Hot Melt Extrusion (HME) to Oral Solid Dosage Forms(OSDFs). By the following methods:
- to Convert ASDs into tablets through **Direct Compression.**
- to Encapsulate ASD powders or granules into **Capsule**.
- to Develop ASD-based **3D-printed tablets** for personalized drug delivery and controlled release.

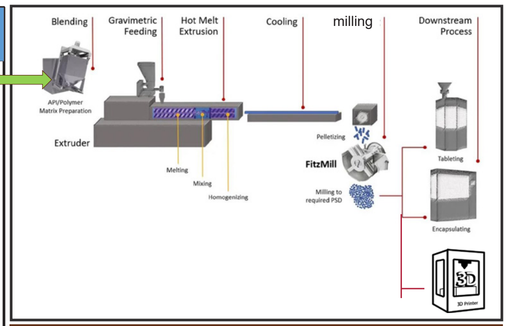


## 2- Challenges

**Physical Stability of ASDs**.
- Risk of crystallization or phase separation.
Process optimization & Selecting the Right Route.
**Performance of the Final Dosage Form**.
- compare the performance of the produced tablets, capsules or the 3D printed tablets.

## 3- Methodology

Production of ASDs via Hot Melt Extrusion

API and polymer blends will be processed through a HME system to produce stable amorphous extrudates.

-Why HME?

-Solvent free.

- Molecular Uniformity

- solubility and bioavailability enhancement.

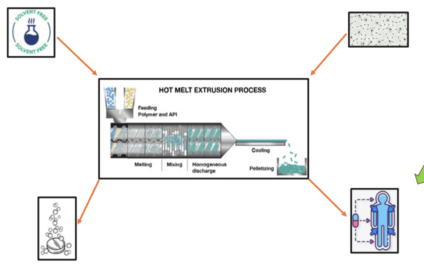


## Down stream processing

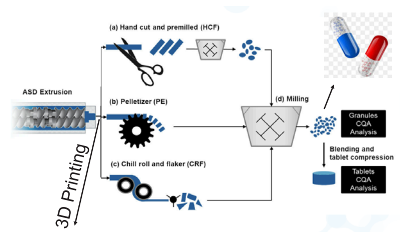


1- Proposed manufacturing routes for the HME extrudate.

(A) Tableting:

Direct compression of the milled extrudate to forms tablets.

(B) Capsule Filling:

Pelletized granules are encapsulated under controlled conditions to ensure uniform dosing and optimized release.

(C) 3D Printing:

By linking HME with 3D Printer

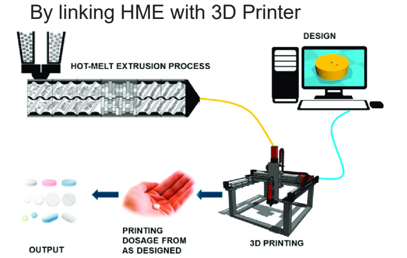


2-Schematic of a combined Hot-Melt Extrusion (HME) and FDM 3D printing into a single continuous process

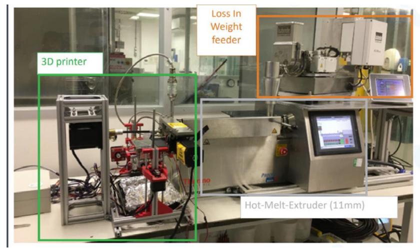


3-Filament free Hot Melt Extrusion 3D printer

## 4-Expected Outcomes

**Solubility Enhancement**: Oral solid dosage forms produced from ASDs are expected to exhibit significant solubility improvements compared to their crystalline counterparts due to the amorphous nature of the API and the inclusion of hydrophilic polymers. However, the specific impact of the OSDF manufacturing route is yet to be determined.

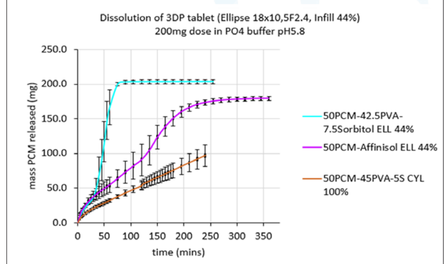


4-impact of formulation and length scale (100% infill versus 44% infil from 3DP dose forms)

A direct head-to-head comparison between 3D printed tablets, capsules and direct compression tablets will be performed to assess release profile and immediate release compliance.

The impact of the OSDF manufacturing route on the ability to sustain the API in the amorphous form and inhibit its crystallisation during dissolution will be assessed.

The addition of additional excipients, such as surfactants and disintegrants, will be considered to enhance dissolution rates by improving wetting and disintegration in aqueous environments

### Characterization of Feedstocks

Change in downstream equipment after the extruder barrel results in differently shaped and sized feedstock materials for milling

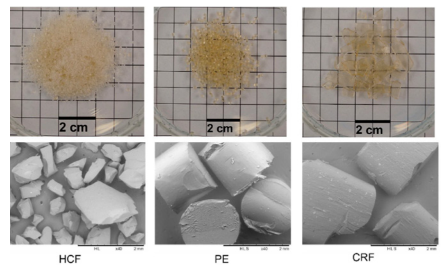


5-Photograph (top) and SEM micrograph (bottom) of different feedstocks for milling. From left to right: HCF,PE, CRF.

## 5-Future Work

- characterization and testing different oral solid dosage forms (OSDFs) to ensure their suitability for pharmaceutical applications.
- Solid-State Characterization.

## References

[1,5] -Downstream Processing of Itraconazole: HPMCAS Amorphous Solid Dispersion: From Hot-Melt Extrudate to Tablet Using a Quality by Design Approach.
[2] - Advanced Pharmaceutical Applications of Hot-Melt Extrusion Coupled with Fused Deposition Modelling (FDM) 3D Printing for Personalized Drug Delivery.
[3,4] -Prasad E, Islam MT, Goodwin DJ, Megarry AJ, Halbert GW, Florence AJ, Robertson J 2019. Development of a hotmelt extrusion (HME) process to produce drug loaded Affinisol™ 15LV filaments for fused filament fabrication (FFF) 3D printing. Additive Manufacturing 29:100776.

## Acknowledgement

The authors would like to acknowledge the advices from Ecaterina Bordos and John Robertson.

## POSTER 40

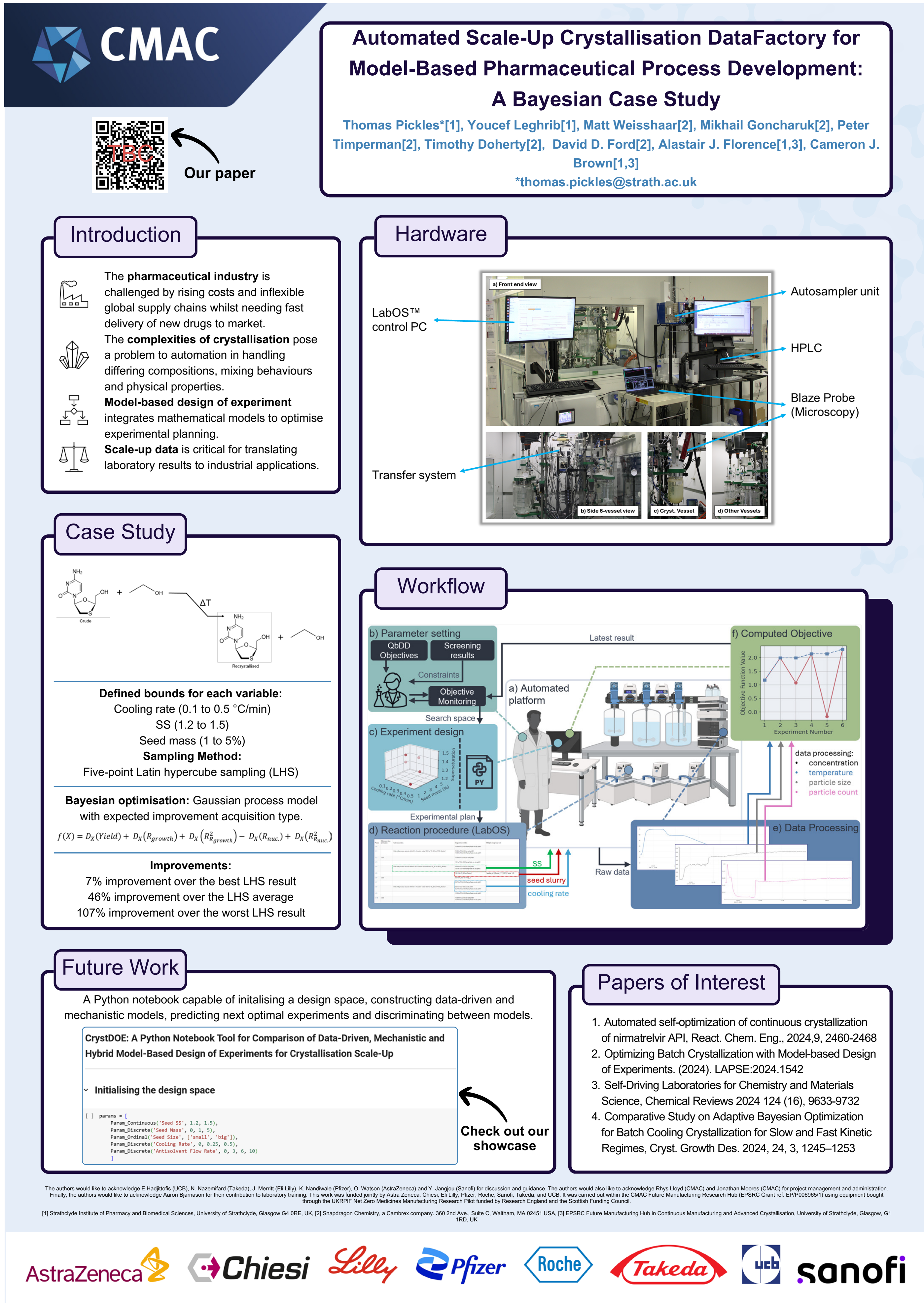


## POSTER 41

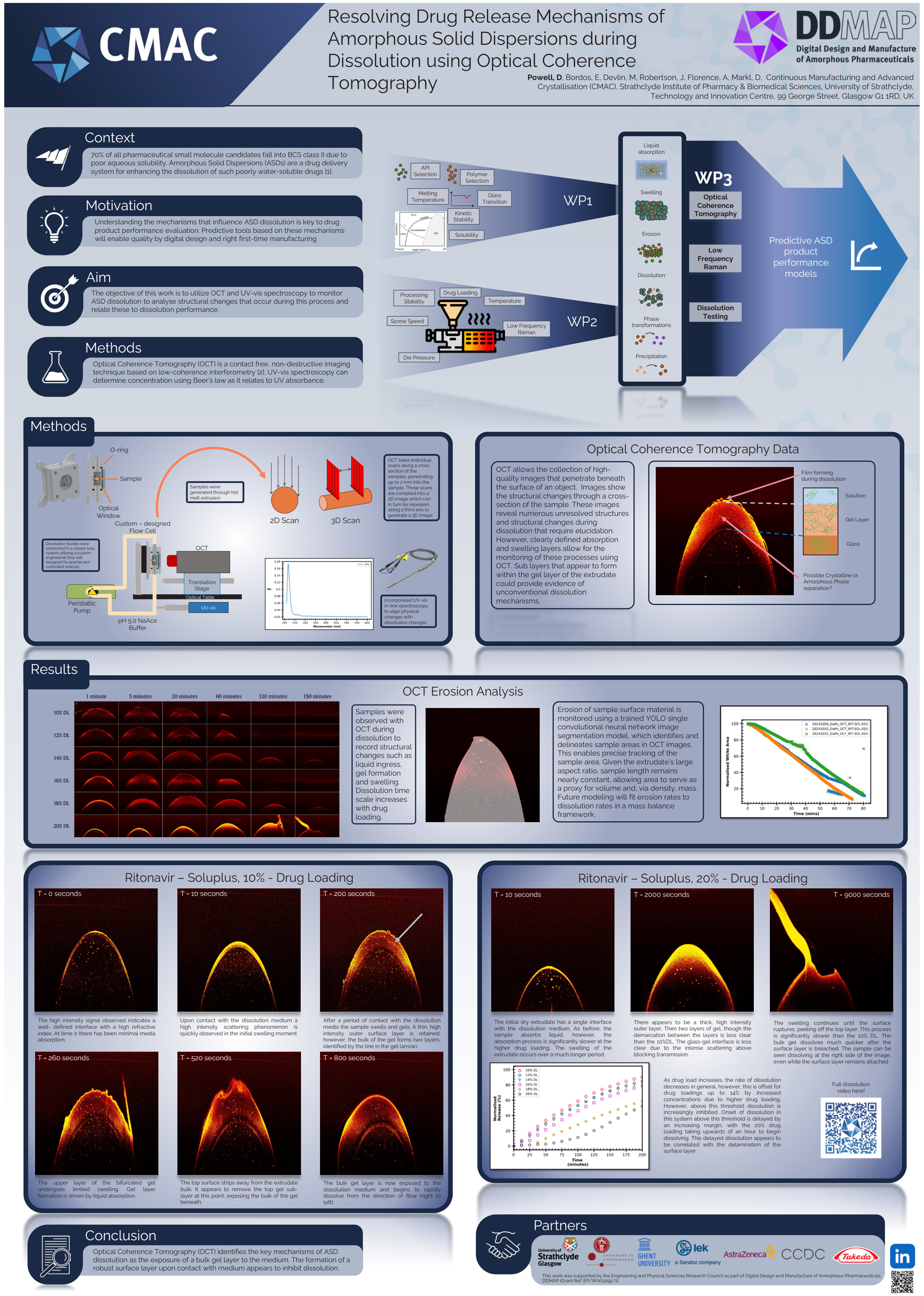

POSTER 42

# Crystallisation Screening DataFactory

Martin Prostredny, Christopher Boyle, Murray Robertson, Sahil Salekar, Parandeep Sandhu, Amal Osman, Connor Clark, Farha Kamaal, Fraser Paterson, Cameron Brown, Javier Cardona, Blair Johnston, Jan Sefcik, John Robertson, Helen Feilden, Alastair Florence

CMAC, University of Strathclyde, Glasgow, UK

## Introduction

Embedded in Platform 1 of the EPSRC MediForge Hub, this cyber-physical system provides a material-sparing, self-optimised, high-throughput sustainable process enabling data integration with models as part of the crystallisation classification system (CCS) model toolbox. Aligned with the industrially relevant RAMI 4.0 framework, the architecture will enable up to 36,000 experiments annually through an autonomous workflow for solvent selection and model-driven experimental design.

This is aligned with **Industry 5.0** through:

- **Sustainability** – 60% material usage reduction target with impact on energy use and waste generation
- **Resilience** – FAIR data management and robust cybersecurity of data fabric, transferable and scalable technology adaption
- **Human-centricity** – up to 90% reduction of repetitive tasks freeing researchers for creative tasks, intelligent decision support

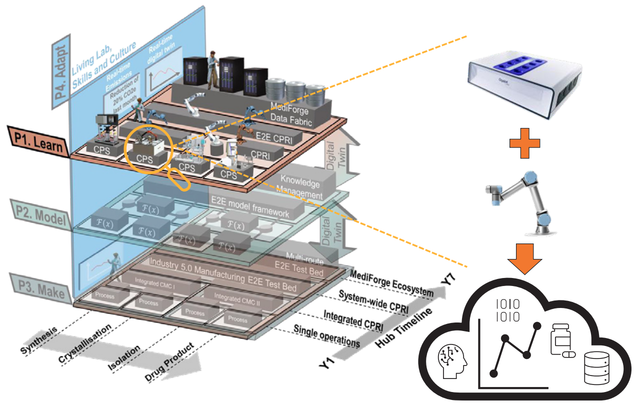


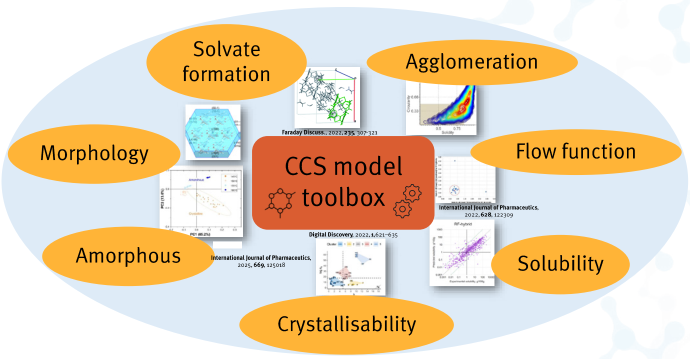


## CSDF vial journey and capabilities

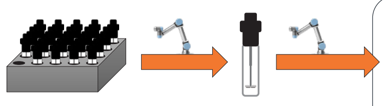

### Vial labelling

Automated QR-code vial labelling using a Leibinger IQJET printer

### Vial dosing

Automated dosing of solids and liquids into the vials using Chemspeed FLEX POWDERDOSE

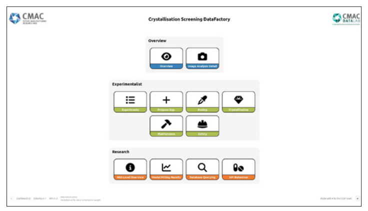

### Crystallisation experiments

Autonomous operation of six Crystalline instruments, including 48 independent reactors, is achieved using a bespoke, in-house-built software solution, enabling experiment queuing, ensuring FAIR data generation, and direct integration with the CMAC data fabric

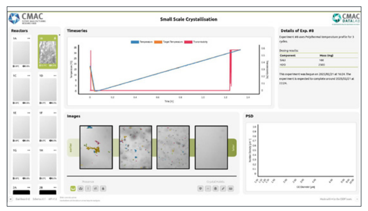

### Post-experiment vial imaging

Identification of fouling, encrustation, crowning, and other effects after crystallisation experiments

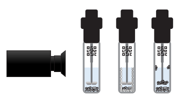

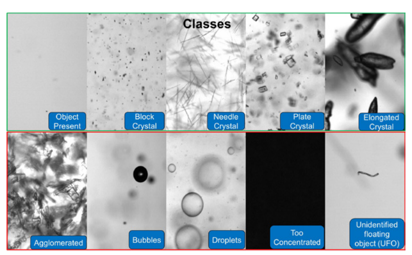


### Online image analysis

Automated detection of cloud & clear points, multi-label classification (crystal shape, agglomeration, bubbles, droplets), particle size and shape data

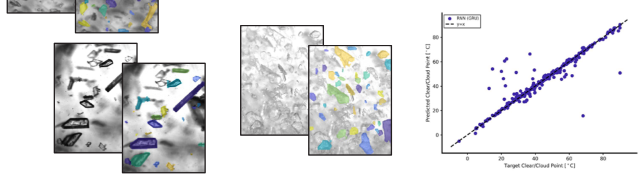

### Raman spectroscopy analysis

Rapid online analysis of solid form using Raman spectroscopy directly after crystallisation experiments prior to isolation using a Tornado HyperFlux PRO Raman with Hudson S04 probe head

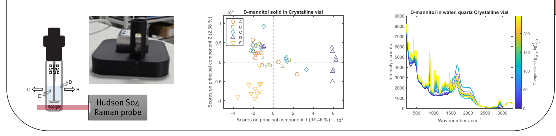

### Sample isolation

Filtration to obtain powder for subsequent analysis (e.g. X-Ray)

### X-Ray diffraction

High-throughput X-Ray diffraction analysis of solid form using the Bruker D8 ENDEAVOR

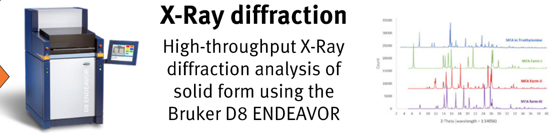

**Acknowledgements**

This work was supported by Research England and the Scottish Funding Council under the UK Research Partnership Investment Fund CMAC Data Lab: A Digital Medicine Manufacturing Research Accelerator and Net Zero Medicines Manufacturing Research Pilot. This work was also supported by EPSRC MediForge Hub: Industry 5.0 Medicines Manufacturing Research Hub (EP/Z532964/1) and Made Smarter Innovation - Digital Medicines Manufacturing Research Centre (EP/V062077/1).

POSTER 43

# Automation of amorphous solid dispersions physical stability prediction

Lewis Ross, Michael Devlin, John Robertson Alastair Florence

CMAC & Strathclyde Institute of Pharmacy and Biomedical Sciences (SIPBS)

DDMAP Digital Design and Manufacture of Amorphous Pharmaceuticals

### Motivation

- Amorphous active pharmaceutical ingredients (API) may offer improved pharmacokinetic performance over poorly soluble crystalline API.
- However, they may exhibit poor chemical and physical stability through a higher free energy state. This may lead to subsequent crystallisation during storage or after ingestion
- Amorphous solid dispersions (ASD) offer a viable approach to enhance the physical stability of an amorphous system since they may restrict molecular mobility and reduce the thermodynamic driving force for crystallisation for an API.
- This project leverages automation to create a large stability database, improving predictive tools for material -sparing ASD stability assessment.

### Objectives

- Build an end-to-end automated workflow which enables a high throughput screening of ASD stability
- Autonomous high throughput screening workflow utilising an automated dosage platform
- Image analysis to autonomously capture and report sample stability
- Machine learning model for prediction of ASD stability

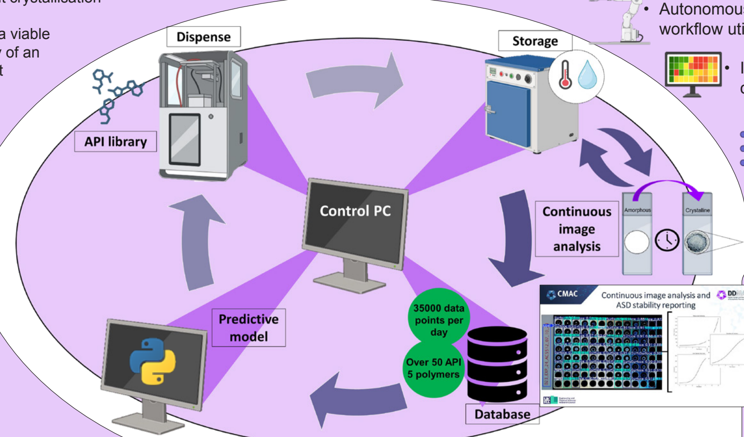


### Why Automate?

- Automated workflow: higher throughput and 24/7 operation
- FAIR database principles enhance data integrity
- Consistency and traceable samples throughput entire workflow
- Ensures reproducibility
- Limits human error and exposure to hazardous chemicals or repetitive manual tasks

### Autonomous analysis of samples

**Well classes**

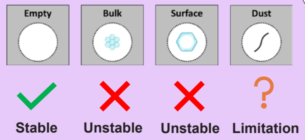


- Sample stability distinguished using classifiers above
- Image analysis model has been trained using 8000 annotated images
- Each well is imaged every 2 hours to capture:

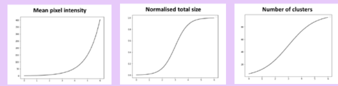


- To characterise ASD stability, polarised light imaging is used to detect birefringence within individual samples.
- Samples autonomously monitored to report the onset of crystallisation and monitor subsequent growth rates *in-situ*.

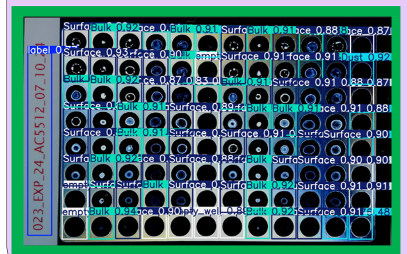

| Well classes | mAP50 (Accuracy) |
|---|---|
| Empty well | 0.956 |
| Surface | 0.833 |
| Bulk | 0.872 |
| Dust | 0.925 |

Validation of model using a pre-split dataset following 80:20

### Bespoke storage solution

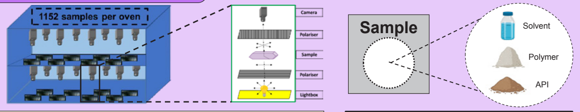


| Conditions | Storage time |
|---|---|
| 40 °C/ 75 % RH | 3 months |
| 30 °C/ 30% RH | 3 months |
| 40 °C/ 0% RH | 3 months |

Per oven there are:
- 12 API mixed with 5 polymers at 8 DL's
- 1152 samples per oven (we have 3 oven conditions)
- 50 APIs at 3 varied stability conditions
  - 12,300 samples
- Imaged once every 2 hours = millions of data points…

Currently running three full ovens:
= 3456 samples continuously monitored
= 41472 data points per day

- Polymer + API solutions prepared using DMSO
- Samples dosed onto a 96-well plate
- Only 60 µg of material used

**Amorphous** – When samples remain amorphous, there is no effect on the polarised light since the material is isotropic. This is a stable amorphous system

**Crystalline** – Once a sample crystallises, it is anisotropic and causes the polarised light to 'split', enabling us to visibly see light through the sample

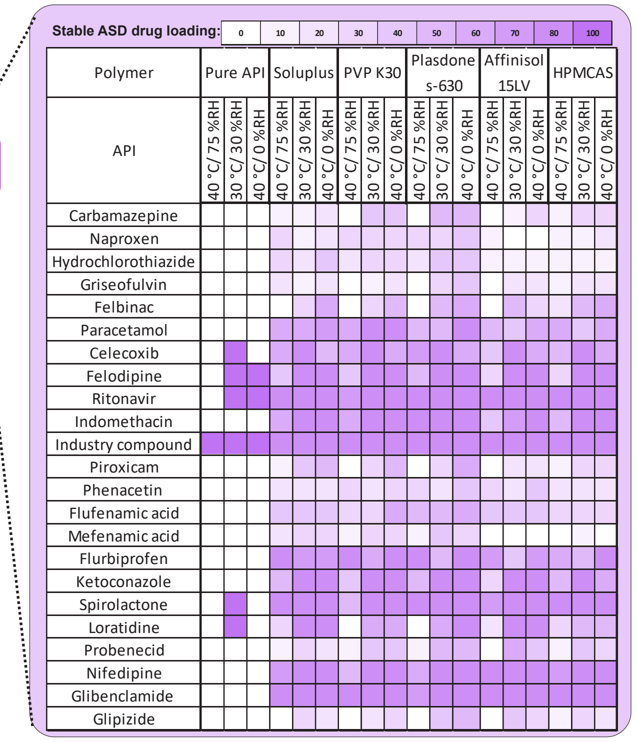


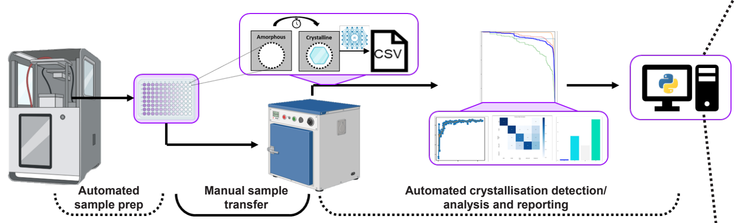


### Conclusions and further work

- Successfully implemented an automated workflow to prepare over 15000 ASD samples for stability testing
- Image analysis can detect the onset of crystallisation for ASDs and subsequently report this as a csv to a database
- Continue implementing workflow to obtain stability data for over 50 API
- Generation of a machine learning model from experimental results to predict the stability of ASDs and extract governing factors in amorphous stability

### References

[1] – Taresco et al, Rapid Nanogram Scale Screening Method of Microarrays to Evaluate Drug-Polymer Blends Using High-Throughput Printing Technology, *Mol Pharm*, **14**, 2079-2087 (2017)
[2] – Eerdenbrugh et al, Small scale screening to determine the ability of different polymers to inhibit drug crystallization upon rapid solvent evaporation, *Mol Pharm*, **7**, 1328-1337, (2010)

### Acknowledgements

This work was supported by the Engineering and Physical Science Research Council as part of Digital Design and Manufacture of Amorphous Pharmaceuticals, DDMAP (Grant Ref: EP/W003295/1), EPSRC DTP REA scheme, University of Strathclyde and CMAC Tier 1 membership

POSTER 44

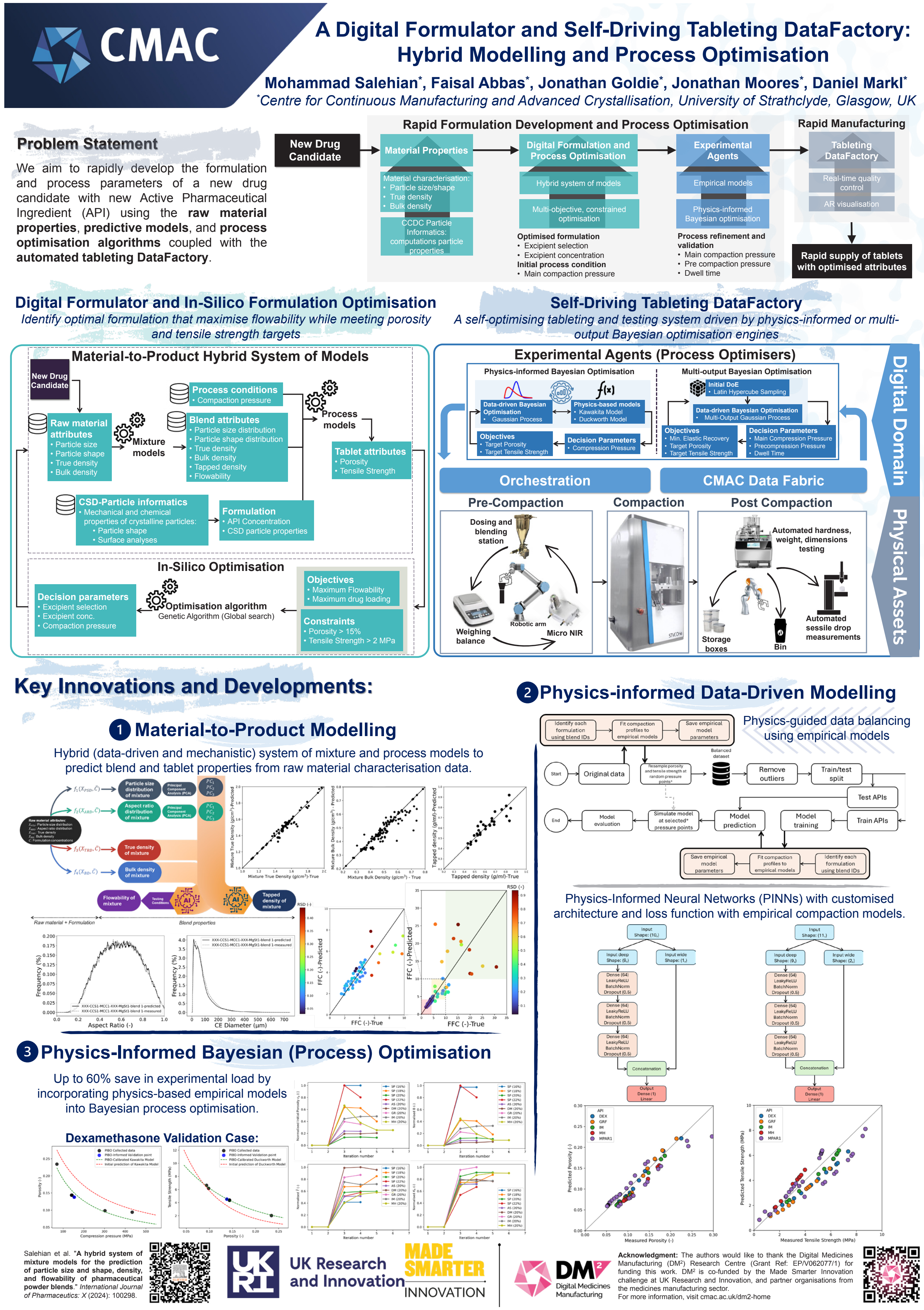


POSTER 45

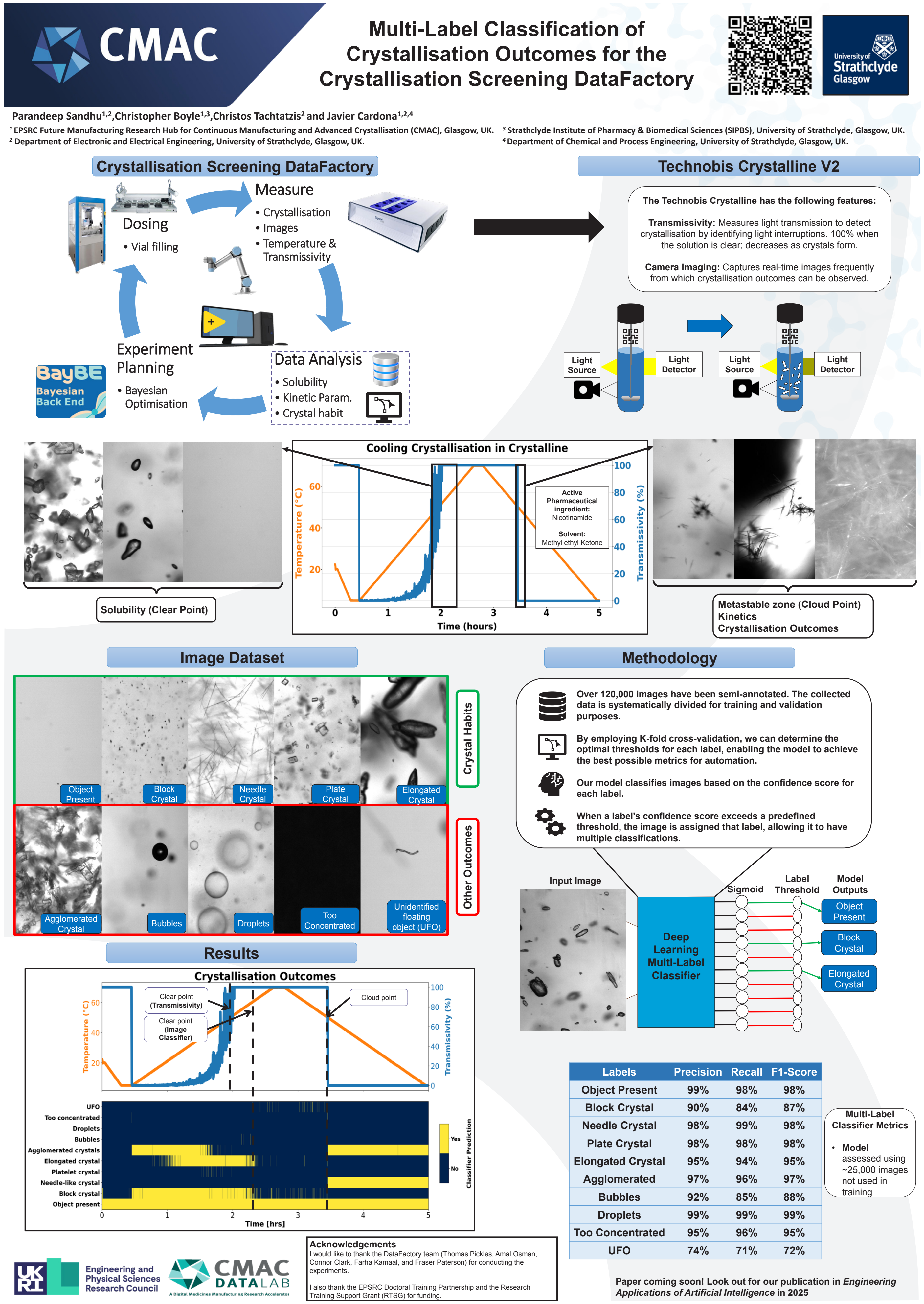


| Labels | Precision | Recall | F1-Score |
| --- | --- | --- | --- |
| Object Present | 99% | 98% | 98% |
| Block Crystal | 90% | 84% | 87% |
| Needle Crystal | 98% | 99% | 98% |
| Plate Crystal | 98% | 98% | 98% |
| Elongated Crystal | 95% | 94% | 95% |
| Agglomerated | 97% | 96% | 97% |
| Bubbles | 92% | 85% | 88% |
| Droplets | 99% | 99% | 99% |
| Too Concentrated | 95% | 96% | 95% |
| UFO | 74% | 71% | 72% |

POSTER 46

# Innovative Approaches to Near-InfraRed Partial Least Squares Calibration: 1) Microscale Blending DataFactory and 2) Digital NIR Spectroscopy

A.Tsioutsios*[1,2], F.Abbas[1,2], J.Goldie[1], M.Salehian[1,2], B.Johnston[1,2], D. Markl[1,2]
[1]Centre for Continuous Manufacturing and Advanced Crystallisation (CMAC), University of Strathclyde
[2]Strathclyde Institute of Pharmacy and Biomedical Sciences (SIPBS), University of Strathclyde

## Keywords

- Innovation
- Automation
- Sustainability
- Efficiency

## Challenges in NIR PLS calibration

**Workload**
Intensive blend prep, NIR, and HPLC tasks

**Material Usage**
High material demand for powders and solvents

## Aims

1. Develop PLS models for API conc. prediction using a robotic microscale blending process coupled with NIRS for sustainable calibration.
2. Train Random Forest ML to predict Blend NIR spectra from Raw Material NIR spectra, providing a robust alternative to PLS model calibration.

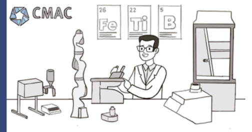

## Automated Robotic-Assisted Microscale Blending coupled with NIRS

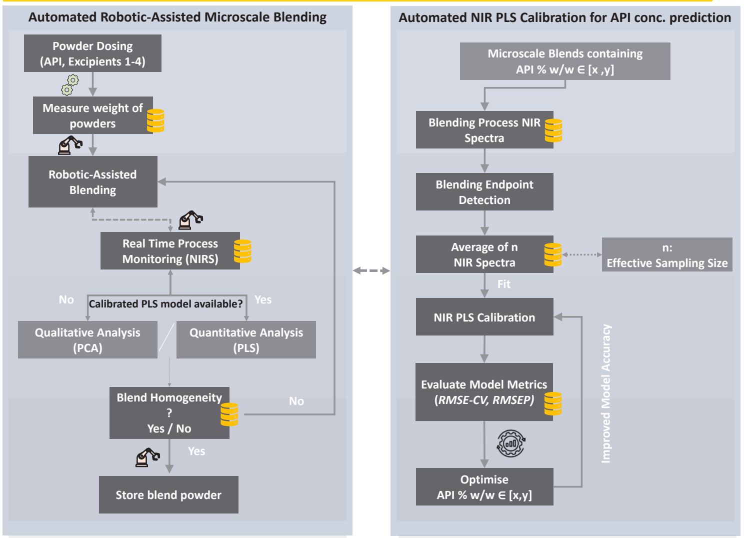


PLS: Partial Least Squares
PC : Principal Component
MBSD: Moving Block Standard Deviation

Qualitative Process Monitoring of Microscale Blending

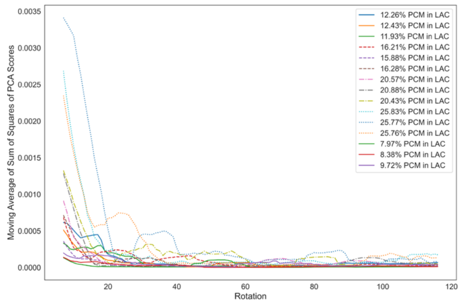


**NIR PLS K-Fold Cross Validation**

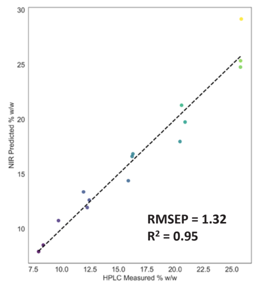


**NIR PLS Test**
Blends tested were prepared using the Turbula T2GE blender

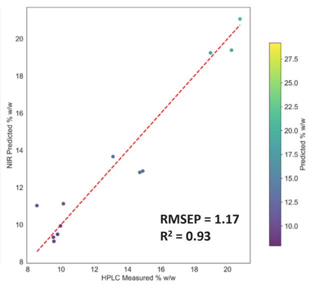


## Digital NIR Spectrometer Workflow

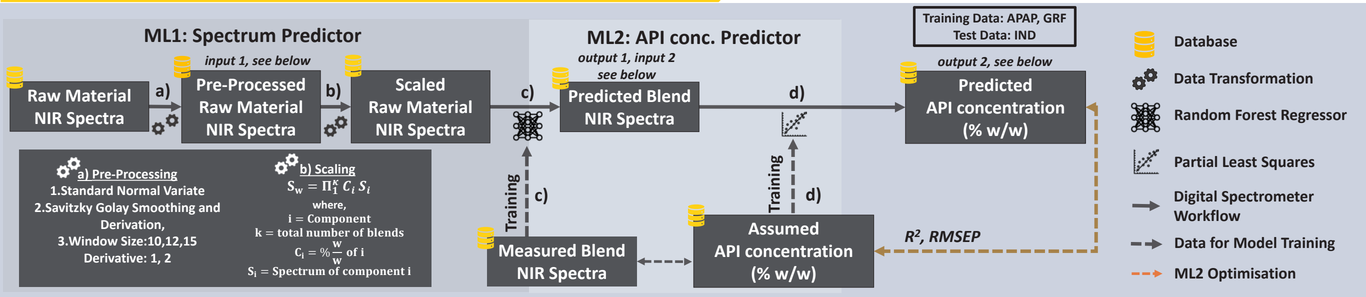


**Input 1: Measured Raw Material NIR Spectra Pre-Processed and Scaled**

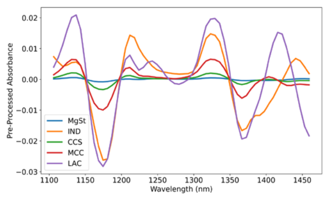


**Output 1: Predicted Blend Spectrum**
(e.g. IND = 30%, CCS = 5%, MCC = 18%, LAC = 46%, MgSt = 1%)

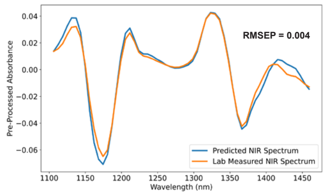


**Input 2: Predicted Blend Spectra Range 5-30 % w/w of IND**

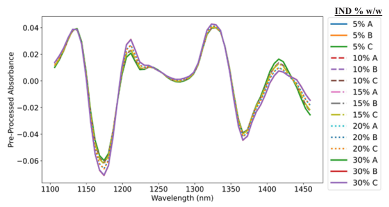


**Output 2: Predicted API Conc.**

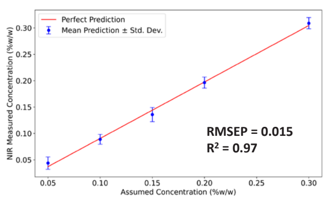


## Future Work

1. Enhance the efficiency of the automated microscale blending process by improving the precision of material transfer from vials to the 3D-printed Transportation Unit (3D-TU).
2. Leverage these advancements to expand the NIR spectral data library, enabling more robust training of machine learning models for accurate prediction of NIR blend spectra.

## References

1. Daniel Markl, Martin Warman, Melanie Dumarey, Eva-Lotta Bergman, Staffan Folestad, Zhenqi Shi, Leo Francis Manley, Daniel J. Goodwin, J. Axel Zeitler, Review of real-time release testing of pharmaceutical tablets: State-of-the art, challenges and future perspective, International Journal of Pharmaceutics, Volume 582, 2020, 119353.
2. Natasha L. Velez, James K. Drennen, Carl A. Anderson, Challenges, opportunities and recent advances in near infrared spectroscopy applications for monitoring blend uniformity in the continuous manufacturing of solid oral dosage forms, International Journal of Pharmaceutics, 615, 2022, 121462.

UK Research and Innovation
MADE SMARTER INNOVATION
DM² Digital Medicines Manufacturing

**Acknowledgment:** The authors would like to thank the Digital Medicines Manufacturing (DM²) Research Centre (Grant Ref: EP/V062077/1) for funding this work. DM² is co-funded by the Made Smarter Innovation challenge at UK Research and Innovation, and partner organisations from the medicines manufacturing sector. For more information, visit cmac.ac.uk/dm2-home

DM² website

POSTER 47

# Advanced characterization: X-ray capability within CMAC national facility

Martin R. Ward, Rachel Feeney, Alan Martin – email: cmac-national-facility@strath.ac.uk
*The University of Strathclyde, CMAC National Facility*

## Single crystal diffraction

- 2 diffractometers (Cu, and Mo sources)
- Latest technology detector (Photon III CMOS) – provides highest sensitivity
- Both equipped with cryostat for variable temperature studies
- Cu system ideally suited to routine structure and absolute configuration determination

***High pressure crystallography***
- Mo system dedicated to high pressure diffraction
- Single crystal and powder
- High brilliance
- Routine structure solution at high pressure conditions
- Can also provide insitu high pressure PXRD

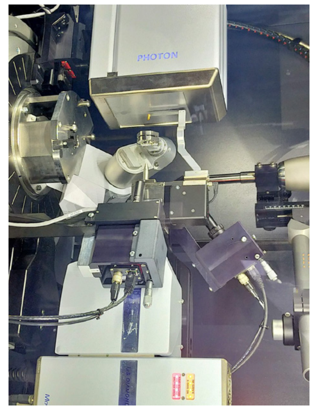

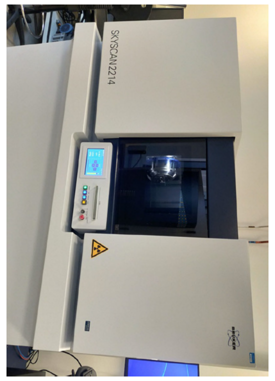

## Xray microscopy

Bruker Skyscan 2214 nano-CT:
- < 500 nm spatial resolution
- 2 detector options:
- Flat panel – large format/fast imaging
- sCMOS – high resolution imaging
- High power source (160 kV, x uA) required for dense material imaging and optimizing for composite device imaging
- Can image vast range of materials from individual particles, to tablets, and complex medical devices

## X-ray Pair Distribution Function (x-PDF)

- Dedicated instrument for x-PDF data collection
- Multiple samples per day throughput
- Analysis of amorphous structure
- Relate changes in amorphous structure to stability
- Nanoparticle characterisation

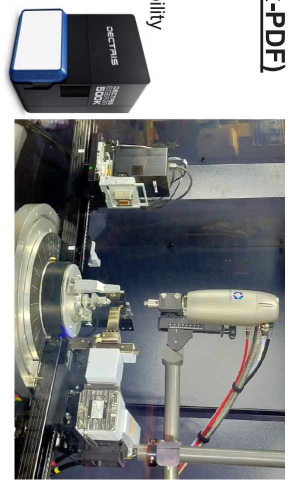

## Powder x-ray diffraction

Wide range of kit available in lab:
- Capillary PXRD
  - High resolution data
  - Indexing, Rietveld refinement, Quantitative PXRD, structure solution from powder data
  - Cryostat for variable temperature measurement (80-500 K)
    - Phase transitions, desolvation/hydration, stability testing etc.
- Screening PXRD
  - High throughput (40 sample plate)
  - Transmission geometry
  - Excellent signal:noise
    - Identify samples of interest for high resolution data collection, e.g. new forms, ID impurities etc.
- Reflection PXRD
  - Can accommodate large sample sizes, and highly absorbing materials
  - Number of useful accessories:
  - Anton Paar CHC+ temperature and humidity stage
  - Provides insitu PXRD testing during controlled temperature and humidity runs
  - Goebel mirror – allows setup for thin film testing and surface measurement

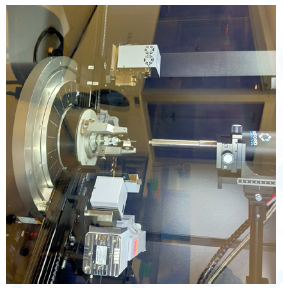

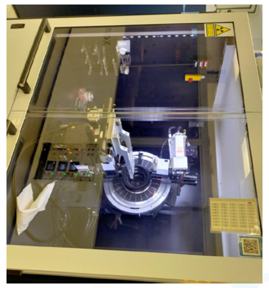

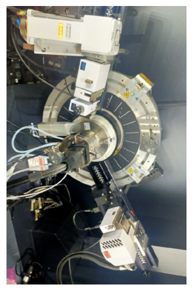

xenocs
Exploring the very small

## Small angle x-ray scattering (SAXS)

Xenocs Xeuss 2.0 SAXS system (2.5 m sample-detector distance)
- 3 xray source options (Cu, Mo, and Cr)
- Large area detector (Dectris 1M)
- Combined SAXS/WAXS
- Insitu PXRD
- GISAXS

Example application areas:
- Size/shape analysis lipid-nanoparticles
- Nanomedicines stability/binding
- Stress-strain analysis

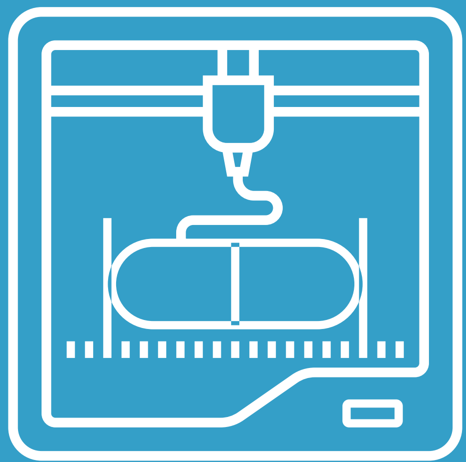

# MicroFactories & Advanced Process Technology

POSTER 49

## CORE project: Industrialisation of Spherical Agglomeration

Bilal Ahmed – CMAC,
University of Strathclyde

This poster will be available at the conference

## POSTER 50

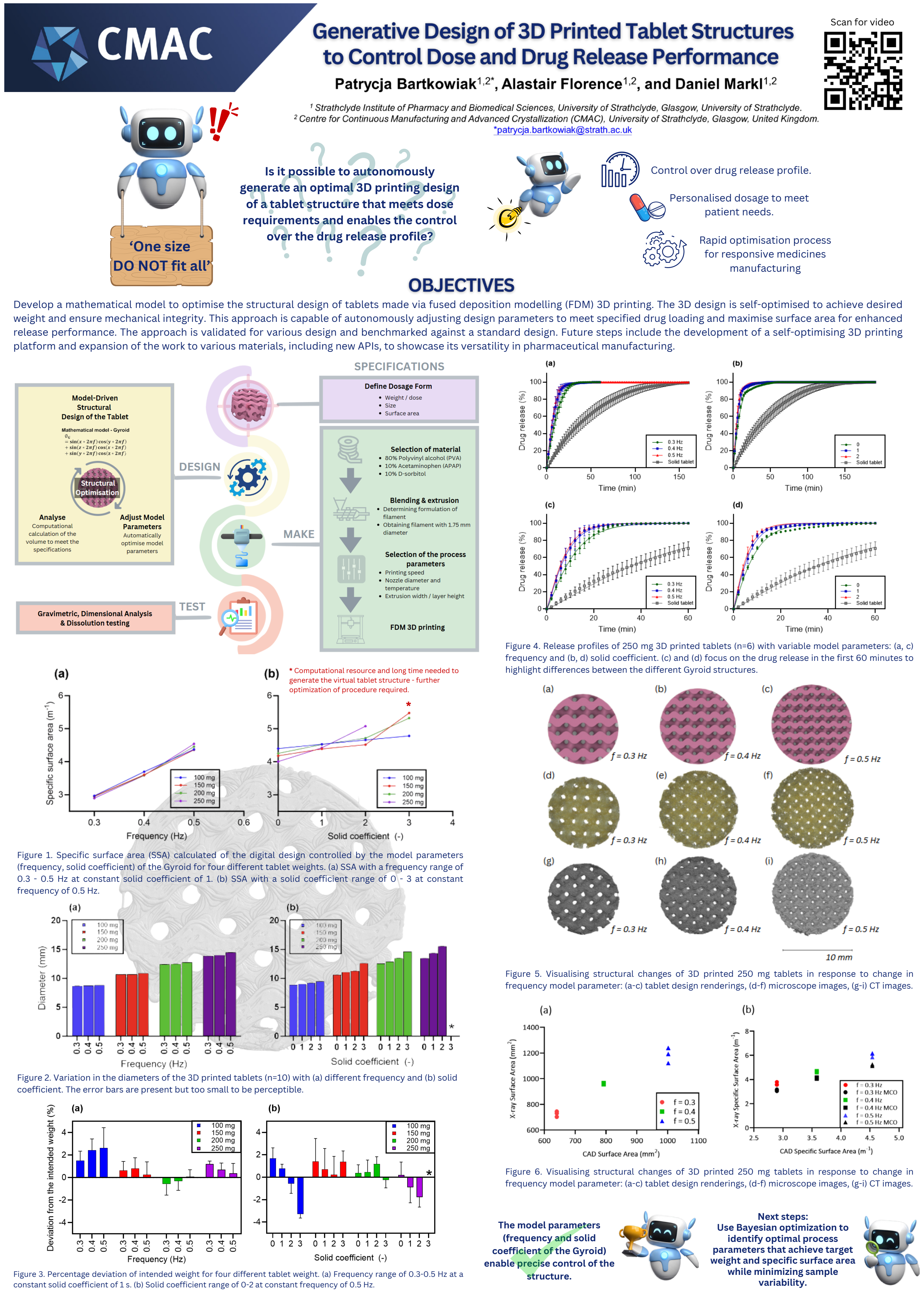


## POSTER 51

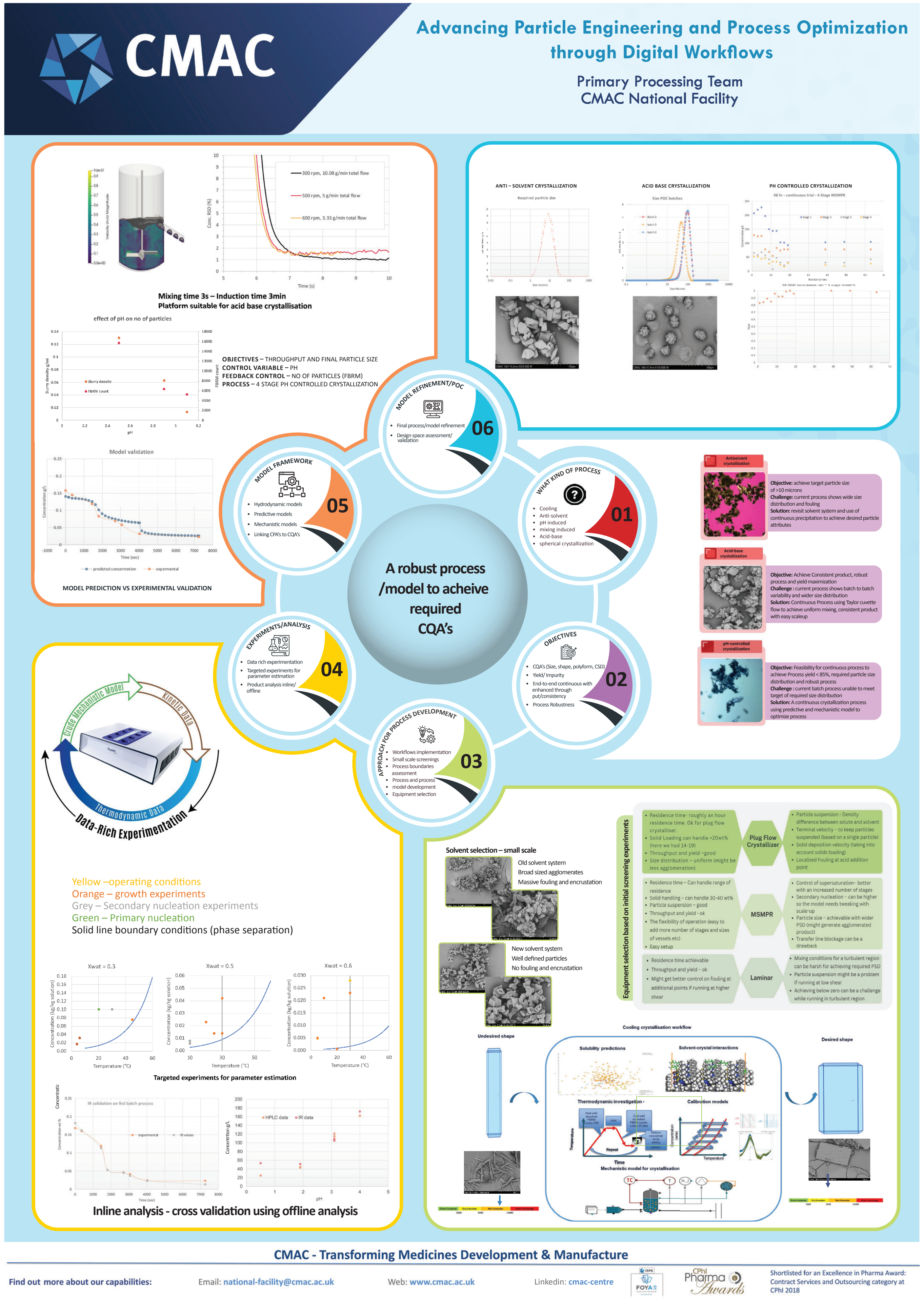

## POSTER 52

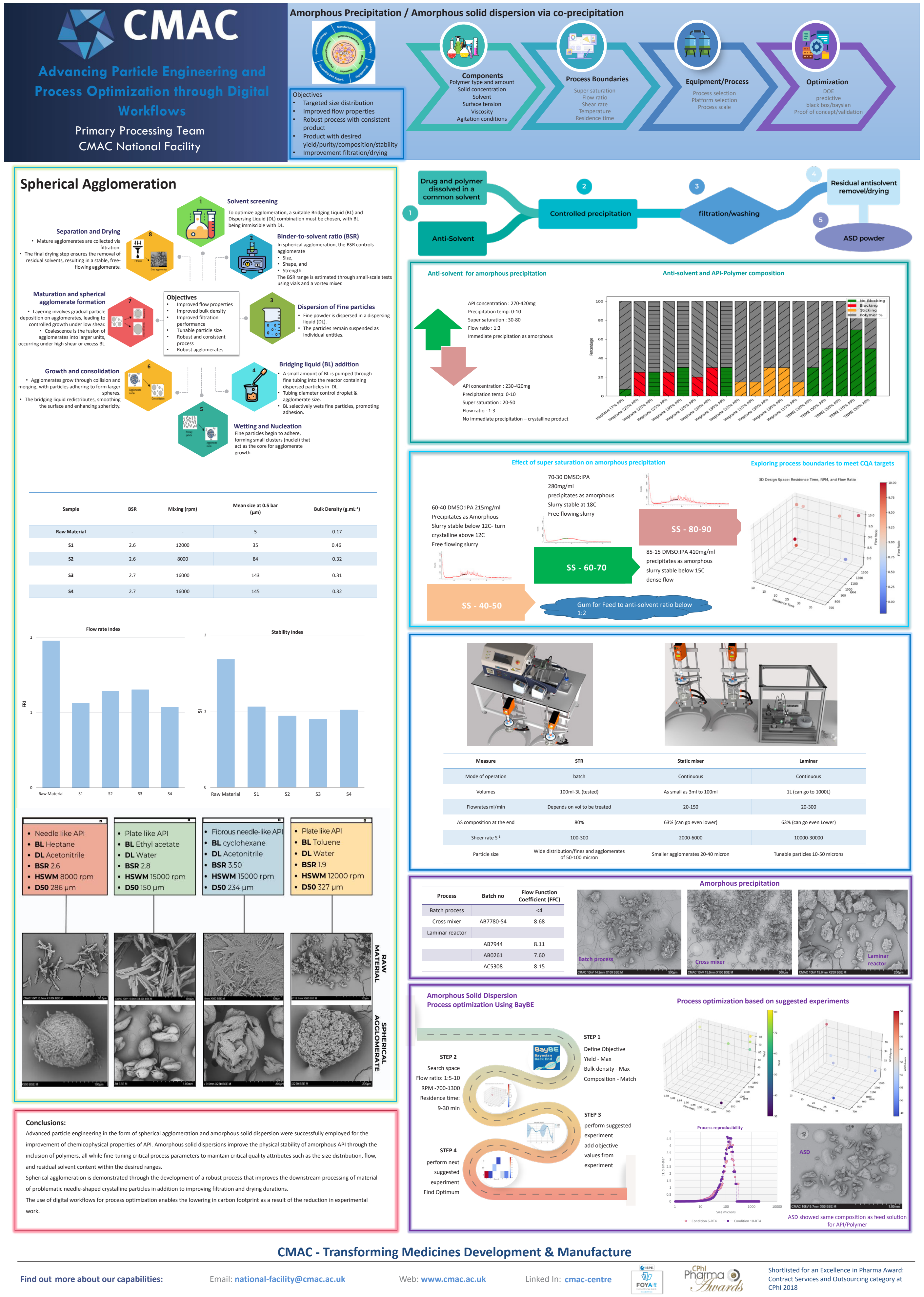


## POSTER 53

# Breaking the crystal lattice: navigating the development of stable amorphous drug products via the API-polymer solubility challenge

Ecaterina Bordos – CMAC, University of Strathclyde

This poster will be available at the conference

POSTER 54

## Advancing UV Calibration and Control Strategies for Real-Time Supersaturation Management in Crystallisation

Humera Siddique – CMAC, University of Strathclyde

This poster will be available at the conference

POSTER 55

## Self-optimisation of dynamic heterogeneous catalytic systems

Soya Dohi – University of Leeds

This poster will be available at the conference

POSTER 56

# SCALING UP AGITATED FILTER DRYERS: THE EFFECTS OF AGITATION ON AGGLOMERATION RATES

Suruthi Gnanenthiran[1], Pari Rao[2], Christopher Hewitt[2], Kate Pitt[1] & Rachel Smith[1]

1. School of Chemical, Materials and Biological Engineering, University of Sheffield, UK 2. Chemical Development, Pharmaceutical Technology & Development, Operations, AstraZeneca, Macclesfield, UK

## INTRODUCTION

Agitated filter dryers (AFDs) are commonly used in the pharmaceutical industry for efficient filtration and drying. The agitation improves heat and mass transfer, resulting in better product uniformity and shorter drying times.[1] Ideally, materials are dried without altering any properties achieved during crystallisation to preserve drug performance behaviour. However, intense agitated drying conditions can result in undesired particle agglomeration, leading to manufacturing challenges such as out-of-specification products, additional milling, and extended cycle times.

## MOTIVATION

Drying in AFDs is a dynamic process where heating and agitation of the wet cake can result in the formation of solid bridges leading to agglomeration.[1] Previous work implemented a mechanistic approach to isolate the effects of agitation during drying. Building on this, the current study evaluates constant tip speed as a scaling index to determine whether agglomeration behavior can be successfully scaled up in a larger AFD when geometric similarity is maintained. The extent of agglomeration is investigated for samples with an average initial moisture content of 20 % subjected to various agitation speeds and time periods. Existing knowledge of wet granulation processes is used to design this work as similar mechanisms may occur (Figure 1).

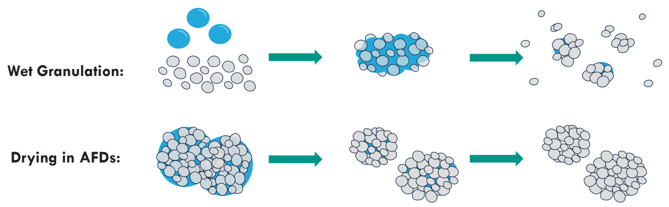


*Figure 1 – Contrasting mechanisms of wet granulation to drying in AFDs*

## RESULTS OF SCALE UP

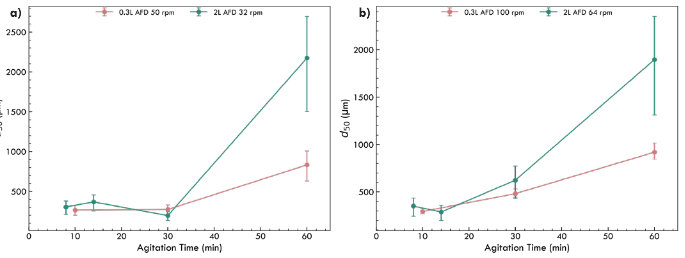


*Figure 2 – $d_{50}$ values over time at (a) low speeds and (b) high speeds*

- At low speeds, scale-up data shows good agreement, indicating tip speed scaling effectively matches energy input per unit mass, resulting in comparable granule dynamics.
- Initial balance between agglomeration and breakage shifts toward agglomeration dominance at 60 mins, more prominently in the larger AFD.
- At higher speeds, agglomeration increasingly dominates over breakage with longer agitation, though $d_{50}$ values diverge due to greater breakage promoting snowballing in the larger AFD.
- Agglomeration trends provide further insight into underlying mechanisms.
- Scaling with tip speed replicates agglomeration behaviour qualitatively however quantitative differences are observed.

## MATERIALS AND METHODS

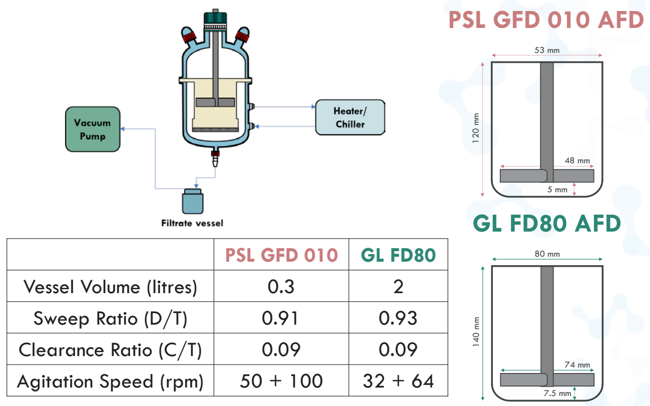


| | PSL GFD 010 | GL FD80 |
|---|---|---|
| Vessel Volume (litres) | 0.3 | 2 |
| Sweep Ratio (D/T) | 0.91 | 0.93 |
| Clearance Ratio (C/T) | 0.09 | 0.09 |
| Agitation Speed (rpm) | 50 + 100 | 32 + 64 |

**Jacket Temperature**
25 °C
**Impeller geometry**
45° pitch blade
**Agitation time**
8 to 60 min

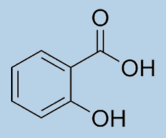

**API**
Salicylic acid
$d_{10}$ = 22.3 μm
$d_{50}$ = 52.3 μm
$d_{90}$ = 111.0 μm
(Mastersizer)
**Solvent**
Distilled water

| Measurement | Characterisation Technique |
|---|---|
| Moisture Content | Moisture Analyser |
| Agglomerate Size Analysis | Sieving |
| Imaging | Scanning Electron Microscopy (SEM)<br>Micro-computed tomography (Micro-CT) |

## MORPHOLOGY OF AGGLOMERATES

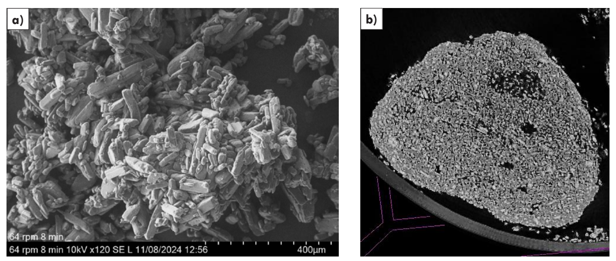


*Figure 3 – (a) SEM image and (b) Micro-CT cross-section of dried agglomerates*

Large clusters of particles visible in SEM image, highlighting extensive agglomeration. Micro-CT cross-sectional image indicates packing of fines on the outer surface of an agglomerate, consistent with a snowballing mechanism. This growth mechanism results from fines generated from breakage adhering to wet agglomerates to promote further growth.

## CONCLUSIONS AND OUTLOOK

Tip speed scaling qualitatively replicates agglomeration behavior across scales. → Quantitative differences due to increased breakage in the larger AFD. → Investigate other scaling indices for improved quantitative scaling.

REFERENCES
1. H. L. Lim, K. P. Hapgood and B. Haig, *Powder Technol*, 2016, **300**, 146–156.

ACKNOWLEDGEMENTS
Funding: EPSRC and AstraZeneca, Technical support: CMBE Mechanical Workshop

POSTER 57

# Co-Processing of Amorphous Solid Dispersions via Co-precipitation with Continuous Taylor-Couette Flow Reactor

CMAC, Strathclyde Institute of Pharmacy and Biomedical Sciences (SIPBS)
*lewis.macqueen@strath.ac.uk

Lewis MacQueen*, Kenneth Smith, Humera Siddique, Michael Devlin, John Robertson, Alastair Florence

## What is the Laminar Platform?

The Laminar Platform is a horizontal, jacketed, 300mL, Taylor-Couette flow reactor (TCR). An inner rotor spins to create different modes of Taylor-Couette flow. These modes influence different particle formations and morphologies.

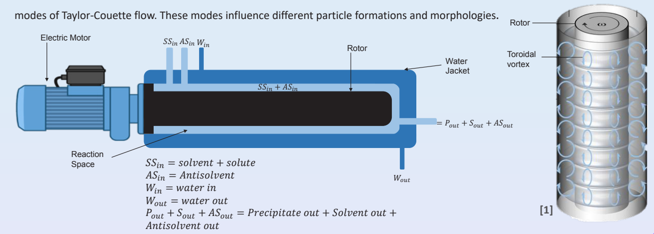


## Aims - Characterisation of the Laminar Platform

**Heat transfer** – Evaluate the temperature control within the reactor
**Minimum suspension** – Determine the minimum rotor RPM for total solid suspension
**Solid and Liquid residence time distribution** – Quantify the mode of flow at different rotor RPMs and net flow
**Effect of shear rate on particle formation** – Measure particle size and shape of an antisolvent recrystallisation of lactose monohydrate
**Inefficiencies and fouling** – Determine the limitations of this reactor

## Minimum suspension

Minimum suspension experiments were conducted using a two-part method, where, a visual confirmation method was utilised first, followed by a quantitative analysis:

- A slurry density of 5 wt% lactose in EtOH at 0.809 $g/cm^3$ was selected based on visual contrast, higher densities did not give the contrast needed to confirm full suspension
- A lower slurry density of 2 wt% was used to quantify the effect of net flow rate on particle suspension to allow better confirmation on effects
- Quantitative analysis using an FBRM probe to measure particle count at a range of RPMs
- It was concluded that from visual confirmation that 190 RPM was the lower limit for full suspension of 5 wt% lactose
- This was backed by quantitative analysis shown by instability starting from 190 RPM


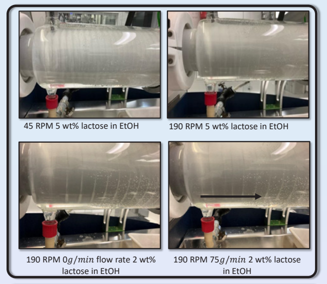


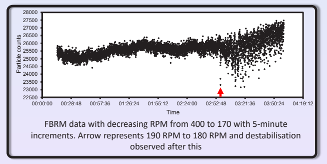

FBRM data with decreasing RPM from 400 to 170 with 5-minute increments. Arrow represents 190 RPM to 180 RPM and destabilisation observed after this

## Heat Transfer

- Heat transfer experiments were conducted using six different water flow rates - 50, 100, 150, 200, and 300 mL/min - pumped through the annular space. The water temperature was maintained at 50°C using jacketed lines to ensure consistent thermal conditions
- Chiller temperature was maintained at 15°C and at a flow rate of 5.1L/min
- The rotor was cycled through 300, 600, 900 and 1200 RPM
- A Prandtl number of 32.18 indicates that the boundary layer is thin, heat transfer between the walls of the reactor is effective, and the benefits from the inter-vortex mixing are apparent. This allows for momentum to dominate over thermal diffusion
- The reactor did not reach its operational limitations, and it was found that heat transfer was not affected by the flow rate

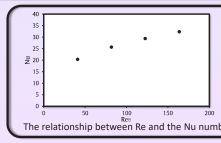

The relationship between Re and the Nu numbers

Increasing $Re_\theta$ the Nusselt number also increases which shows that convective heat transfer is the dominant mode, and therefore higher heat transfer between the boundaries.

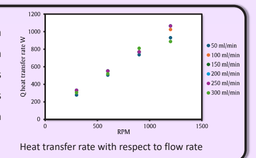


Heat transfer rate with respect to flow rate

Increasing the rotational speed leads to a higher heat transfer coefficient which enhances the convective heat transfer. This data shows that the reactor did not hit its operational limits and performs within future experimental requirements.

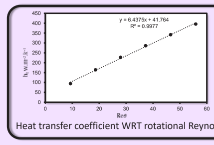


Heat transfer coefficient WRT rotational Reynolds number

The system was operated above the critical Taylor no (105) hence, the heat transfer coefficient indicates that convection (forced convection) is the dominant mode of heat transfer between the annular space and the jacket.

## Solid and liquid residence time distribution

**Liquid RTD**

- A calibration of sodium benzoate using a Carl Zeiss MCS5000 UV spectrometer was carried out with a transflectance probe with a path length of 5mm
- Water was used as a carrier liquid pumped in at different flow rates, an injection of 3mL of 30mg/L sodium benzoate is introduced
- Flow rates of 12.5, 25, 50, 75, and 100g/min and 300, 600, 900 and 1200 RPM were used to determine the effects of net flow and RPM on RTD
- Time of total elution of sodium benzoate was recorded to determine the effects of RPM and net flow

**Solid RTD**

- A Mettler Toledo G400 FBRM is used to measure the residence time of a 5mL injection of MCC (PH101) 10 wt% suspension of 50, 75, 100 and 125g/min and 300, 600, 900 and 1200 RPM
- Water was used as a carrier with flow rates of 50, 75, 100 and 125g/min and 300, 600, 900 and 1200 RPM
- Higher flow rates are used with the knowledge of particle settling in tubing lines from the minimum suspension work

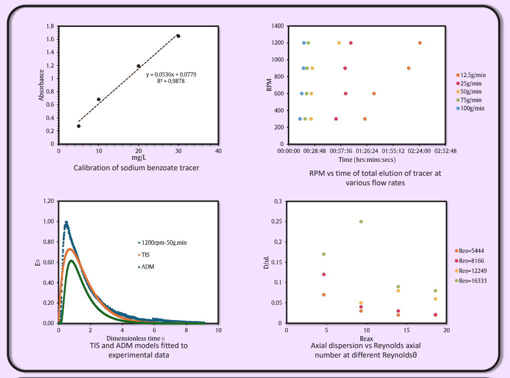


Calibration of sodium benzoate tracer

RPM vs time of total elution of tracer at various flow rates

TIS and ADM models fitted to experimental data

Axial dispersion vs Reynolds axial number at different Reynoldsθ

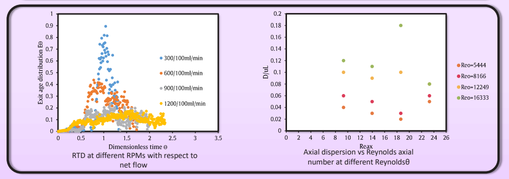


RTD at different RPMs with respect to net flow

Axial dispersion vs Reynolds axial number at different Reynoldsθ

**Liquid RTD – results**

- With increasing RPM, intervortex mixing was more apparent and therefore an increase in axial dispersion
- Lower flow rates and higher axial dispersion was observed longer time spent by the tracer within the annular space allows more interaction between vortex structures
- At 1200 RPM, three ranks could describe the system moving towards plug flow at 300 RPM with a maximum of 20 tanks, analogous to the number of vortex structures present
- Vortices have minimal intervortex mixing at lower RPMs and each behaves as a tank-in-series
- Optimal plug flow conditions seen at 300 RPM

**Solid RTD – results**

- Solid RTD indicates that lowering RPM makes the system move towards plug flow, higher RPM tends towards a fully mixed system, this agrees with the liquid RTD
- The minimum number of tanks at 1200 rpm was 3 and increased to 20 at 300 rpm
- Optimal plug flow conditions seen at 300 RPM

## Effect of shear rate on particle formation

- An antisolvent recrystallisation of lactose monohydrate is carried out at 20°C
- Lactose dissolved in water at 19.1$g/L$
- Ethanol used as the antisolvent
- Table 1 shows the conditions used during the antisolvent recrystallisation

| Condition | Lactose: Antisolvent | RPM of Laminar | | | | Volume flow rate mL/min lactose | Volume flow rate mL/min antisolvent | Total volume flow rate mL/min | RT (minutes) |
|---|---|---|---|---|---|---|---|---|---|
| 1 | 1:2<br>13:26 | 300 | 600 | 900 | 1200 | 12.04 | 33.33 | 45.37 | 7.27 |
| 2 | 1:3<br>9.5:28.5 | 300 | 600 | 900 | 1200 | 8.79 | 36.54 | 45.33 | 7.27 |
| 3 | 1:4<br>7.5:30 | 300 | 600 | 900 | 1200 | 6.94 | 38.46 | 8.72 | 7.27 |

Table 1: Conditions for antisolvent recrystallisation

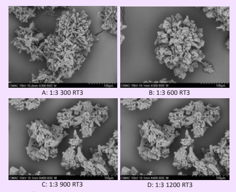

A: 1:3 300 RT3
B: 1:3 600 RT3
C: 1:3 900 RT3
D: 1:3 1200 RT3

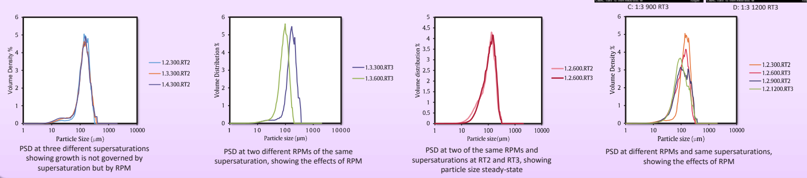


PSD at three different supersaturations showing growth is not governed by supersaturation but by RPM

PSD at two different RPMs of the same supersaturation, showing the effects of RPM

PSD at two of the same RPMs and supersaturations at RT2 and RT3, showing particle size steady-state

PSD at different RPMs and same supersaturations, showing the effects of RPM

## Conclusions

Heat transfer was efficient and performed above its usual experimental conditions, recrystallisation of lactose proved that particle size can be controlled, solid and liquid RTD showed that the platform can perform at near plug flow conditions at 20 tanks for both instances and the minimum suspension RPM is sufficient to provide the conditions needed to operate at plug flow Taylor-Couette ranges for a suspension density of 0.809 $g/cm^3$.

## Future work

To use the platform within its characterised operating ranges to coprecipitate amorphous solid dispersions. Coprecipitation of drug stabilised by polymer will determine the viability of drug systems produced on the Laminar platform and may fill in gaps where hot melt extrusion and spray drying are not viable options based on operating conditions.

## ASD systems for Laminar processing

| API/polymer 40°C/75%RH | Soluplus | PVP K30 | Plasdone | Affinisol | HPMC-AS |
|---|---|---|---|---|---|
| Carbamazepine wt% | 10 | 0 | 0 | 0 | 10 |
| Ritonavir wt% | 80 | 70 | 80 | 80 | 80 |
| Paracetamol wt% | 60 | 60 | 50 | 50 | 60 |
| Naproxen wt% | 30 | 30 | 30 | 10 | 10 |
| Celecoxib wt% | 60 | 60 | 70 | 40 | 50 |
| Felodipine wt% | 40 | 40 | 50 | 30 | 30 |

Table 2: 3-month stability for API loadings in polymer

Based on API/polymer stability at 40°C/75%RH within DDMAP by Lewis Ross, a selection of ASD systems will be processed in coprecipitation experiments completed in the Laminar platform. A selection of compatible, miscible solvent/antisolvents will be used.

## Acknowledgments

Thanks to the EPSRC and CMAC for funding. Thanks to Dr Michael Devlin and Dr Daniel Powell for their ongoing support and Lewis Ross for providing me with invaluable API/polymer stability data

References
[1] **Taylor-Couette reactor: Principles, design, and applications** Schrimpf M, Esteban J, Vorholt A *AIChE Journal (2021) 67(5) e17228*

POSTER 58

## Drug product formulation and manufacturing at National Facility

Carlota Mendez – CMAC,
University of Strathclyde

This poster will be available at the conference

POSTER 59

## Transfer learning for reaction development

Benedetta Bassetti –
University of Leeds

This poster will be available at the conference

## POSTER 60

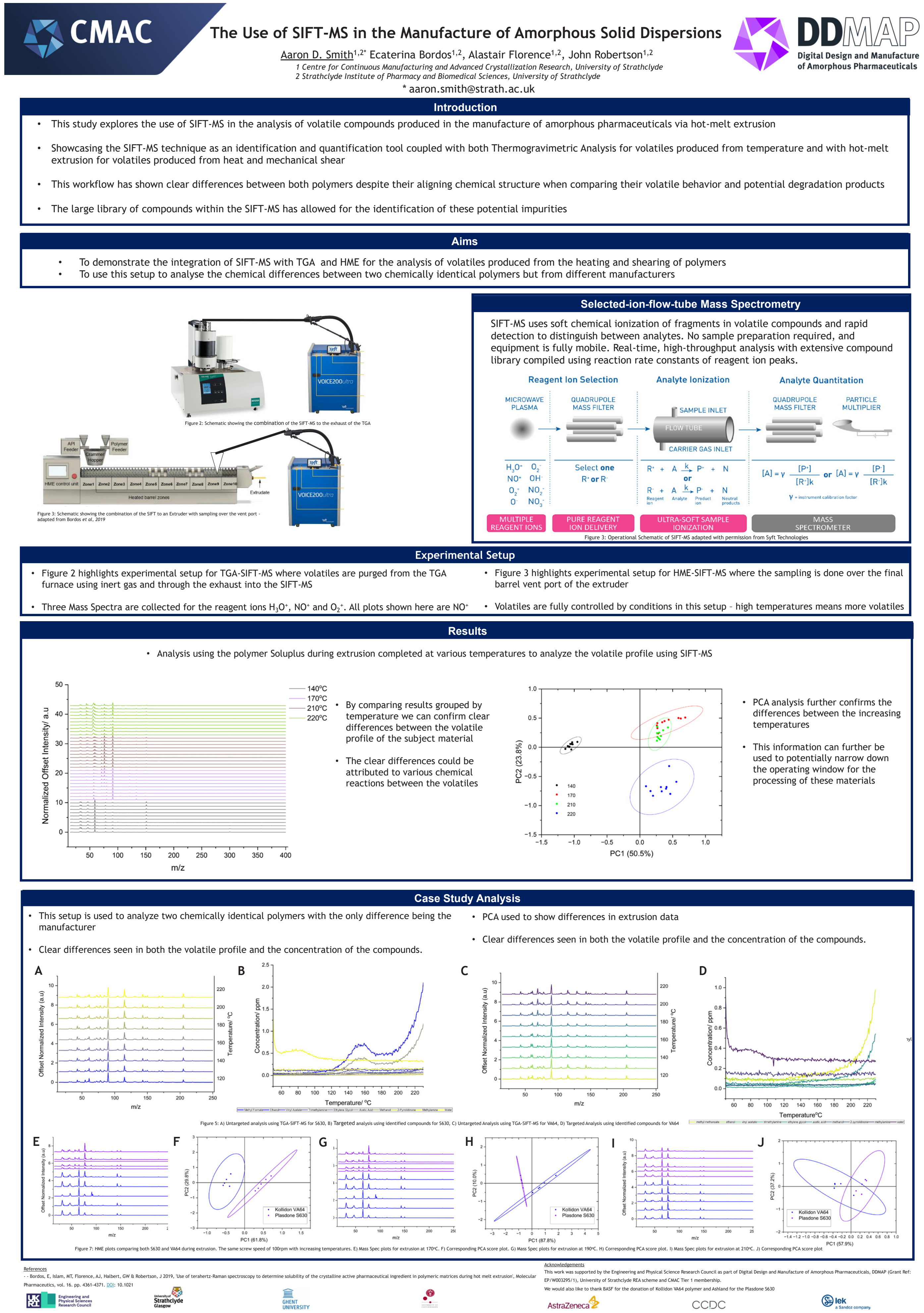


## POSTER 61

# Telescoped self-optimising systems: making long reaction campaigns shorter

## Kalum Thurgood-Parkes – University of Leeds

This poster will be available at the conference

POSTER 62

# Multi Routes to Amorphous Solid Dispersions: Spray Drying vs Hot Melt Extrusion

Colette Tierney – CMAC, University of Strathclyde

This poster will be available at the conference

POSTER 63

# In-situ Studies of Crystallization and Filtration Processes Using Time-resolved Synchrotron Based X-ray Phase Contrast Imaging (XPCI)

Oliver V. Towns[1,2*], Ameer Alshukri[1], Nathan Hennessy[1], Tariq Mahmud[1], Joanna Leng[3], Sara Ottoboni[2,4], Chris J. Price[2,4], Helen Wheatcroft[5], Anna Jawor-Baczynska[5], Sven L. M. Schroeder[1,2]

[1]Chemical and Process Engineering, University of Leeds, Leeds, LS2 9JT, UK

[2]EPSRC Centre for Innovative Manufacturing in Continuous Manufacturing and Crystallisation, University of Strathclyde, Glasgow, G1 1RD, UK

[3]School of Computer Science, University of Leeds, Leeds, LS2 9JT, UK

[4]Department of Chemical and Process Engineering, University of Strathclyde, Glasgow, G1 1RD, UK

[5]Chemical Development, Pharmaceutical Technology & Development, Operations, AstraZeneca, Macclesfield, UK

*cm15ovt@leeds.ac.uk

## Introduction

Synchrotron X-ray phase contrast imaging (XPCI) allows **rapid microscopic imaging** of multiphase systems with low absorption contrast between the components, such as organic crystals in solvents. This permits **time-resolved studies of the structural evolution of dynamic systems**. This technique has been applied to both **crystal growth**, using 2D radiographic imaging (which will be extended to 3D in the future), and to **filtration processes**, using time-resolved 3D tomography scans.

## Crystal Growth Radiography

**Current industrial standards** for monitoring crystallisations are **limited** in the information that is gained, eg:

- **FBRM** and **Laser Light Scattering**: only give **1D** length information
- **Microscopy Probes**: Only give **2D** information and can be **difficult to process**.

**XPCI** has the following **advantages** over standard techniques:

- **Easier background correction** due to parallel rays, so no crystals are out of focus.
- Phase contrast also can **reveal other phase behaviour** (anti-solvent mixing, oiling out, etc.)
- Can be **paired with other X-ray modalities**, such as diffraction, for more information
- Has the potential to extract **time-resolved 3D information**, building a more complete picture of the process and therefore influencing more accurate models.

A bespoke object detection algorithm has been created to automatically segment crystals from the background.

Thickness information may be extracted using the Paganin filter as shown in figure 2 (1).

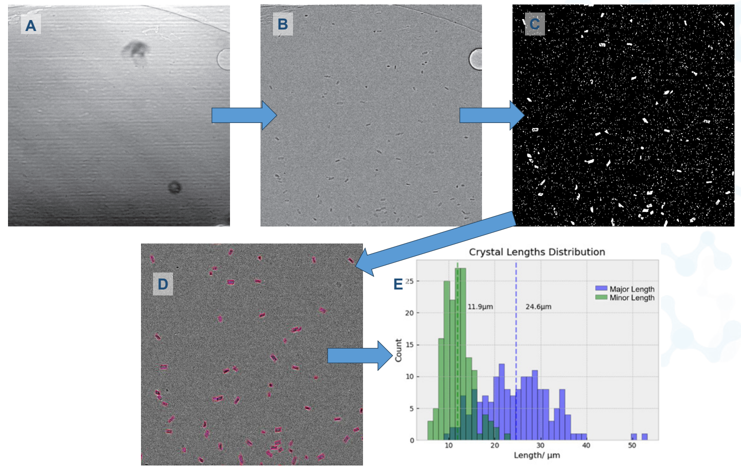


**Figure 1.** Screenshots of frame from the video processing pipeline. A: Raw video frame. B: Background corrected frame. C: Binary threshold frame. D: Contour labelled frame. E: Example of figure extracted from frame, major (blue) and minor (green) lengths with labelled averages.

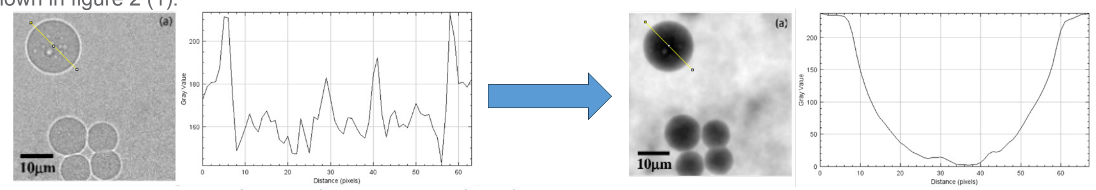


**Figure 2.** XPCI images of latex spheres taken from reference 1 with associated pixel intensity graphs plotted along yellow line.

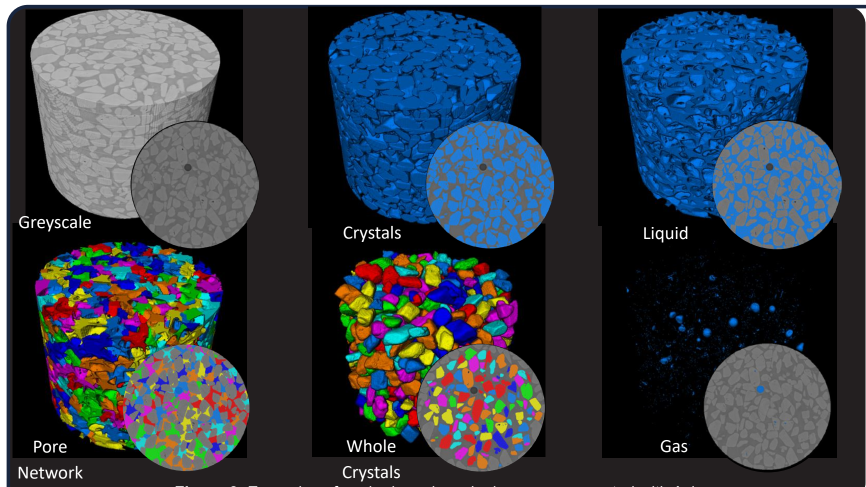


**Figure 3.** Examples of each phase in a single scan, segmented with Avizo.

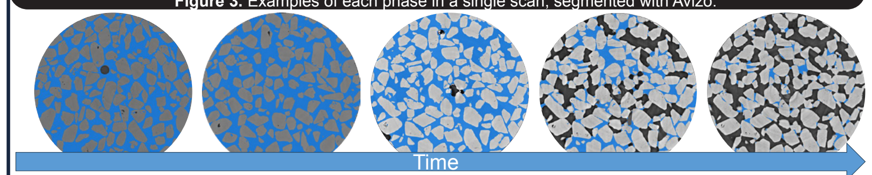


**Figure 4.** Z-slice of granular paracetamol filtration, washing and drying through time. Liquid phase highlighted in blue.

## Filtration Tomography

Synchrotron based X-ray phase contrast tomography has been used to visualise the **filtration, washing and drying** of pharmaceutical solids. 3D scans are taken in less than a minute meaning that they can be taken throughout each step, allowing us to build a **4D picture** of the whole process.

Paracetamol (granular and micronized) and metacetamol (needle-like) were used for different **sizes and morphology** examples, and the **filtration conditions were investigated**, such as: flow-rate, drying-rate and stopping points.

Phase contrast allows for each phase to be segmented and analysed individually in **3D, and through time**. Data on the following can be extracted:

- **Particle shape** and **size distributions** in 3D
- Phase variation with height
- Where liquid, and therefore **impurities**, is retained
- How the pore network changes

With a **better understanding** of the filtration, washing, and drying process efforts can be made to implement **more efficient processing**.

1. Paganin, D., Mayo, S., Gureyev, T., Miller, P. and Wilkins, S. 2002. Simultaneous phase and amplitude extraction from a single defocused image of a homogeneous object. *Journal of Microscopy*. **206**(1), pp.33-40.

POSTER 64

## Analysis of Spherical Agglomerate Morphology and Processability

Rachel Feeney – CMAC,
University of Strathclyde

This poster will be available at the conference

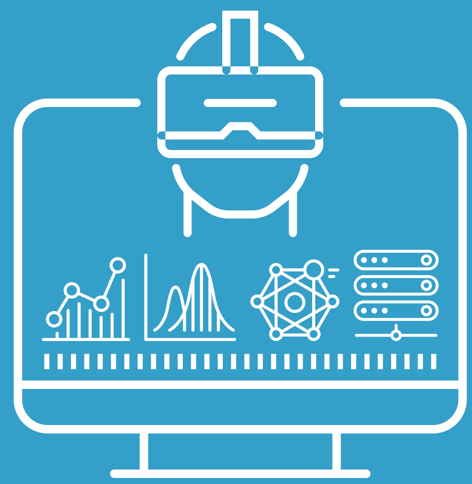

# Quality by Digital Design & Digital Workflows

## POSTER 66

# A New Centre of Excellence for Regulation to Accelerate Digital Adoption in Medicines Development and Manufacturing

Ian Houson - CMAC, University of Strathclyde

This poster will be available at the conference

## POSTER 67

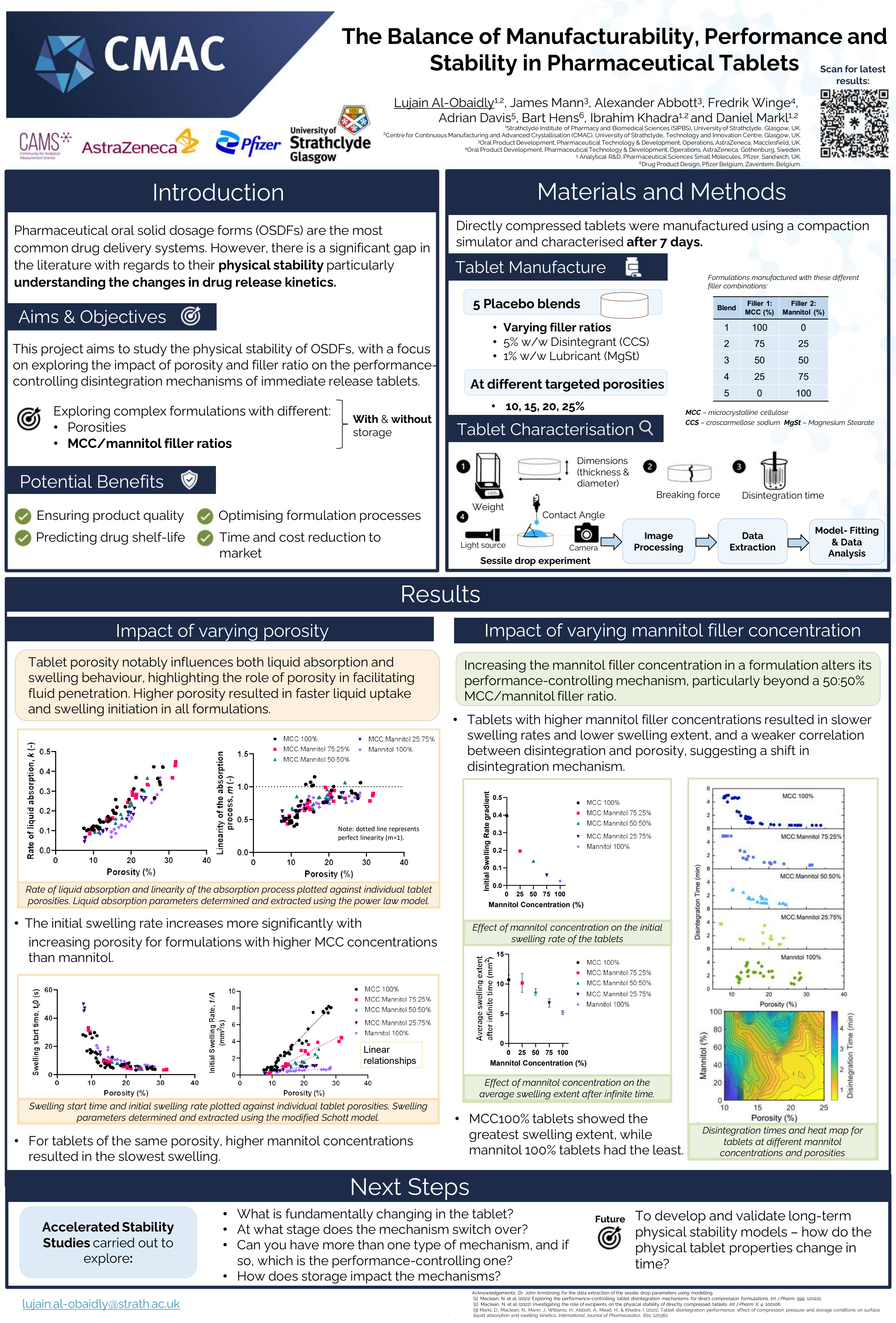

## POSTER 68

# Innovative Nanoparticle Production

Hakam Alaqabani, Jade Forrester, and Yvonne Perrie

*CMAC National Facility, University of Strathclyde*

## Introduction

Our research team focuses on the advanced development and manufacture of targeted drug delivery systems, including lipid nanoparticles (LNPs), polymer-lipid hybrid systems, and liposomes. By leveraging scalable microfluidic technologies, we are able to optimize and produce formulations with precise control over critical quality attributes, ensuring both consistency and scalability from bench-scale to GMP production. In addition, we provide comprehensive analytical characterization using a variety of techniques to assess particle size, surface charge, chemical composition, and structural integrity. Our team also conducts in-depth biological and in vivo evaluations to assess cellular uptake, toxicity, and the efficacy of drug delivery, as well as tracking via advanced imaging systems.

Drug Discovery → Clinical Development → Approved Drug

## Lab Capabilities

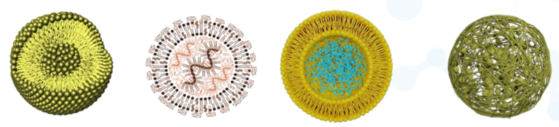


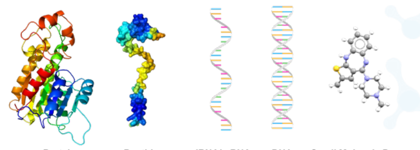


Formulation

### Advanced Formulation Development: Polymer-LNPs-Liposome

- **Designing Drug Delivery Systems (DDS) for Targeted & Sustained Release**
- Development of nanoparticles loaded with **drugs, DNA, siRNA, mRNA, proteins, peptides, and small molecules**
- Scalable **microfluidic mixing** from **bench-scale to GMP production**


Characterization

### Comprehensive Analytical Characterization

- **Particle Attributes**
- **Size & Surface Charge**: ELS (Electrophoretic Light Scattering), DLS (Dynamic Light Scattering), NTA (Nanoparticle Tracking Analysis), DSC (Differential Scanning Calorimetry).
- **Spectroscopic & Chromatographic Techniques**
- **Chemical Characterization**: UV-Vis, FTIR, HPLC, Mass Spectrometry, Fluorescence Spectroscopy, gel electrophoresis , Gas Chromatography
- **Structural & Stability Analysis**
- **Morphology & Composition**: Cryo-TEM, SEM, Xenocs Small Angle X-ray Scattering (SAXS)
- **Stability & Quality Control**: Freeze Drying, pH Monitoring, Long-Term Stability Testing

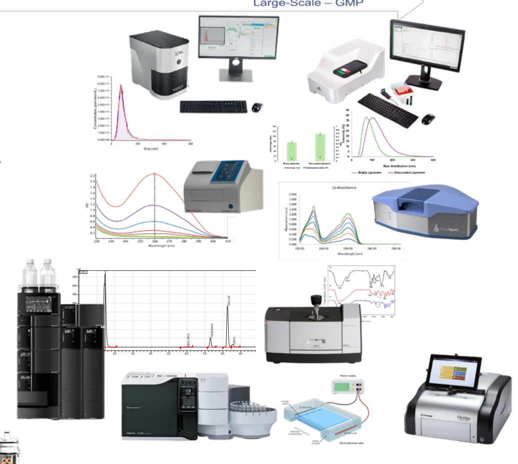

Purification & Release

### Production Attributes

- **Stability Testing:** Freeze drying, pH monitoring, temperature cycling, and long-term stability studies
- **Purification Techniques:** Dialysis, Tangential Flow Filtration (TFF), and Spin Columns
- **Drug Release Kinetics:** Controlled release studies using the USP 4 SOTAX apparatus

Biological

### In vitro and in vivo

- **Biological & In Vivo Evaluation**
- **Cellular Studies**
- **Viability, Toxicity, Uptake** across various cell lines
- **Intracellular Trafficking** via Confocal Fluorescence Microscopy
- **Antibody Studies** using Flow Cytometry
- **In Vivo Imaging & Tracking**
- Bioluminescence & Fluorescence Imaging (IVIS & GX Systems)

Applications

### Research development

- **Formulation Parameter Optimization**: Enhancing stability, bioavailability, and controlled release
- **Vaccine Development**: In vitro and in vivo studies for immunogenicity and efficacy
- **Anti-Cancer Investigations**: Targeted drug delivery and therapeutic efficacy assessments

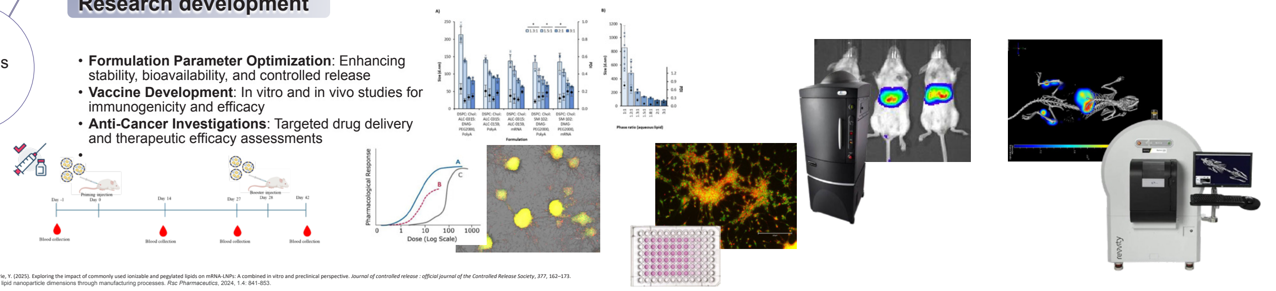


Reference:
Binici, B., Rattray, Z., Zinger, A., & Perrie, Y. (2025). Exploring the impact of commonly used ionizable and pegylated lipids on mRNA-LNPs: A combined in vitro and preclinical perspective. *Journal of controlled release : official journal of the Controlled Release Society*, *377*, 162–173.
MCMILLAN, Caitlin, et al. Tailoring lipid nanoparticle dimensions through manufacturing processes. *Rsc Pharmaceutics*, 2024, 1.4: 841-853.

## POSTER 69

# Autonomous Physical Stability Model Development

Maria Chang[1,2], Lee Ashworth[3], James Mann[3], Faisal Abbas[1,2], Daniel Markl[1,2]
[1]Centre for Continuous Manufacturing and Advanced Crytalllisation (CMAC), University of Strathclyde, Glasgow UK
[2]Strathclyde, Institute of Pharmacy & Biomedical Sciences, University of Strathclyde, Glasgow, UK
[3]Global Product Development, Pharmaceutical Technology & Development, Operations, AstraZeneca, Macclesfield, UK

### Project Aims

**Connecting systems** to enable **accelerated development** of performance and stability models for **pharmaceutical tablets**

### Objectives

**ONE** – Connect **Self-driving Tableting System** with **Fully Automated Dissolution System**

**TWO** – Connect linked systems from **Objective 1** with **Fully Automated Storage System** to enable simultaneous optimization of **manufacturability** and **performance**

**THREE** – Combining the **Dissolution Modelling Predication** with **Stability Prediction** that can then be used **iteratively**.

### Self-Driving Laboratory

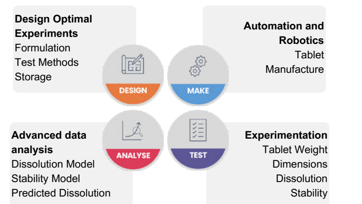


### Data Output

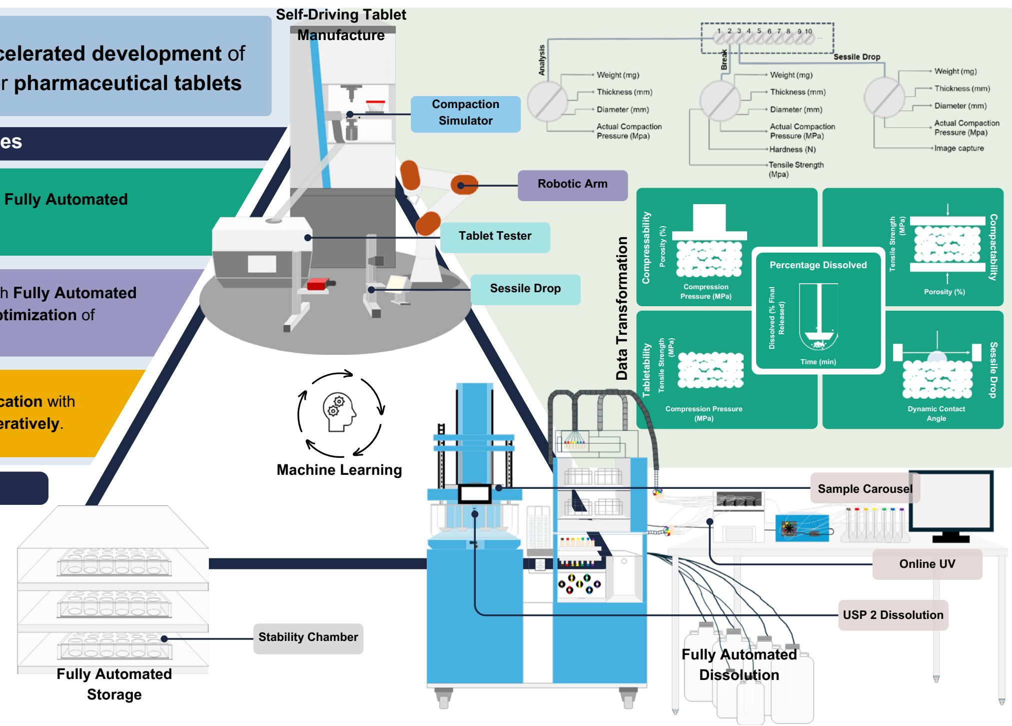


### Enabling Big Data with Automated Dissolution and Self-Driving Tablet Manufacture

#### Experiment Objective

**Investigating the impact of disintegrant level on dissolution performance enabled by self-driving tablet manufacture and automated dissolution**

#### Experimental Design

| Tablet Dimensions | | | |
|---|---|---|---|
| Weight (mg) | 250 | Shape | Flat, Round |
| Diameter (mm) | 9 | Porosity | 10%, 15% & 20% |

| Tablet Component | Excipient | %w/w | | |
|---|---|---|---|---|
| | | F1 | F2 | F3 |
| API | Ibuprofen 50 | 10 | 10 | 10 |
| Filler 1 | Microcrystalline Cellulose | 43.5 | 42 | 40.5 |
| Filler 2 | Lactose | 43.5 | 42 | 40.5 |
| Disintegrant | Croscamellose Sodium | 2 | 5 | 8 |
| Lubricant | Magnesium Stearate | 1 | 1 | 1 |

#### Per Formulation

- Automated Tableting Bayesian Optimisation: 00:57:27
- Self-Driving Tablet Manufacture (Analysis, Break, Sessile Drop: 01:57:57
- Fully Automated Dissolution: 04:45:00
- Total Experiment Time (Tablet Manufacture + Dissolution): 07hr 40min 24 sec
- Number of Tablets per formulation: 84

**Total Experiment Time: (3 Formulations x 3 Porosities)** 23 hr 01 min 12 sec

v

**Total Experiment Time (Manually Operated at CMAC):** 2 days 1 hr

Note: Total time is cumulative total, timing does not take into account working hours

#### Proposed Integrated Workflow

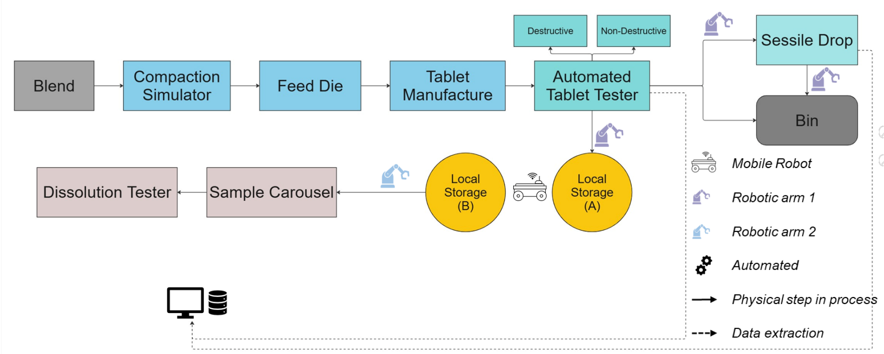


### Next Steps

- ETL – Define Meta Data Workflow
- Increase experiment design
- Dissolution Prediction Models
- Further Enhance Automated Dissolution's Automated Capabilities

Engineering and Physical Sciences Research Council

POSTER 70

# mRNA-LNP Vaccines; A Case Study

Jade Forrester, Hakam Alaqabani and Yvonne Perrie
*CMAC National Facility, University of Strathclyde*

## Introduction

At continuous manufacturing, we specialise in precision nanoparticle formulation, encompassing lipids, solid lipid, polymeric nanoparticles, and nano emulsions. Utilising a wide variety of microfluidic techniques, we formulate these nanoparticles with unprecedented accuracy and scalability. In parallel, we explore the exciting potential of messenger RNA (mRNA) vaccines. This study highlights pivotal data on the CQAs and in vitro and in vivo efficacy and behaviour of mRNA vaccine formulations.

## Materials and Methods

In this study, the impact of structure on potency was investigated by formulating a range of mRNA-LNP vaccines with varied ionizable and PEGylated lipids. All formulations were manufactured using a microfluidic mixer (NanoAssemblr® Benchtop from Cytiva) and standard critical quality attributes were analysed including particle size, polydispersity, zeta potential and mRNA encapsulation and recovery. The mRNA-LNP vaccines were also evaluated in both in vitro (HEK-293) assays as well as preclinical in vivo studies (BALB/c mice).

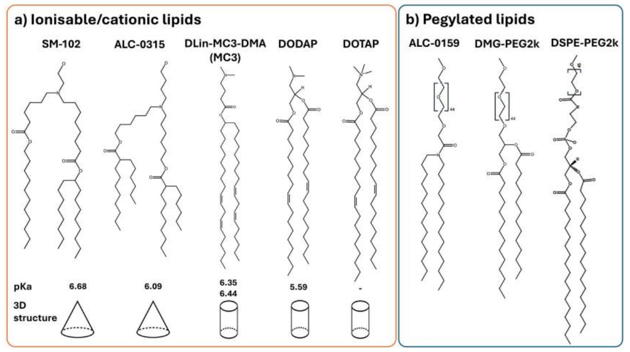


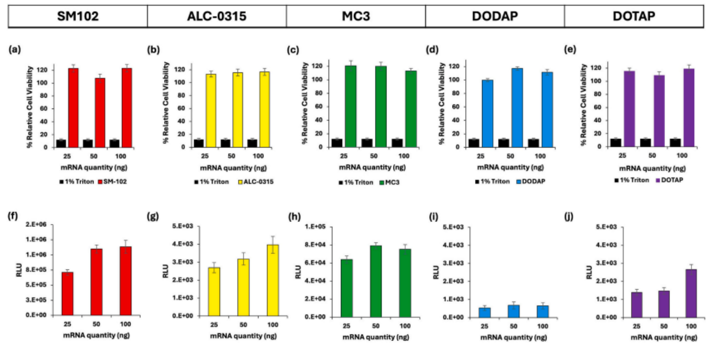


| Cationic/Ionizable lipids | Day | Diameter (nm) | PDI | Zeta potential (mV) | EE (%) | Mass balance (%) |
|---|---|---|---|---|---|---|
| SM-102 | 0 | 64.9 ± 5.3 | 0.04 ± 0.03 | −1.0 ± 0.9 | 97 ± 1 | 85 ± 16 |
| | 7 | 67.9 ± 6.8 | 0.03 ± 0.01 | −1.5 ± 0.9 | 96 ± 0 | 84 ± 14 |
| ALC-0315 | 0 | 55.2 ± 0.5 | 0.11 ± 0.02 | −2.1 ± 1.1 | 93 ± 2 | 93 ± 11 |
| | 7 | 56.3 ± 1.0 | 0.12 ± 0.02 | −3.7 ± 2.3 | 95 ± 1 | 100 ± 1 |
| MC3 | 0 | 60.8 ± 1.3 | 0.11 ± 0.02 | −1.6 ± 1.6 | 93 ± 2 | 93 ± 5 |
| | 7 | 60.6 ± 2.0 | 0.10 ± 0.02 | −2.2 ± 0.5 | 93 ± 1 | 93 ± 6 |
| DODAP | 0 | 69.0 ± 2.8 | 0.04 ± 0.02 | −1.4 ± 1.3 | 91 ± 1 | 97 ± 6 |
| | 7 | 66.1 ± 7.5 | 0.06 ± 0.02 | −1.4 ± 1.0 | 87 ± 2 | 94 ± 2 |
| DOTAP | 0 | 49.8 ± 5.9 | 0.24 ± 0.04 | 2.4 ± 1.9 | 99 ± 0 | 89 ± 10 |
| | 7 | 68.7 ± 10.9 | 0.29 ± 0.03 | 4.8 ± 1.2 | 99 ± 1 | 87 ± 8 |

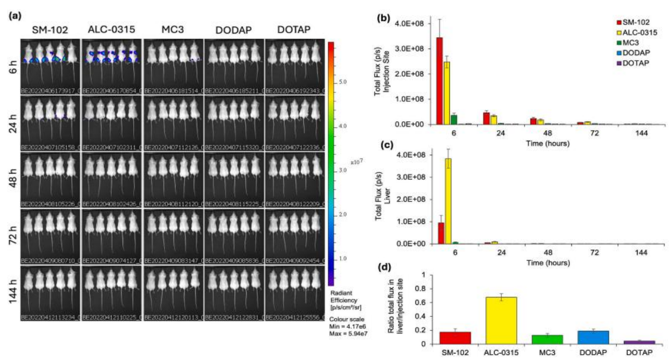


## Results

All LNP formulations exhibited similar CQAs, including particle sizes <100 nm, low PDI (<0.2), near-neutral zeta potential, and high encapsulation efficiency (>90%). However, the potency of these LNPs, as measured by in vitro mRNA expression and in vivo expression following intramuscular injection in mice varied significantly. LNPs formulated with SM-102 exhibited the highest expression in vitro, whilst in vivo SM-102 and ALC-0315 LNPs showed significantly higher mRNA expression than DLin-MC3-DMA, DODAP and DOTAP LNPs.

Reference:

Binici, B., Rattray, Z., Zinger, A., & Perrie, Y. (2025). Exploring the impact of commonly used ionizable and pegylated lipids on mRNA-LNPs: A combined in vitro and preclinical perspective. *Journal of controlled release : official journal of the Controlled Release Society*, *377*, 162–173.

POSTER 71

# Challenging the Concept of Strain Rate Sensitivity: Feedframe Dynamics Drive Tensile Strength Reduction in High-Speed Tabletting

Musab Osman[1,2], Daniel Markl[1,2], Gavin Reynolds[3], Catherine Yates[3], Pratik P. Upadhyay[4] and John Robertson[1,2]
[1]Strathclyde Institute of Pharmacy & Biomedical Sciences, University of Strathclyde, Glasgow, UK
[2]CMAC Future Technology and Innovation Centre, University of Strathclyde, 99 George Street, Glasgow, G1 1RD, UK
[3]Oral Product Development, Pharmaceutical Technology and Development, AstraZeneca, Macclesfield, SK10 2NA, UK
[4]Oral Product Development, Pharmaceutical Technology and Development, AstraZeneca, Gothenburg, Sweden

## INTRODUCTION

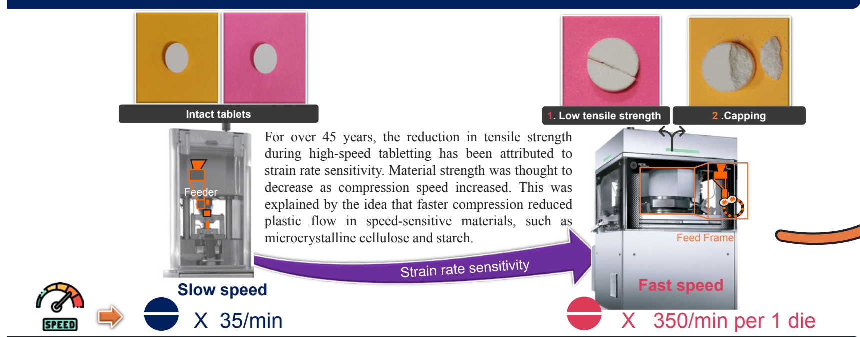


For over 45 years, the reduction in tensile strength during high-speed tabletting has been attributed to strain rate sensitivity. Material strength was thought to decrease as compression speed increased. This was explained by the idea that faster compression reduced plastic flow in speed-sensitive materials, such as microcrystalline cellulose and starch.

This study challenges the assumption that tensile strength (TS) reduction in high-speed tableting stems from strain rate sensitivity (SRS). Instead, we demonstrate that feedframe paddle rotation weakens interparticle bonding by increasing lubrication extent, reducing TS.

## RESULTS

- Is scaling up simply increasing tablet output (e.g. dwell time 15 ms)?

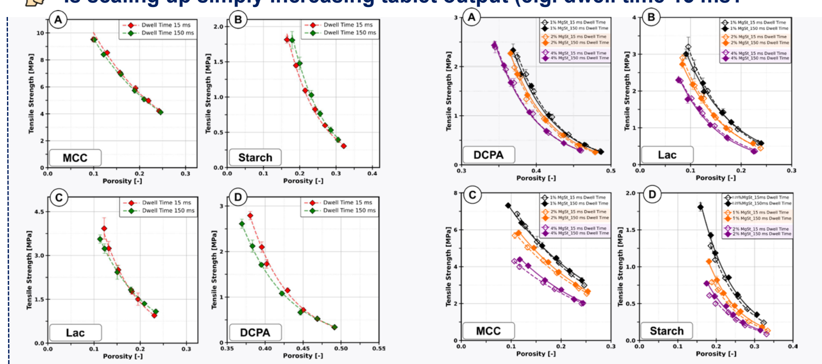


**Fig.1.** Effect of Dwell Time on Tensile Strength of Pure Materials: MCC, Starch, Lactose, and DCPA

**Fig.2**. Effect of Dwell Time and Lubrication Level (MgSt) on Tensile Strength of MCC, Starch, Lactose, and DCPA.

**Dwell time** = the time during which compaction force is more or equal to 90% of its peak value
**rpm** = feeder rotation per minute
**DCPA** = Dibasic calcium Phosphate Anhydrous
**Lac** = Lactose monohydrate
**MCC** = Microcrystalline cellulose
**Starch** = Partially Pregelatinised Maze Starch

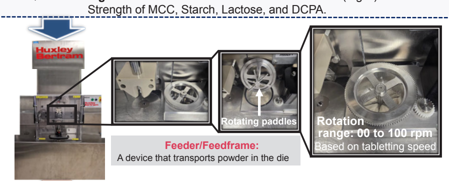


**Feeder/Feedframe:**
A device that transports powder in the die

- What is actually happening during Scaling up ?

Feedframe rotation speed is increased—up to 100 RPM or more—to ensure consistent die filling at high tabletting speeds

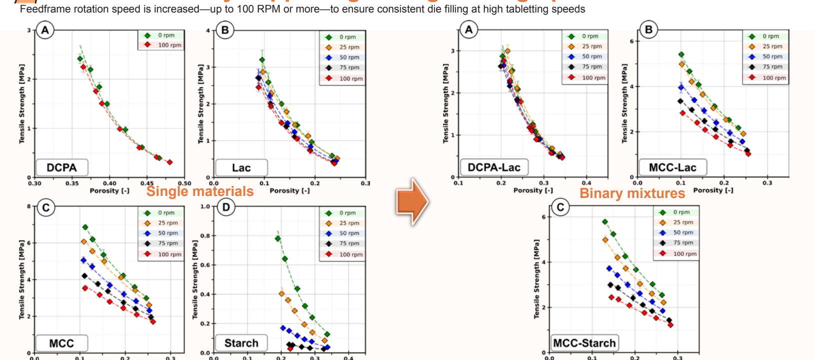


Fig.3. Effect of Feedframe Paddle Speed on Tensile Strength of Lubricated Materials (1% MgSt): DCPA, Lac, MCC & Strach.

Fig. 4. Impact of Feedframe Speed on Tensile Strength of Binary Mixtures at 1% Lubrication Level (MgSt): DCPA-Lac, MCC-Lac, and MCC-Starch.

## CONCLUSION

- **Dwell time does not affect the tensile strength** of the studied materials, except for DCPA, which shows a slight increase at high speed.
- **Dwell time does not impact the tensile strength** of Lac and DCPA, **regardless of lubrication levels.** For MCC, a slight decrease in tensile strength is observed at 2% and 4% lubrication, and for starch at 1% and 2%. However, these changes are minor and fall within the standard error range.
- **Feed frame paddle rotation weakens the tensile strength** of lubricated materials.
- **Thus; what has traditionally been attributed to strain rate sensitivity in tablet manufacturing is, in fact, a lubrication problem caused by increased feedframe paddle rotational speeds.**
- **Feed frame-induced tensile strength reduction** in **binary mixtures** is **governed** by the sensitivity of their **individual components** to feedframe speed

## ACKNOWLEDGEMENT

- The authors would like to acknowledge the contributions of CMAC National Facility Team for their technical support. MO would also like to thank EPSRC and AstraZeneca, Macclesfield, UK for funding.

## REFERENCES

[1] M. T. Ende *Chemical Engineering in the Pharmaceutical Industry: Drug Product Design, Development, and Modeling*, Second Edi. New Jerssey, USA: John Wiley & Sons, Inc, 2019.
[2] C. C. Sun, "Development of a High Drug Load Tablet Formulation Based on Assessment of Powder Manufacturability : Moving Towards Quality by Design," vol. 98, no. 1, pp. 239–247, 2009, doi: 10.1002/jps.
[3] M. C. Monedero "Effect of Compression Speed and Pressure on the Physical Characteristics of Maltodextrin Tablets," vol. 9045, p. 10, 2008, doi: 10.3109/03639049809082362

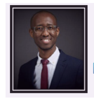

Musab Osman
Musab.Osman@Strath.ac.uk

POSTER 72

# Developing Workflows to Drive Autonomous Experimentation

Murray Robertson[1], Helen Feilden[1], Ian Houson[1], Cameron Brown[1], Blair Johnston[1], Chantal Mustoe[1] & Alice Turner[1]
1. The EPSRC Future Manufacturing Research Hub in Continuous Manufacturing and Advanced Crystallisation, University of Strathclyde, Glasgow
www.cmac.ac.uk
murray.robertson@strath.ac.uk

## Introduction – QbDD Workflows

- Quality by Digital Design (QbDD) is a framework to accelerate medicines development and enable regulatory innovation for new medicines approvals.
- It exploits emerging capabilities in industrial digital technologies and accelerates the identification and exploration of more robust design spaces.
- The QbDD Workflows help guide implementation of the QbDD framework.

From QbD to QbDD

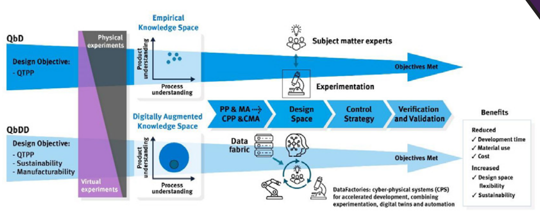

Figure 1: From QbD to QbDD: The transition from QbD to QbDD with reference to its effect on the knowledge space and the use of an existing data fabric to inform experimentation and CPSs at each stage of development (as part of self-driving DataFactories) to enable a range of benefits.

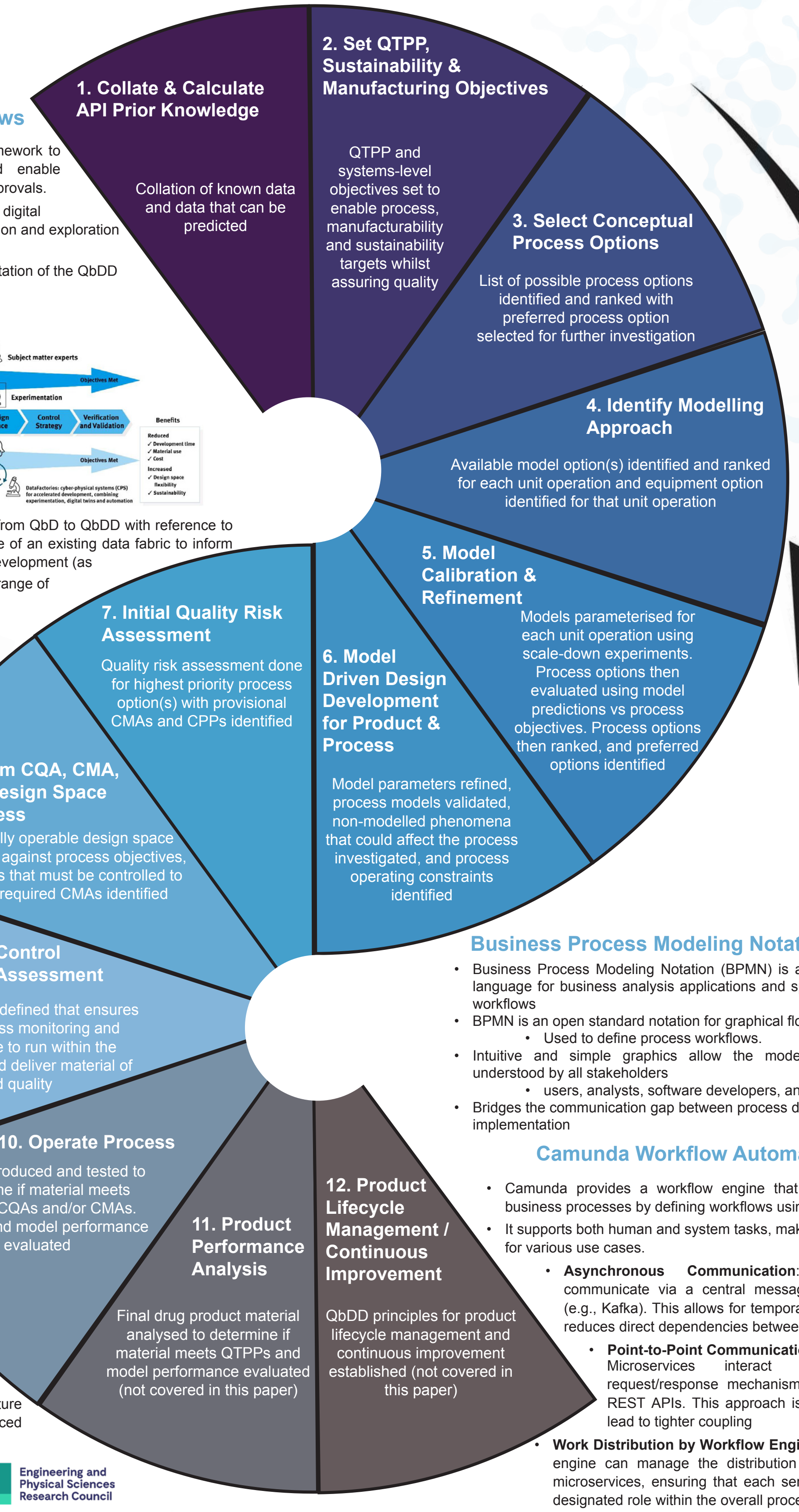


Figure 2: Workflow stages and outputs.

## Business Process Modeling Notation (BPMN)

- Business Process Modeling Notation (BPMN) is a visual modeling language for business analysis applications and specifying process workflows
- BPMN is an open standard notation for graphical flowcharts
  - Used to define process workflows.
- Intuitive and simple graphics allow the models to be easily understood by all stakeholders
  - users, analysts, software developers, and data architects
- Bridges the communication gap between process design and implementation

## Camunda Workflow Automation

- Camunda provides a workflow engine that helps automate business processes by defining workflows using BPMN
- It supports both human and system tasks, making it versatile for various use cases.
  - **Asynchronous Communication**: Microservices communicate via a central message or event bus (e.g., Kafka). This allows for temporal decoupling and reduces direct dependencies between services
    - **Point-to-Point Communication**: Microservices interact directly using request/response mechanisms, often through REST APIs. This approach is simpler but can lead to tighter coupling
- **Work Distribution by Workflow Engine**: The workflow engine can manage the distribution of tasks across microservices, ensuring that each service performs its designated role within the overall process

## Acknowledgements

This work was funded as part of the Future Continuous Manufacturing and Advanced Crystallisation Research Hub EP/P006965/1



POSTER 73

# Advanced Formulation Mixture Rule Optimisation for Enhancing Predictability of Tablet Compressibility and Compactability

Theo Tait – CMAC,
University of Strathclyde

This poster will be available at the conference

POSTER 74

# Developing a methodology for the use of sustainability objectives in API crystallisation process development and optimisation

Nicola Voiculescu – CMAC, University of Strathclyde

This poster will be available at the conference

POSTER 75

CMAC

# Understanding Punch Sticking in Pharmaceutical Tablet Compression

Lilly

Ishwari Wale[1,2], John Robertson[1,2], Aditya Bharadwaj Singaraju[3], Daniel Markl[1,2]

[1]Strathclyde Institute of Pharmacy & Biomedical Sciences, University of Strathclyde, Glasgow, UK

[2]Centre for Continuous Manufacturing and Advanced Crystallisation, Technology and Innovation Centre, University of Strathclyde, 99 George Street, Glasgow , G1 1RD ,UK

[3] Lilly Research Labs, Eli Lilly and Company, Indianapolis, IN 46285, USA

## Common Tablet Defects

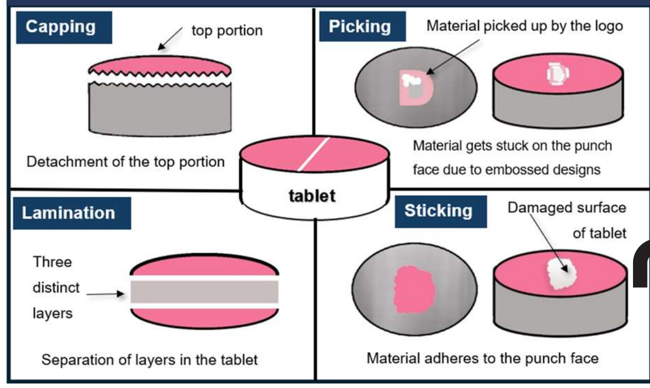


## Stages of Powder Adherence

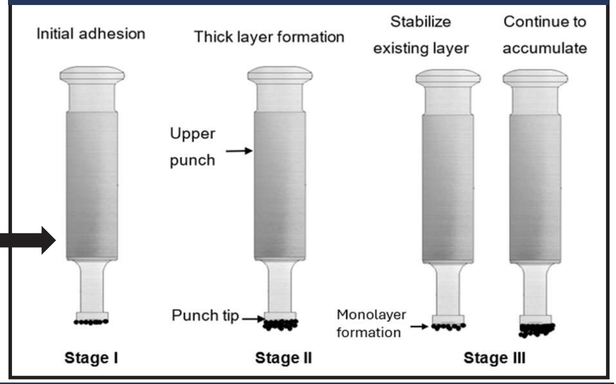


## Methods to Assess Punch Sticking

| Category | Method | Mechanism | Quantitation | Specificity | Time |
|---|---|---|---|---|---|
| Powder method | Centrifugal method | Centrifugal force | I | N | M |
| | Rheometry | Adhesion - Cohesion forces | I | N | S |
| Compaction method | Punch tip weight | Interaction between punch tip & tablet material | D | N | F |
| | Compaction parameter analysis | Interaction between punch tip & tablet material | I | N | M |
| Powder residual method | HPLC - UV spectroscopy | Chemical interaction | D | Y | F |
| Tablet method | Atomic Force Microscopy (AFM) | Atomic-Level Stick-Slip | D | N | F |
| Miscellaneous method | Scanning Electron Microscopy | Electromagnetic radiation | D | N | F |
| Advanced methods | Lasor Sensor based | Infrared radiation | D | Y | F |

Abbreviations and Definitions: Indirect Method refers to characterizing the affinity between material and punch face (**I** - Indirect Method); Direct Method refers to characterizing the amount of material (**D** - Direct Method); Time refers to the duration required to perform the experiment and analyze results (**F** - Fast (<5 minutes), **M** - Moderate (5 minutes to 1 hour), **S** - Slow (>1 hour)); Specificity indicates the ability to identify components from the adhered material (**Y** - Yes, **N** - No).

## Reflection on an Experimental Journey

**Rheometry**

- Based on adhesive and cohesive force
- Calculation of Sticking Index (SI)
- Uses very low pressure , Lack of specificity

**Image analysis**

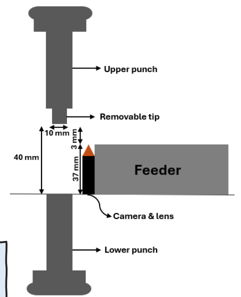


- Lack of specificity
- Restricted for monolayer adhesion

**Raman spectroscopy**

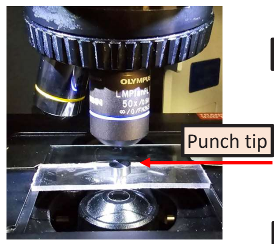


- Quantification and specificity is possible
- Non-destructive and no sample preparation

**Weighing tip & HPLC analysis**

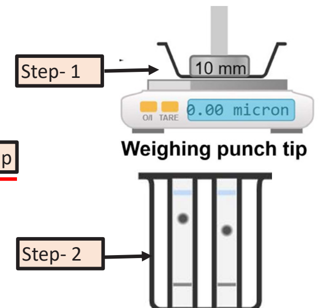


- Traditional method
- Provides qualitative & quantitative analysis
- Requires solvent compatibility with adhered material , time consuming

**Morphology Directed Raman Spectroscopy**

- Raman equipped with morphology
- New approach to assess sticking
- Linking PSD to adhered material

## Conclusion

Early detection of sticking in pharmaceutical tablet compression is essential for reducing batch failures, minimizing wastage, and lowering costs. Implementing reliable assessment methods and proactive monitoring can help identify and address sticking issues promptly, ensuring consistent and high-quality production of pharmaceutical tablets.

## References

1.Paul, S., Taylor, L.J., Murphy, B., Krzyzaniak, J., Dawson, N., Mullarney, M.P., Meenan, P. and Sun, C.C., 2017. Mechanism and kinetics of punch sticking of pharmaceuticals. *Journal of pharmaceutical sciences*, *106*(1), pp.151-158.

2. Saddik, J.S. and Dave, R.H., 2021. Evaluation of powder rheology as a potential tool to predict tablet sticking. Powder Technology, 386, pp.298-306.

PSD – Particle Size Distribution

# Notes

CMAC


General Enquiries
E: info@cmac.ac.uk

/cmac-centre
@CMAC_Centre
@CMAC_Centre
@CMAC_Centre

www.cmac.ac.uk



UKRI Engineering and Physical Sciences Research Council